Coordination Chemistry Reviews 502 (2024) 215599

Contents lists available at ScienceDirect

Coordination Chemistry Reviews

journal homepage: www.elsevier.com/locate/ccr

Review

Syntheses and structures of transition metal complexes of quinoline-containing multidentate amine ligands

Bronte Carr, Cassandra L. Fleming, Allan G. Blackman *

Department of Chemistry, Auckland University of Technology, Private Bag 92006, Auckland 1142, New Zealand

ARTICLE INFO

Keywords:
Quinoline
Multidentate
Transition metal
X-ray
Amine ligands

ABSTRACT

The literature pertaining to tri-, tetra-, penta-, and hexadentate amine ligands containing unsubstituted quinoline moieties is reviewed. The syntheses of these 46 ligands are detailed, and all X-ray structurally characterised transition metal complexes of these ligands are compiled and discussed. Comparisons to the analogous pyridine complexes, where they exist, are made. Most differences are found amongst the five-coordinate complexes, where the quinoline complexes mostly exhibit square pyramidal geometries, while the analogous pyridine complexes are predominantly trigonal bipyramidal. A structural feature we term the quinolyl split, where one or two quinolyl rings bisect an X-M-X angle, in contrast to their pyridine congeners, is identified.

1. Introduction

The recent synthesis and characterisation of the family of TEtra-Quinoline macrocycles (TEQs)[a] outlined in Fig. 1 serves as an elegant example of the use of the quinoline moiety in multidentate ligands. [1].

Quinoline was first isolated from coal tar by Runge in 1834 and shortly thereafter, in 1842, was obtained from destructive distillation of quinine, itself obtained from cinchona bark in 1820. [2] Although it is difficult to exactly pinpoint the earliest characterised transition metal complex of quinoline, research into the interactions of transition metals with quinoline was occurring around the turn of the 20th century, [3–5] while the earliest crystal structure of a transition metal complex of quinoline in the CSD dates from 1967. [6] Given the ubiquity of pyridine and its derivatives as ligands in transition metal complexes, it is therefore somewhat surprising that quinoline and quinoline-containing ligands have not been more widely used in coordination chemistry. The exception to this is the chelating ligand 8-hydroxyquinoline (also known as oxine), by far the most widely used of all quinoline-based ligands, with metal complexes of this, and its derivatives, finding use as antimicrobial, anti-metastatic, antiviral and antileukemia agents, [7–10] radiopharmaceuticals, [11] electroluminescent devices, [12] and in PET imaging, [13] amongst many other applications. Quinoline is attractive as a ligand both because as it can be viewed as a bulky substituted pyridine, and that the quinoline nucleus can be modified through reaction with electrophiles and nucleophiles more easily than is the case for pyridine. The p*K*a of the quinolinium ion (4.92) is close to that of the pyridinium ion (5.23), suggesting that the electronic properties of both molecules are similar and that differences in coordination properties may be predominantly attributable to steric effects. Interestingly, there are no examples of structurally characterised homoleptic four-, five- or six-coordinate quinoline complexes with which the corresponding homoleptic pyridine complexes can be compared in order to confirm this contention. The nearest example is *trans*-[Ni(quinoline)$_4$(NCS)$_2$], in which the Ni-N$_{quinoline}$ bonds are 0.03 – 0.13 Å longer than the Ni-N$_{pyridine}$ bonds in *trans*-[Ni(py)$_4$(NCS)$_2$], [14,15] consistent with the greater steric bulk of quinoline compared to that of pyridine. As is also found for pyridine, quinoline binds to transition metals almost exclusively as a monodentate ligand through the lone pair on the N atom; the lone structurally characterised exception appears to be [η^6-quinoline]Mo(PMe$_3$)$_3$, which exists in isomeric [η^6-(*C*$_6$)quinoline]Mo(PMe$_3$)$_3$ (**OHAPES**) and [η^6-(*C*$_5$*N*)-quinoline]Mo(PMe$_3$)$_3$ (**OHAPIW**) forms (Fig. 2). [16] The former was prepared from the reaction of [Mo(PMe$_3$)$_6$] with quinoline and this was converted to the latter by heating at 150 °C in cyclohexane for 3 days. The former was also shown to undergo hydrogenation of the pyridine ring and deligation of the resulting tetrahydroquinoline by heating at 80 °C in an H$_2$ atmosphere for 7 days.

* Corresponding author.
E-mail address: allan.blackman@aut.ac.nz (A.G. Blackman).

[a] Abbreviations: TEQ = TEtraQuinoline macrocycle, py = pyridine, dca = dicyanamide, DEAD = diethyl azodicarboxylate, NDSA = 1,5- naphthalenedisulfonate anion, tcc = tetrachlorocatechol dianion, dhbq = deprotonated 2,5-dihydroxy-1,4-benzoquinone, PET = photoinduced electron transfer, BP = tetradeprotonated 4,4′-bis(3-*tert*-butyl-1,2-catechol), DBcat = dianion of 3,5-di-*tert*-butylcatechol, CHEF = chelation enhanced fluorescence, DBSQ = 3,5-di-*tert*-butyl-1,2-semiquinone.

https://doi.org/10.1016/j.ccr.2023.215599
Received 18 October 2023; Accepted 27 November 2023
Available online 22 December 2023

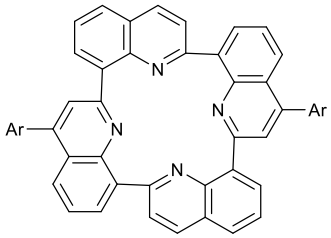

Fig. 1. General structure of a TEQ macrocycle.

The quinoline nucleus has been incorporated in a number of multidentate amine ligands, and these form the basis of this review. Herein we detail structurally characterised examples of transition metal complexes that incorporate multidentate amine ligands containing unsubstituted quinoline moieties. The discussion is limited to tri-, tetra-, penta-, and hexadentate amine ligands, and only those for which at least one structurally characterised transition metal complex is available. It should be noted that there are, somewhat surprisingly, no structurally characterised lanthanoid or actinoid complexes of the ligands reported herein. The structures of these complexes are compared to the analogous pyridine congeners where they exist, which are designated with an asterisk (in other words, **5*** is the pyridine congener of ligand **5**). All X-ray structures discussed are given the 6 letter CSD Refcode where available, and hydrogen atoms in the corresponding diagrams are omitted for clarity. While we have attempted to be comprehensive, we apologise in advance for any omissions. While this manuscript was in review, an article focusing on the applications of quinoline-based metal complexes was published. [17] The two are complementary, with the current paper being centred on synthesis and structure, while readers interested in applications are referred to the above reference.

2. Tridentate ligands

2.1. Tridentate ligands containing one quinolyl moiety

The structures of these ligands are outlined in Fig. 3.

2.1.1. N-(quinoline-2-ylmethyl)ethane-1,2-diamine (1) [18–22]

The reaction between quinoline-2-carbaldehyde and N-(2-aminoethyl)acetamide gives the corresponding imine, and borohydride reduction of this affords **1**. [19] This ligand can also be prepared by reacting 2-(chloromethyl)quinoline hydrochloride with ethylenediamine. [20].

The six-coordinate complex *fac*-[Tc(**1**)$(CO)_3$]Cl·H_2O (Fig. 4, **SINLIL**) [19] has technetium coordinated to three nitrogen atoms from the ligand in a *fac* configuration, and three CO ligands, resulting in a distorted octahedral geometry about the metal centre. The *cis* N-Tc-N bond angles range from 74.25° to 88.89°, *cis* N-Tc-O angles lie between 90.55° and 105.59°, and *cis* O-Tc-O angles are from 83.84° to 90.62°. The *trans* N-Tc-O angles are between 170.50° and 174.95°. The Tc-$N_{tertiary}$ bond lengths are 2.205 Å – 2.219 Å, the Tc-$N_{quinoline}$ bond lengths are 2.244 Å and 2.283 Å, and the Tc-C bond lengths range from 1.917 Å to 1.939 Å.

The corresponding pyridine complex, *fac*-[Tc(**1***)$(CO)_3$]Cl (**SINLOR**), [19] has been reported, and displays a very similar geometry to the quinoline-containing analogue.

2.1.2. N-methyl-N'-(2-quinolylmethyl)piperazine (2) [23]

Ligand **2** can be prepared from the reaction of N-methylpiperazine and 2-(chloromethyl)quinoline hydrochloride in the presence of anhydrous K_2CO_3. [23] Two copper complexes, monomeric [Cu(**2**)$(NCS)_2$] and polymeric {[Cu(**2**)$(\mu_{1,5}$-dca)]$ClO_4\}_n$, have been prepared and structurally characterised. The Cu(II) ion in [Cu(**2**)$(NCS)_2$] (Fig. 5, **REQHAY**) [23] is pentacoordinate, with the Cu(II) ion bound to two terminal thiocyanato ligands and the three nitrogen atoms of the ligand. The geometry about the metal centre can be described as a distorted tetragonal pyramid ($\tau_5 = 0.33$). The bond angles between the Cu(II) ion and the ligand (N-Cu-N) range from 73.09° to 154.84°, N-Cu-NCS angles from 93.26° to 135.14°, and the SCN-Cu-NCS angle is 105.24°. Cu-$N_{thiocyanato}$ bond lengths are 1.989 Å and 2.062 Å and the ligand Cu-N distances range between 2.022 Å and 2.066 Å. The Cu(II) ion sits 0.517 Å above the plane of the square base which is formed by the ligand nitrogen atoms and one of the thiocyanato N atoms. Polymeric {[Cu(**2**)$(\mu_{1,5}$-dca)]$ClO_4\}_n$ (**BOLSUT**) [23] comprises 1-D chains of [Cu(**2**)(dca)]$^+$ units bridged by dicyanamide ligands, with all Cu(II) ions being five-coordinate and displaying distorted geometries closer to square pyramidal than trigonal bipyramidal.

The corresponding pyridine ligand forms an analogous complex, [Cu(**2***)$(NCS)_2$] (**REQHEC**), [23] which displays a more square pyramidal geometry ($\tau_5 = 0.11$), with the Cu(II) ion sitting 0.421 Å above the square plane. The Cu-$N_{pyridine}$ and Cu-$N_{quinoline}$ bond lengths are identical. The major difference between the two structures is the orientation of the aromatic rings relative to the thiocyanato ligands. In [Cu(**2***)$(NCS)_2$], the pyridine ring lies nearly coplanar with a Cu-$N_{thiocyanate}$ bond while in [Cu(**2**)$(NCS)_2$], the phenyl ring of the quinoline moiety effectively bisects the $N_{thiocyanate}$-Cu-$N_{thiocyanate}$ bond, increasing it slightly compared to the pyridine congener (105.24° versus 102.87°, respectively); this arrangement avoids destabilising interactions between H-8 of the quinoline moiety and the thiocyanato ligands, and appears to be a common feature in five-coordinate complexes of tridentate quinoline-containing ligands. We term such behaviour the quinolyl split.

2.1.3. 1-(Quinol-2-ylmethyl)-1,4-diazacycloheptane (3) [24,25]

Palaniandavar and coworkers reported the synthesis of **3** from the reaction of 2-(chloromethyl)quinoline hydrochloride and homopiperazine in the presence of triethylamine.

The five-coordinate copper complex [Cu(**3**)Cl_2]·CH_3CN (Fig. 6, **LETMAZ**) [24] has $\tau_5 = 0.08$, consistent with a square pyramidal

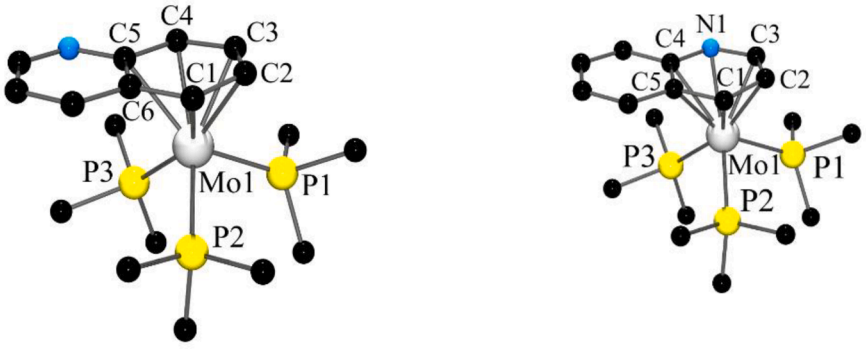

Fig. 2. Examples of π-bound quinoline. η^6-(C_6) (left) and η^6-(C_5N) (right) binding.

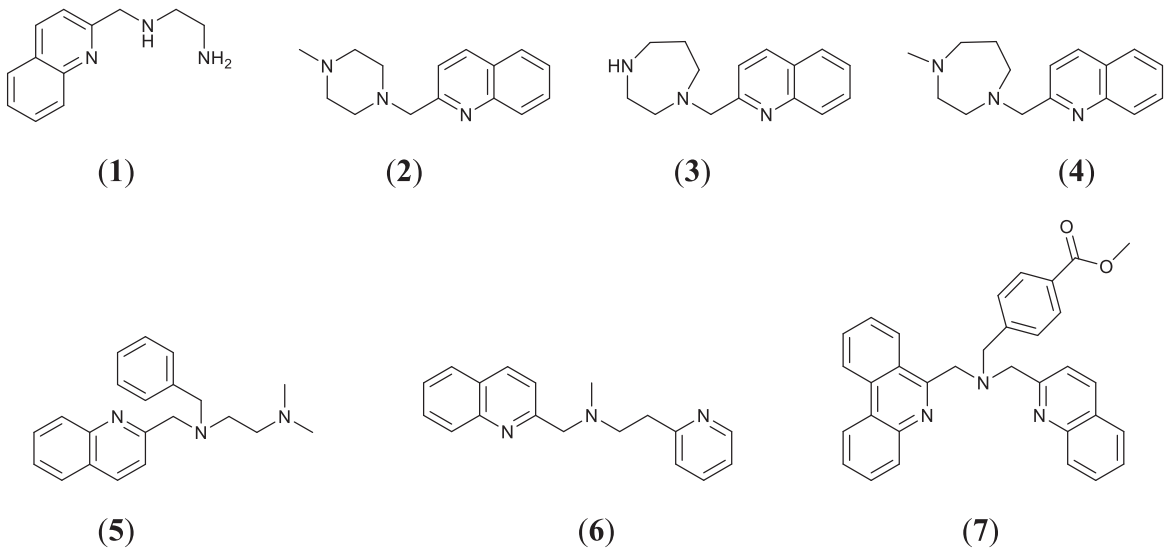

Fig. 3. Structures of the tridentate ligands containing one quinolyl moiety.

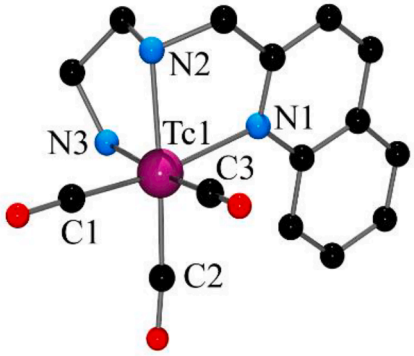

Fig. 4. Structure of the *fac*-[Tc(**1**)$(CO)_3]^+$ cation. Selected bond lengths (Å) and angles (°): Tc1-N1 2.283, Tc1-N2 2.205, Tc1-N3 2.209, Tc1-C1 1.917, Tc1-C2 1.939, Tc1-C3 1.931; N1-Tc1-N2 74.26, N1-Tc1-N3 88.89, N2-Tc1-N3 78.36, N1-Tc1-C2 105.59, N2-Tc1-C1 96.53, CC1-Tc1-C2 83.84, C1-Tc1-C3 88.20, N1-Tc1-C1 170.50, N2-Tc1-C2 172.78, N3-Tc1-C3 174.88.

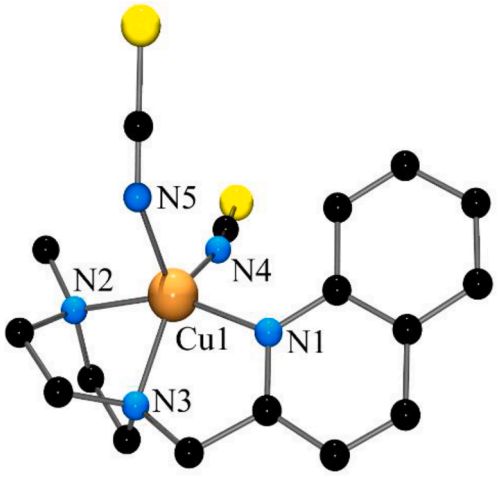

Fig. 5. Structure of the [Cu(**2**)$(NCS)_2$] complex. Selected bond lengths (Å) and angles (°): Cu1-N1 2.024, Cu1-N2 2.066, Cu1-N3 2.022, Cu1-N4 1.989, Cu1-N5 2.062; N1-Cu1-N2 154.84, N1-Cu1-N3 82.74, N2-Cu1-N3 73.09, N1-Cu1-N4 99.17, N2-Cu1-N5 95.13, N3-Cu1-N4 135.14, N3-Cu1-N5 118.18.

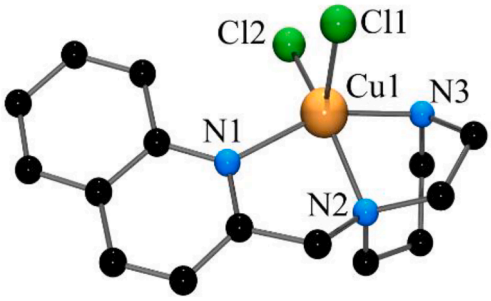

Fig. 6. Structure of the [Cu(**3**)Cl_2] complex. Selected bond lengths (Å) and angles (°): Cu1-N1 2.135, Cu1-N2 2.039, Cu1-N3 2.036, Cu1-Cl1 2.456, Cu1-Cl2 2.272; N1-Cu1-N2 81.19, N2-Cu1-N3 76.59, N1-Cu1-N3 154.90, N1-Cu1-Cl1 93.78, N1-Cu1-Cl2 103.67, N2-Cu1-Cl2, N2-Cu1-Cl2 90.23, N2-Cu1-Cl2 149.96.

geometry. The square planar base consists of the three ligand nitrogen atoms, with Cu-$N_{homopiperazine}$ bond lengths of 2.036 Å and 2.039 Å, and a Cu-$N_{quinoline}$ bond length of 2.135 Å. The fourth equatorial position is occupied by a chlorido ligand (Cu-Cl = 2.272 Å) while the remaining chlorido ligand is axial (Cu-Cl = 2.456 Å).

The pyridyl analogue of this ligand gives dimeric bis(μ-chlorido) [Cu(**3***)$Cl_2]_2(ClO_4)_2$ (**XIZSUU**) [26] on reaction with Cu^{2+}, presumably owing to its less sterically demanding nature.

2.1.4. 4-Methyl-1-(quinol-2-ylmethyl)-1,4-diazacycloheptane (4) [24,27,28]

Ligand **4** was prepared in a similar fashion to **3** (Section 2.1.3), from the reaction of 2-(chloromethyl)quinoline hydrochloride and *N*-methylhomopiperazine in the presence of triethylamine. The ligand was isolated as a yellow oil after a basic work-up of the crude material.

There are two independent molecules of the five-coordinate complex [Cu(**4**)Cl_2] (**LETMED**) [24] in the asymmetric unit. The Cu(II) ion in each of these is coordinated by three nitrogen atoms from the ligand and two chlorido ligands. The coordination geometry around the Cu(II) ion lies almost exactly between trigonal bipyramidal and square planar as revealed by the τ_5 values (0.48 and 0.45) and the authors described this geometry as trigonal–bipyramidal distorted square-based pyramidal. Therefore, the N-methyl substituent present in this ligand has a significant effect on the geometry of the resulting [Cu(**4**)Cl_2] complex, as the analogous complex containing the N-H version of the ligand (Section

2.1.3, **LETMAZ**) [24] has $\tau_5 = 0.08$. The N-Cu-N bond angles of both the molecules are 78.23, 78.24°, 83.05°, 83.35, 161.08 and 161.28°, the N-Cu-Cl angles range from 91.92° to 133.79°, and the Cl-Cu-Cl angles are 109.72 and 114.82°. The ligand binds to the metal centre with bond lengths ranging between 2.039 Å and 2.068 Å, and the Cu-Cl bond lengths are 2.304 Å, 2.318 Å, 2.430 Å and 2.462 Å[24].

The complex [Cu(**4**)((*p*-NO_2Ph)$_2PO_2)_2$]·H_2O (**IREFIV**) [27] was obtained as part of an investigation into the reaction of Cu(II) complexes with phosphate esters. **4** is coordinated to the Cu(II) ion via the three nitrogen atoms, and two monodentate bis(*p*-nitrophenyl)phosphate ligands give a five-coordinate complex. The τ_5 value (0.37) is indicative of a trigonal bipyramidal distorted square pyramid. As with other complexes of the same, or similar, ligands the square base is comprised of all three nitrogen atoms from the ligand and one of the phosphate ester oxygen atoms. The Cu-N bond lengths are 2.017 Å (quinoline), 2.011 Å and 2.021 Å, while Cu-O distances are 2.023 Å and 2.120 Å. The N-Cu-N bond angles are 79.47°, 84.01° and 163.38°, N-Cu-O angles are between 91.16° and 140.73°, and the O-Cu-O angle is 99.14°.

Again, replacement of the quinoline moiety of the ligand with a less sterically demanding pyridine unit results in formation of a dicopper complex; in this case the Cu^{2+} ions are bridged in a μ-1,3 fashion by two bis(*p*-nitrophenyl)phosphate ligands (**IREFER**). [24,27].

2.1.5. *N' -benzyl-N'-(quinol-2-ylmethyl)-N,N-dimethylethylenediamine (5)* [29]

This ligand was first prepared in 2011 [29] from reductive amination of quinoline-2-carbaldehyde with N'-ethyl-N,N-dimethylethylenediamine in dichloromethane using sodium triacetoxyborohydride as the reductant.

The complex [Cu(**5**)Cl_2] (Fig. 7, **ALISOE**) [29] is the only complex of this ligand to have been structurally characterised. The Cu(II) centre is coordinated to the three of the nitrogen atoms of the ligand and two chlorido ligands. The τ_5 value of 0.01 is consistent with the observed square pyramidal geometry, with the three nitrogen atoms from the ligand lying in the square plane. The Cu-Cl bond distances are 2.307 Å and 2.414 Å while the Cu-N bond lengths are 2.069 Å (quinoline), 2.069 Å, and 2.088 Å.

The complex [Cu(**5***)Cl_2].CH_3OH (**ALISEU**), [29] which contains the analogous pyridine ligand **5***, [30] is structurally very similar (τ_5 = 0.01).

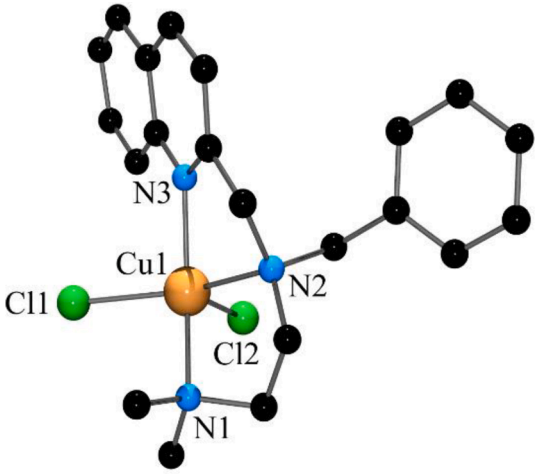

Fig. 7. Structure of the [Cu(**5**)Cl_2] complex. Selected bond lengths (Å) and angles (°): Cu1-N1 2.069, Cu1-N2 2.088, Cu1-N3 2.069, Cu1-Cl1 2.307, Cu1-Cl2 2.069; N1-Cu1-N2 83.89, N2-Cu1-N3 79.40, N1-Cu1-N3 153.58, N1-Cu1-Cl1 91.96, N1-Cu1-Cl2 99.46, N2-Cu1-Cl1 154.13, N2-Cu1-Cl2 102.92, N3-Cu1-Cl2 104.11, Cl1-Cu1-Cl2 102.94.

2.1.6. *2-(2-ethylpyridyl)-(2-methylquinolyl)-methylamine (6)* [31]

Ligand **6** was obtained as a viscous yellow oil from the reaction of 2-(2-methylaminoethyl)pyridine and 2-(chloromethyl)quinoline hydrochloride in the presence of Cs_2CO_3. It should be noted that the diagram of the ligand given in the original paper is in error, as it contains an isoquinoline, rather than a quinoline, unit. [31].

The dinuclear complex *mer*-[Cd_2(**6**)$_2$(μ-1,3-N_3)$_2$(N_3)$_2$] (Fig. 8, **HIKTAY**) [31] has been synthesised from the reaction between equimolar amounts of **6** and $Cd(NO_3)_2{\cdot}4H_2O$, and two equivalents of NaN_3 in methanol. The structure of this complex consists of two *mer*-[Cd(**6**)N_3]$^+$ units connected by two bridging azido ligands. The Cd(II) centres are octahedrally coordinated by the three nitrogen donor atoms of **6** in a *mer* configuration, the N atoms from two bridging azido ligands, and a terminal azido ligand (Cd-N = 2.276 Å). The Cd(II) ions are 5.975 Å apart and the Cd-N bond lengths involving the bridging azido ligands range from 2.296 Å to 2.568 Å. The Cd-N bond lengths involving **6** range from 2.306 Å to 2.46 Å. Bond angles involving the metal ions and the N atoms of **6** are 155.10° (*trans* N-Cd-N) and 71.11° and 84.27° (*cis* N-Cd-N), while those involving the bridging azido and terminal azido ligands are 171.68° and 172.95° (*trans* N/N_3-Cd-N_3) and 82.88° and 106.21° (*cis* N/N_3-Cd-N_3). Intermolecular π-π stacking interactions of adjacent aromatic rings of the **6** are observed, with separation of the pyridyl and quinolyl moieties ranging from 3.510 Å to 3.966 Å.

2.1.7. *4-[((6-phenanthridinylmethyl) (2-quinolinylmethyl)amino)methyl] benzoic acid methyl ester (7)* [32]

The ligand **7** was first prepared by Metzler-Nolte [32] and coworkers by refluxing 6-(chloromethyl)phenanthridine, 4-[((2-quinolinylmethyl) amino)methyl]benzoic acid methyl ester and K_2CO_3 for 24 h in acetonitrile. Following purification with silica gel column chromatography the ligand was obtained as a light yellow solid.

The only structurally characterised complex of this ligand is the distorted octahedral Re(I) tricarbonyl complex, *fac*-[Re(**7**)$(CO)_3$]Br. CH_3OH (Fig. 9, **IBOPIB**). [32] The ligand binds to the metal centre via three nitrogen donors and the other three positions are occupied by carbonyl ligands. *Trans* angles around the metal ion range from 171.66° to 173.16° and *cis* angles from 75.07° to 105.51°. Metal-ligand bond lengths are 2.230 Å (Re-$N_{quinoline}$), 2.239 Å (Re-$N_{phenanthridine}$), and

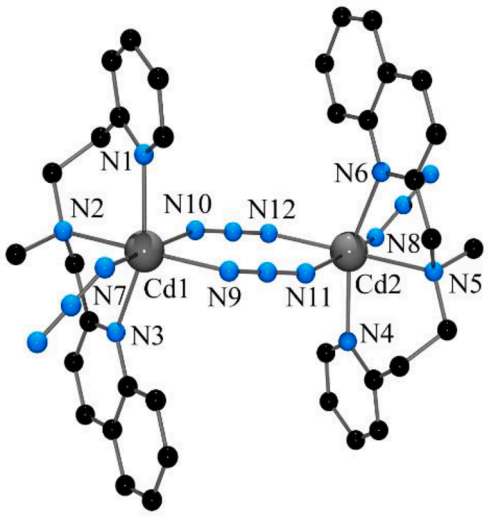

Fig. 8. Structure of the *mer*-[Cd_2(**6**)$_2$(μ-1,3-N_3)$_2$(N_3)$_2$] complex. Selected bond lengths (Å) and angles (°): Cd1-N1 2.306, Cd1-N2 2.465, Cd1-N3 2.333, Cd2-N4 2.306, Cd2-N5 2.465, Cd2-N6 2.333, Cd1-N7 2.276, Cd2-N8 2.276, Cd1-N9 2.296, Cd1-N10 2.568, Cd2-N11 2.568, Cd2-N12 2.296; N1-Cd1-N2 84.27, N2-Cd1-N3 71.11, N1-Cd1-N3 155.10, N1-Cd1-N7 88.98, N4-Cd1-N7 97.45, N1-Cd1-N10 89.10, N9-Cd1-N10 82.88, N4-Cd2-N3 84.27, N5-Cd2-N6 71.11, N4-Cd2-N6 155.10, N4-Cd2-N8 88.98, N5-Cd2-N8 97.09, N8-Cd2-N12 91.06, N6-Cd2-N11 87.73, N11-Cd2-N12 82.88.

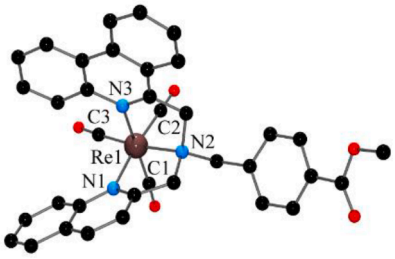

Fig. 9. Structure of the *fac*-[Re(**7**)$(CO)_3$] $^+$cation. Selected bond lengths (Å) and angles (°): Re1-N1 2.230, Re1-N2 2.230, Re1-N3 2.239, Re1-C1 1.924, Re1-C2 1.907, Re1-C3 1.916; N1-Re1-N2 79.02, N1-Re1-N3 80.52, N2-Re1-N3 75.07, N1-Re1-C1 105.51, N2-Re1-C2 98.58, N3-Re1-C1 100.85, N1-Re1-C3 172.10, N2-Re1-C1 173.50, N3-Re1-C2 171.21.

2.230 Å (Re-$N_{tertiary}$), with Re-C distances ranging from 1.907 Å to 1.924 Å.

The complex *fac*-[Re(**7***)$(CO)_3$]Br.CH_3OH (**IBOPAT**) [32] containing the analogous pyridine ligand exhibits a very similar geometry; the only difference of note is the slightly shorter Re-$N_{pyridine}$ bond distance (2.167 Å) in comparison to the Re-$N_{quinoline}$ bond length (2.230 Å).

2.2. Tridentate ligands containing two quinolyl moieties

The structures of these ligands are outlined in Fig. 10.

2.2.1. N-Benzyl-N,N-di(quinolin-2-ylmethyl)amine (8) [33–40]

The ligand **8**, first reported in 2005, [37] can be prepared from the reaction of 2-(chloromethyl)quinoline hydrochloride, benzylamine and Na_2CO_3. [34,37] Minor modifications to this method involve replacing Na_2CO_3 with aqueous NaOH [39], or K_2CO_3 [34,36]. The X-ray structure of the ligand (**XAWRIA**) [40] shows it to adopt a tripodal geometry.

Four-, five- and six-coordinate complexes of **8** have been reported, and structural data for the five and six coordinate complexes are summarised in Tables 1 and 2.

The four-coordinate Cu(I) complex [Cu(**8**)(CO)]ClO_4 (**GETFIV**) [33] displays a distorted tetrahedral geometry (τ_4 = 0.78) about the metal ion, with three nitrogen atoms from the ligand and one carbonyl ligand forming the primary coordination sphere. The bond angles range from 82.04° to 125.61°, the Cu-N bond lengths from 2.049 Å to 2.109 Å, and Cu-C is 1.797 Å for the carbonyl ligand. [33]. The complex of the analogous pyridine ligand (**GETDUF**) [33] displays a similar structure. Likewise, the dimeric bis(μ-hydroxo) cations $[Cu_2(\mu\text{-}OH)_2(\mathbf{8})_2]^{2+}$ (**GETGIW**) [33] and $[Cu_2(\mu\text{-}OH)_2(\mathbf{8}^*)_2]^{2+}$ (**PIVKOV**), [41] containing the quinolyl and pyridyl tridentate ligands, respectively, display very similar structures, with the Cu-Cu separation being only slightly greater in the quinoline complex (3.001 Å versus 2.922 Å). The phenyl rings in both cations exhibit intramolecular π-π interactions with the quinoline and pyridine rings (centroid–centroid distances < 3.9 Å).

The complex [Cu(**8***)Cl_2] (**EZERAE**) [42] adopts a slightly distorted square-pyramidal geometry (τ_5 = 0.11), while the quinolyl analogue (**WEFCOC**), [34] which has a much larger Cl-Cu-Cl bond angle (131.10° versus ~ 108°, Figs. 11 and 12), consequently has τ_5 = 0.54,. This is another example of the quinolyl split (Section 2.1.2), where the more sterically bulky quinoline moieties essentially bisect the Cl-Cu-Cl angle, whereas the two pyridine moieties are nearly coplanar with one of the Cu-Cl bonds in the former complex.

2.2.2. (1-Phenylethyl)bis(quinolin-2-ylmethyl)amine (9) [43]

Both enantiomers of **9** were synthesised from the reaction of either (+) or (-)-1-phenylethylamine with 2-(bromomethyl)quinoline in the presence of NaOH. [43].

[Cu(**9**)$(H_2O)_2$]$(ClO_4)_2$ (**OKIROP**) [43] is a pentacoordinate Cu(II) complex, with three donor N atoms from the ligand and O atoms from two aqua ligands. The Cu(II) exhibits a geometry almost exactly between square pyramidal and trigonal bipyramidal (τ_5 = 0.49). The N-Cu-N bond angles are 83.39°, 84.06° and 165.19°, while those for N-Cu-O range from 91.38° to 136.09° and the O-Cu-O angle is 111.58°. Cu-$N_{quinoline}$ bond lengths are 1.980 Å and 1.968 Å and the Cu-$N_{tertiary}$ distance is 2.056 Å. The Cu-O bond lengths are 2.062 Å and 2.170 Å.

The complex [Cu(**9**)$(CH_3CN)(ClO_4)$](ClO_4) (Fig. 13, **OKIRUV**) [43] comprises a Cu(II) metal centre bonded to the three N atoms of the ligand, an N atom from an acetonitrile ligand and an O atom from a perchlorato ligand. The geometry about the metal ion is similar to the complex above, with τ_5 = 0.48. The N-Cu-N bond angles are 83.72°, 84.00° and 165.17°, those for N-Cu-$N_{acetonitrile}$ are 95.49°, 97.95° and 121.07°, the N-Cu-O angles are 91.36°, 91.80° and 136.37°, and the O-Cu-$N_{acetonitrile}$ bond angle is 102.54°. Cu-N_{ligand} distances lie between 1.997 Å and 2.042 Å, Cu-$N_{acetonitrile}$ = 2.086 Å, and Cu-O = 2.164 Å.

Both of the above complexes manifest the quinolyl split, with the quinoline phenyl rings bisecting the angle between the ancillary ligands.

2.2.3. (1-(1-Naphthylethyl))bis(quinolin-2-ylmethyl)amine (10) [43–45]

Ligand **10** was originally prepared using the synthetic procedure reported by Zhang, [43] in which (*S*)-1-napthylethylamine is reacted with ethanolic 2-(bromomethyl)quinoline, with NaOH as the base. This ligand has also been prepared from the reaction of 2-(chloromethyl) quinoline hydrochloride and (*S*)-1-naphthylethylamine, in the presence of K_2CO_3 and KI. [44].

The zinc complex [Zn(**10**)$(ONO_2)_2$] (Fig. 14, **RUVDOD**) [44] is five-coordinate, with the three nitrogen donors from the ligand and two monodentate nitrato ligands bound to the Zn(II) metal centre, affording the complex a distorted trigonal bipyramidal geometry (τ_5 = 0.30). The N-Zn-N bond angles are 79.84°, 80.16°, and 158.22°, N-Zn-O angles range from 93.31° to 139.96°, and the O-Zn-O angle is 91.62°. Zn-N bond lengths lie between 2.115 Å and 2.198 Å, and the Zn-O bond lengths are 2.025 Å and 2.086 Å. The quinolyl split is again apparent.

2.2.4. (Bis(2-quinolylmethyl)aminomethyl)benzoic acid (11) [46]

The ligand **11** was obtained from base hydrolysis of (bis(2-quinolylmethyl)aminomethyl)benzoic acid methyl ester with aqueous NaOH. [46].

Fac-[Re(**11**)$(CO)_3$]Cl (Fig. 15, **UWOTAD**), [46] the only reported structurally characterised complex of **11**, contains a six-coordinate Re(I) ion in which the tridentate ligand **11** binds via all three available nitrogen donors in a *fac* configuration. The other three coordination sites are occupied by CO ligands and the complex displays a distorted octahedral geometry. The *cis* bond angles vary between 75.09° and 104.76°, and the *trans* angles are 171.64°, 171.91° and 173.78°. The Re-N bond lengths are between 2.221 Å and 2.238 Å, and the Re-C bonds range from 1.929 Å to 1.943 Å, similar to related complexes [47,48 46].

2.2.5. 1-{5-[(Bis(quinolin-2-ylmethyl)amino)methyl]-4-hydroxytetrahydrofuran-2-yl}-5-methyl-1H-pyrimidine-2,4-dione (12) [49]

The thymidine nucleoside-based tridentate ligand, **12**, is obtained from the reductive amination reaction of 1-(5-(Aminomethyl)-4-hydroxytetrahydrofuran-2-yl)-5-methyl-1*H*-pyrimidine-2,4-dione and quinoline-2-carbaldehyde in 1,2-dichloroethane in the presence of $NaBH(OAc)_3$.

The six-coordinate complex *fac*-[Re(**12**)$(CO)_3$]Br·0.5$NaPF_6$ (**KAMJOY**) [49] was obtained from the reaction of **12** and [NEt_4][Re$(CO)_3Br_3$]. The Re-$N_{quinoline}$ bond lengths (2.236 Å and 2.211 Å) are both similar to the Re-$N_{tertiary}$ distance (2.233 Å), and the Re-C bond lengths range from 1.868 Å to 1.919 Å, consistent with those in other similar complexes [50–52]. Bond angles between 172.45° and 174.45° (*trans* N-Re-C), 73.92° and 89.50° (*cis* N-Re-N), 87.80° and 104.27° (*cis* N-Re-C), and 83.04° and 89.46° (*cis* C-Re-C) are consistent with a distorted octahedral geometry.

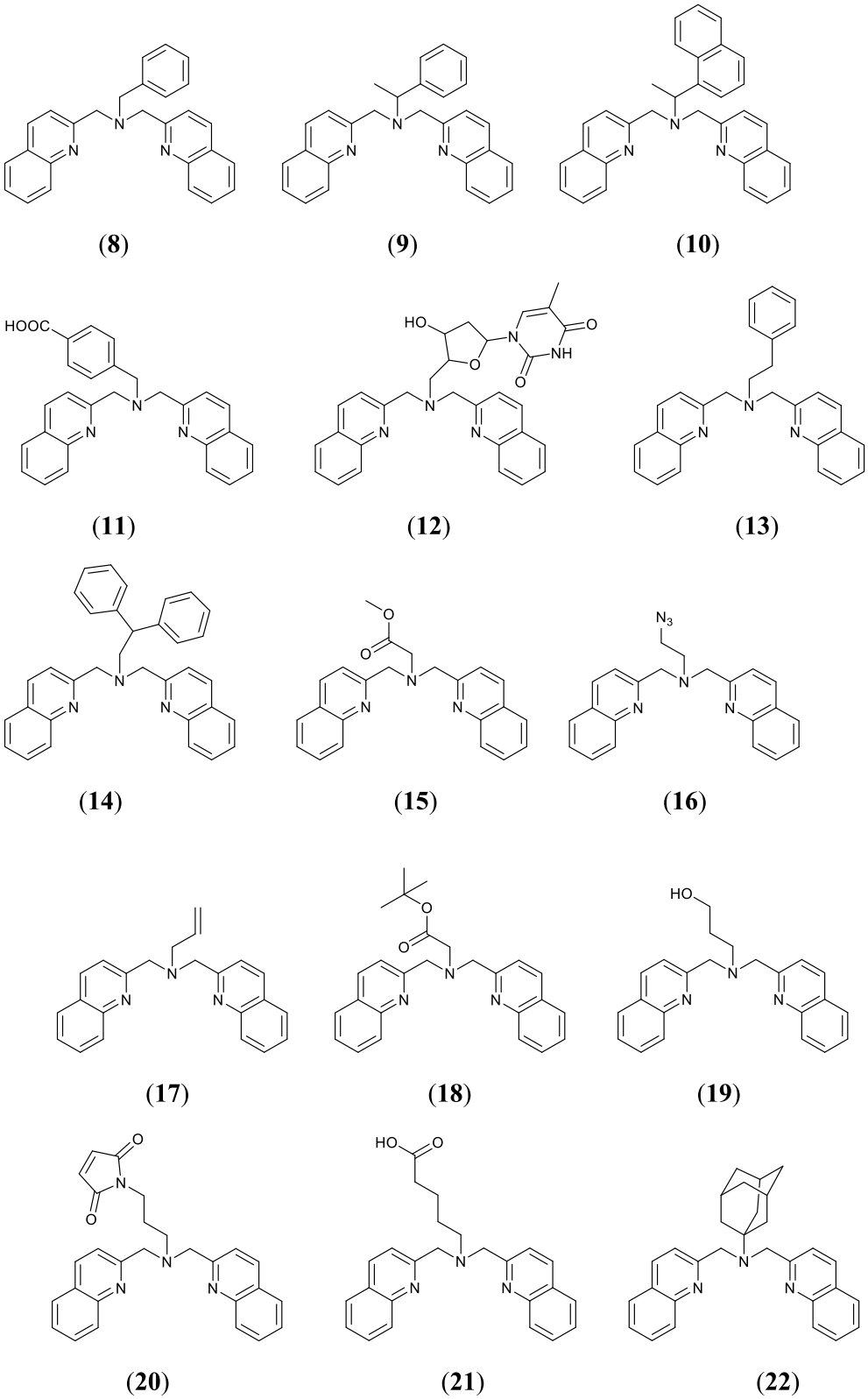

Fig. 10. Structures of the tridentate ligands containing two quinolyl moieties.

2.2.6. N,N-Bis(2-quinolylmethyl)-2-phenylethylamine (13) [33,53]

The ligand **13** was prepared from the reductive amination of 2-phenylethylamine with quinoline-2-carbaldehyde in acetic acid / methanol, with $NaBH_3CN$ as the reductant. [53].

Of the five structurally characterised complexes containing this ligand, monomeric [Cu(**13**)]ClO_4 (Fig. 16, **GETFOB**) [33] is the most interesting. The Cu(I) ion is four-coordinate, with the metal binding to the three N atoms of the ligand, and a C atom of the phenyl ring (τ_4 = 0.75). The geometry of this latter binding is quite remarkable; as can be seen in Fig. 16, a C atom of the phenyl ring lies 2.217 Å from the Cu(I) ion, displaying a κC-binding mode for what was described as a d-π interaction. The complex cation N-Cu-N bond angles are 82.78°, 83.91°

Table 1
Five-coordinate complexes of **8**.

Complex	N-M-N/°	N-M-X /°	X-M-X /°	M-$N_{quinoline}$/Å	M-$N_{tertiary}$/Å	M-X/Å	τ_5	ref
[Cu(**8**)(η^2-SO_4)] (**FONQEG**)	79.26 85.54 103.62	93.66 104.17 162.60 165.08	71.49	2.040 2.249	2.015	1.978 2.007	0.04	[36]
[Cu_2(μ-OH)$_2$(**8**)$_2$](ClO_4)$_2$ (**GETGIW**)	75.20 83.78 107.73	89.48 95.33 98.01 103.92 161.81 171.15	78.75	2.027 2.370	3.035	1.928 1.956	0.19	[33]
[Cu(**8**)(H_2O)$_2$](ClO_4)$_2$ (**RUBPUB**)	82.39 83.22 165.61 83.01 83.11 166.08 83.04 83.22 166.04	90.69 91.20 94.12 108.88 141.96 91.69 92.04 93.43 97.50 109.00 135.57 91.72 92.73 94.02 96.31 108.96 135.16	108.97 115.35 115.84	1.995 1.995 1.984 1.985 1.982 1.986	2.049 2.056 2.062	2.194 2.163 2.030 2.156	0.51, 0.39, 0.51	[35]
[Cu(**8**)Cl_2]·2CH_3CH_2OH (**WEFCOC**)	81.62 82.20 163.38	92.41 93.58 93.73 93.98 105.68 123.21	131.10	1.988 1.994	2.137	2.328 2.427	0.54	[34]

Table 2
Six-coordinate complexes of **8**.

Complex cation	*Trans* N-M-N/°	*Trans* X-M-N/°	*Trans* X-M-X /°	*Cis* N-M-N/°	*Cis* X-M-N/°	*Cis* X-M-X /°	M-$N_{quinoline}$/Å	M-$N_{aliphatic}$/Å	M-X/Å	Ref
mer-[Fe_2(μ-OH)$_2$(**8**)$_2$(CH_3CN)$_2$](ClO_4)$_2$ (**FEXYUD**)	148.45	171.25	167.50	74.14 74.68	87.11 90.45 91.96 93.91 95.28 100.50 104.18 107.37	79.46 88.05	2.252 2.255	2.254	1.985 2.090 (H_2O) 2.290 (MeCN)	[37]
fac-[Ni(**8**)(η^1-SO_4)(H_2O)$_2$]		169.17 169.73 173.27		78.27 82.05 95.18	86.06 87.69 88.16 93.78 96.46 105.36	85.25 89.58 90.96	2.103 2.120	2.115	2.060 2.066 (H_2O) 2.108 (SO_4)	[36]

[1] The complex [Cu(**8**)(H_2O)$_2$](ClO_4)$_2$ crystallises with three independent moieties in the asymmetric unit.

and 127.57°, and the N-Cu-C angles are 99.64°, 106.76° and 125.43°. The Cu-$N_{quinoline}$ bond lengths are 1.982 Å and 1.989 Å and the Cu-N_{amine} bond length is 2.212 Å.

The Cu(I) complexes [Cu(**13**)NCMe](ClO_4) (**GETFUH**) [33] and [Cu(**13**)CO]ClO_4 (**GETGAO**) [33] have also been structurally characterised and a summary of their bond lengths and angles is given in Table 3.

The asymmetric dimeric Cu(II) complex, [(**13**-O)(**13**)Cu_2.(μ-OH)](ClO_4)$_2$ (**GETGOC**), [33] was obtained from the reaction of [Cu(**13**)]ClO_4 with O_2. Oxygenation of one **13** ligand occurs concomitant with metal oxidation, and the structure consists of two Cu(II) cations each bound by all available nitrogen atoms of the **13** and **13**-O ligands and bridged by a hydroxido ligand and the incorporated oxygen atom. τ_5 values (0.12 and 0.27) for the Cu(II) centres are consistent with distorted square pyramidal coordination geometries. The complex displays N-Cu-N bond angles between 80.46° and 102.12°, N-Cu-O_{oxygen} 85.66°–146.17°, N-Cu-$O_{hydroxido}$ 90.91° – 174.18°, and O_{oxygen}-Cu-$O_{hydroxido}$ angles of 78.48° and 79.48°. The ligand nitrogen atoms are bound to the Cu(II) centres at distances ranging between 2.003 Å and 2.262 Å. Cu-O_{oxygen} and Cu-$O_{hydroxido}$ bond lengths are 1.931/1.942 Å and 1.900/1.930 Å, respectively[33].

[Cu(**13**)(CH_3CN)(ClO_4)](ClO_4).CH_3COCH_3 (**RAYRAL**) [53] has two crystallographically independent 5-coordinate cations within its unit cell, with each comprising a Cu^{2+} ion bound to a **13** ligand, a CH_3CN ligand and a ClO_4^- ligand. Both Cu(II) centres display a distorted square pyramidal geometry (τ_5 = 0.16 and 0.20) and display the quinolyl split. The two cations have N-Cu-N bond angles between 81.19° and 164.50°, N-Cu-X angles ranging from 87.21° – 152.71°, and X-Cu-X of 104.73° and 101.87° (X = acetonitrile or acetone). Cu-$N_{quinoline}$ bond distances

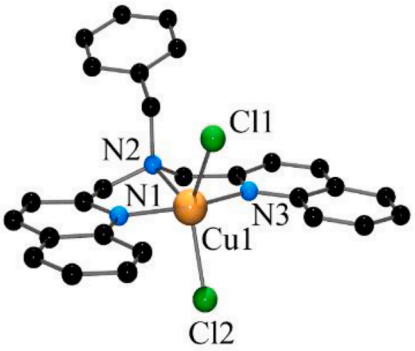

Fig. 11. Structure of the [Cu(**8**)Cl_2] complex. Selected bond lengths (Å) and angles (°): Cu1-N1 1.988, Cu1-N2 2.137, Cu1-N3 1.994, Cu1-Cl1 2.427, Cu1-Cl2 2.328; N1-Cu1-N2 82.10, N1-Cu1-N3 163.38, N2-Cu1-N3 81.62, N1-Cu1-Cl1 93.58, N1-Cu1-Cl2 93.73, N2-Cu1-Cl1 105.68, N2-Cu1-Cl2 123.21, N3-Cu1-Cl1 93.98, N3-Cu1-Cl2 92.41, Cl1-Cu1-Cl2 131.10.

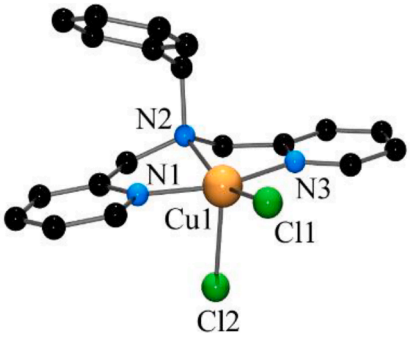

Fig. 12. Structure of the [Cu(**8***)Cl_2] complex. Selected bond lengths (Å) and angles (°): Cu1-N1 2.018, Cu1-N2 2.069, Cu1-N3 1.999, Cu1-Cl1 2.256, Cu1-Cl2 2.471; N1-Cu1-N2 80.98, N1-Cu1-N3 160.88, N2-Cu1-N3 80.67, N1-Cu1-Cl1 97.06, N1-Cu1-Cl2 93.12, N2-Cu1-Cl1 154.21, N2-Cu1-Cl2 98.08, N3-Cu1-Cl1 97.12, N3-Cu1-Cl2 94.86, Cl1-Cu1-Cl2 107.71.

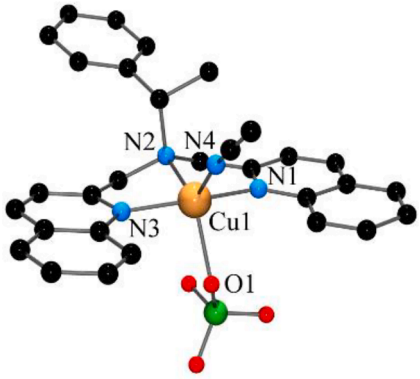

Fig. 13. Structure of the [Cu(**9**)(CH_3CN)(ClO_4)]$^+$ cation. Selected bond lengths (Å) and angles (°): Cu1-N1 1.997, Cu1-N2 2.042, Cu1-N3 2.020, Cu1-N4 2.086, Cu1-O1 2.164; N1-Cu1-N2 84.00, N1-Cu1-N3 165.17, N2-Cu1-N3 83.72, N1-Cu1-N4 97.95, N2-Cu1-N4 121.07, N3-Cu1-N4 95.49, N1-Cu1-O1 91.80, N2-Cu1-O1 136.37, N3-Cu1-O1 91.36, N4-Cu1-O1 102.54.

range between 1.957 Å and 2.035 Å and the Cu-$N_{tertiary}$ bond lengths are 2.026 Å and 2.031 Å.

The pyridine analogue of **13** is found in the complex [Cu(**13***)]ClO_4 (**ENETOG**), [54] which displays the same unusual coordination of the phenyl ring and a similar geometry as found in the quinoline complex above (τ_4 = 0.79 and 0.88). The Cu-C bond length, however, is notably shorter in the pyridine complex (2.163 Å versus 2.217 Å).

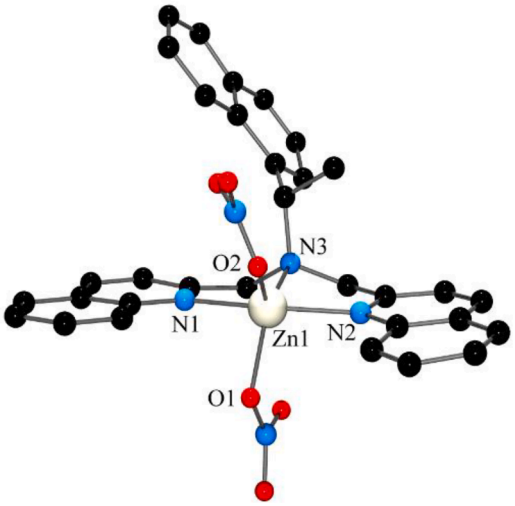

Fig. 14. Structure of the [Zn(**10**)(NO_3)$_2$] complex. Selected bond lengths (Å) and angles (°): Zn1-N1 2.126, Zn1-N2 2.115, Zn1-N3 2.198, Zn1-O1 2.086, Zn1-O2 2.025; N1-Zn1-N2 158.22, N1-Zn1-N3 79.84, N2-Zn1-N3 80.16, N1-Zn1-O1 93.31, N2-Zn1-O1 96.46, N3-Zn1-O1 139.96, N1-Zn1-O2 104.57, N2-Zn1-O2 94.58, N3-Zn1-O2 128.36, O1-Zn1-O2 91.62.

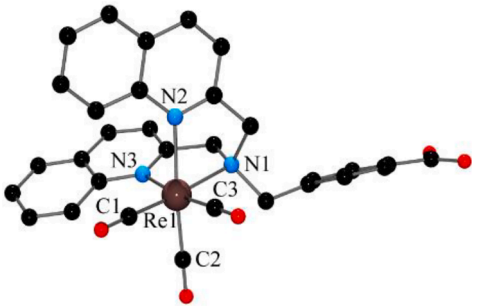

Fig. 15. Structure of the *fac*-[Re(**11**)$(CO)_3$]$^+$cation. Selected bond lengths (Å) and angles (°): Re1-N1 2.238, Re1-N2 2.227, Re1-N3 2.221, Re10C1 1.929, Re1-C2 1.943, Re1-C3 1.930; N1-Re1-N2 75.09, N1-Re1-N3 78.09, N2-Re1-N3 83.52, N2-Re1-C1 99.60, N3-Re1-C1 104.78, C1-Re1-C2 88.14, C1-Re1-C3 82.98, N1-Re1-C1 173.78, N2-Re1-C2 171.91, N3-Re1-C3 171.64.

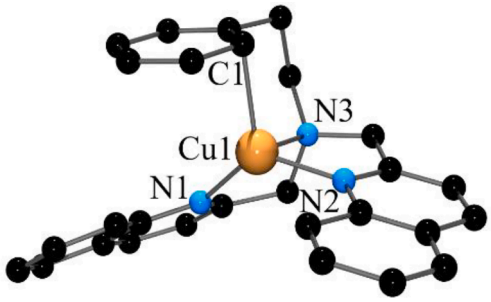

Fig. 16. Structure of the [Cu(**13**)]$^+$ cation. Selected bond lengths (Å) and angles (°): Cu1-N1 1.982, Cu1-N2 1.989, Cu1-N3 2.212, Cu1-C1 2.217; N1-Cu1-N2 127.57, N1-Cu1-N3 83.91, N2-Cu1-N3 82.78, N1-Cu1-C1 125.43, N2-Cu1-C1 106.76, N3-Cu1-C1 99.64.

2.2.7. N,N-Bis(2-quinolylmethyl)-2,2-diphenylethylamine (14) [33,53]

This ligand was prepared in a similar fashion to **13**, from the reductive amination of quinoline-2-carbaldehyde with 2,2-diphenylethylamine in a solution of acetic acid and methanol, with reduction

Table 3
Four-coordinate complexes of **13.**

Complex	N-M-N/°	N-M-X /°	M-$N_{quinoline}$/Å	M-$N_{tertiary}$/Å	M-X/Å	τ_4	ref
[Cu(**13**)(CH_3CN)]ClO_4 (L.CH_3CN)	80.56	117.91	2.025	2.196	1.876	0.77	[33]
	81.98	120.38	2.056				
	107.20	131.75					
[Cu(**13**)(CO)]ClO_4	80.89	123.32	2.030	2.155	1.795	0.76	[33]
	83.00	124.21	2.050				
	100.38	129.31					

effected by $NaBH_3CN$. [53].

The four-coordinate complex [Cu(**14**)]ClO_4 (Fig. 17, **GETGES**) [33] has a similar unusual structure to the analogous complex in Section 2.2.6 above, with the primary coordination sphere comprising three N donors from the ligand and a phenyl C atom 2.175 Å from the metal ion. The Cu-$N_{quinoline}$ bond lengths are 1.995 Å and 2.032 Å and the Cu-$N_{tertiary}$ bond length is 2.214 Å. N-Cu-N bond angles involving only the tridentate ligand are 81.46°, 83.58°, and 124.87°.

The Cu(II) complex [Cu(**14**)(CH_3COCH_3)(ClO_4)][Cu(**14**)(OH_2)(CH_3COCH_3)](ClO_4)$_3$ (**RAYREP**), (incorrectly described as [Cu(**14**)(CH_3COCH_3)(ClO_4)](ClO_4) in the original publication) [53] consists of two separate five-coordinate Cu(II) cations, each bonded to a tridentate **14** ligand and a monodentate acetone ligand, with 5-coordination completed by a monodentate perchlorate ligand on one and a monodentate water ligand on the other. The overall coordination geometry of the Cu(II) centres is distorted square pyramidal (τ_5 = 0.15 and 0.16), with a quinolyl split. N-Cu-N bond angles range from 82.27° to 166.05°, N-Cu-X angles are between 88.12° and 157.04°, and the X-Cu-X angles are 96.95° and 98.98° (X = acetone or water). The Cu-$N_{quinoline}$ bond lengths range from 1.984 Å to 2.037 Å, and the Cu-$N_{tertiary}$ bond lengths are 2.042 Å and 2.048 Å.

2.2.8. *[Bis(quinolin-2-ylmethyl)amino]acetic acid methyl ester (15) [44,55,56]*

Ligand **15** was prepared from the reaction of aminoacetic acid methyl ester hydrochloride and quinoline-2-carbaldehyde in 1,2-dichloroethane, with reduction of the initially formed imine effected by NaBH$(OAc)_3$ [55]. An alternative procedure utilises the reaction between 2-(chloromethyl)quinoline hydrochloride and the methyl ester in the presence of K_2CO_3 and KI in acetonitrile[44].

In the distorted octahedral complex *fac*-[Re(**15**)$(CO)_3$]Br (**KEJLER**), [55] **15** binds in a tridentate *fac* fashion. The *cis* quinoline moieties of the ligand form a cleft, with the shortest centroid–centroid distance being 3.695 Å. As a result, both quinoline N atoms display significantly 'bent' geometries, with angles of ~ 158° between the Re-N vector and the plane of the pyridine ring. The *trans* X-Re-X bond angles lie between 169.55° and 178.46°, and the *cis* range from 77.72° – 103.45°. The Re-$N_{quinoline}$ bond lengths are 2.217 Å and 2.231 Å, Re-$N_{tertiary}$ is 2.237 Å, and the Re-C bond lengths are between 1.903 Å and 1.918 Å.

The five-coordinate complex [Zn(**15**)$(ONO_2)_2$] (Fig. 18, **RUVDET**) [44] features **15** as a tridentate ligand and two monodentate nitrato ligands occupying the other coordination sites, to give a distorted trigonal bipyramidal geometry (τ_5 = 0.30) with the quinoline moieties situated mutually *trans*. The N-Zn-N bond angles are 78.48°, 79.83°, and 157.16°. The N-Zn-O angles range between 89.25° and 139.21°, and the O-Zn-O bond has an angle of 126.83°. The Zn-N bond lengths are between 2.139 Å and 2.179 Å, and the Zn-O bond lengths are 2.045 Å and 2.225 Å[44].

The pyridyl congener of [Zn(**15**)$(ONO_2)_2$], [Zn(**15***)$(ONO_2)_2$] (**RUVDAP**) [44], has also been structurally characterised. This displays an outwardly similar structure to the quinolyl analogue, with τ_5 = 0.24. However, the Zn-$N_{pyridine}$ bond lengths (2.059 Å and 2.068 Å) are considerably shorter than the Zn-$N_{quinoline}$ bonds, as expected from the reduced steric bulk. In addition, the O-Zn-O bond angle, which involves both monodentate nitrato ligands, is much larger in the quinoline complex (126.83°) than in the pyridine complex (82.05°), owing to the greater steric bulk of the tridentate ligand in the former. This is yet another manifestation of the quinolyl split.

2.2.9. *2-azido-N,N-bis((quinolin-2-yl)methyl)ethanamine (16) [57,58]*

Ligand **16** was isolated as a pale yellow solid from the reaction of 2-(bis((quinoline-2-yl)methyl)amino)ethanol [59], triphenyl phosphine, diisopropylazodicarboxylate and diphenylphosphoryl azide in THF[57]. The X-ray structure of the ligand (**KIZTOE**) [58] shows a tripodal, rather than splayed, conformation of the three arms.

The rhenium tricarbonyl complex *fac*-[Re(**16**)$(CO)_3$]Br (Fig. 19, **WAMWUE**), [57] has a distorted octahedral geometry around the metal centre which is coordinated to the quinolyl and tertiary N atoms of the ligand and three CO ligands. The Re-N bond distances are 2.212 Å, 2.220 Å, and 2.226 Å, while the Re-C lengths are 1.905 Å, 1.936 Å, and

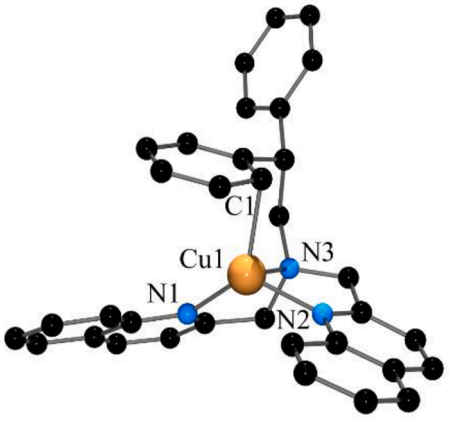

Fig. 17. Structure of the [Cu(**14**)]$^+$cation. Selected bond lengths (Å) and angles (°): Cu1-N1 1.995, Cu1-N2 2.032, Cu1-N3 2.214, Cu1-C1 2.175; N1-Cu1-N2 124.87, N1-Cu1-N3 83.58, N2-Cu1-N3 81.46, N1-Cu1-C1 131.75, N2-Cu1-C1 102.06, N3-Cu1-C1 93.90.

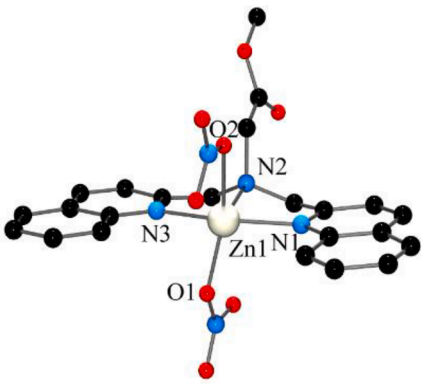

Fig. 18. Structure of the [Zn(**15**)$(NO_3)_2$] complex. Selected bond lengths (Å) and angles (°): Zn1-N1 2.153, Zn1-N2 2.139, Zn1-N3 2.179, Zn1-O1 2.045, Zn1-O2 2.225; N1-Zn1-N2 157.16, N1-Zn1-N3 78.48, N2-Zn1-N3 79.83, N1-Zn1-O1 84.17, N2-Zn1-O1 97.58, N3-Zn1-O1 139.21, N1-Zn1-O2 99.27, N2-Zn1-O2 89.25, N3-Zn1-O2 93.94, O1-Zn1-O2 126.83.

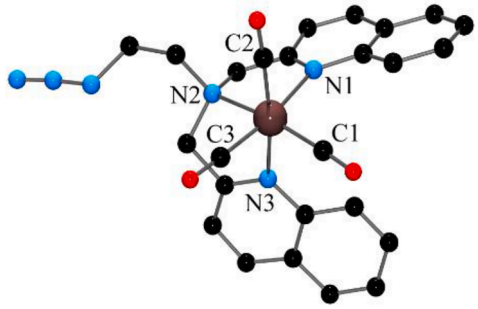

Fig. 19. Structure of the *fac*-[Re(**16**)$(CO)_3]^+$cation. Selected bond lengths (Å) and angles (°): Re1-N1 2.226, Re1-N2 2.220, Re10N3 2.212, Re10C1 1.936, Re1-C2 1.905, Re1-C3 1.939; N1-Re1-N2 78.33, N1-Re1-N3 86.34, N2-Re1-N3 73.22, N1-Re1-C1 103.42, N2-Re1-C2 97.89, N3-Re1-C1 99.00, N1-Re1-C3 170.50, N2-Re1-C1 171.99, N3-Re1-C2 171.09.

1.939 Å. Intercation π-π interactions between quinolyl rings are present, with centroid–centroid distances of 3.646 Å, and there are no close contacts involving the azide group. The complex cation has *cis* X-Re-X angles that vary from 73.22° to 103.42°, and *trans* angles from 170.50° to 171.09°.

2.2.10. 3-[Bis(2-quinolinylmethyl)amino]-prop-1-ene (17) [60–62]

A detailed synthesis of ligand **17** has not been reported, but a reaction scheme in the original paper depicts the reaction of 2-quinolinecarboxaldehde and allylamine in 1,2-dichloroethane and the addition of $NaBH(OAc)_3$ as the reducing agent. [62].

The complex *fac*-[Re(**17**)$(CO)_3](PF_6)$ (**WOXMEE**) [62] exhibits a distorted octahedral geometry, with the Re(I) metal centre bound to the three ligand nitrogen atoms and three CO ligands. The two independent cations in the unit cell have *cis* X-Re-X angles ranging from 81.94° to 104.90°, and *trans* angles lying between 171.69° and 175.10°. Re-$N_{quinoline}$ bond lengths are between 2.206 Å and 2.217 Å, Re-$N_{tertiary}$ distances are 2.200 Å and 2.222 Å, and Re-C bond lengths vary from 1.900 to 1.925 Å.

The pyridine version of **17** is known, and the analogous complex of this, *fac*-[Re(**17***)$(CO)_3](SO_3CF_3)$ (**QEZZIG**) [63], exhibits a very similar structure.

2.2.11. [Bis(quinolin-2-ylmethyl)amino]acetic acid methyl ester (18) [55,56,62]

Ligand **18** was prepared from the reaction of quinoline-2-carbaldehyde and aminoacetic acid methyl ester hydrochloride in 1,2-dichloroethane and subsequent reduction of the imine with $NaBH(OAc)_3$. [55].

The complex *fac*-[Re(**18**)$(CO)_3](PF_6)$.THF (**WOXMOO**) [62] has the six-coordinate Re ion bonded to the three N atoms from the ligand and three carbon atoms from the carbonyl ligands, affording a distorted octahedral geometry at the metal centre with a *fac* configuration of the ligand. *Cis* N-Re-N bond angles are 73.64°, 78.73°, and 86.17°, *cis* N-Re-C angles vary between 89.02° and 103.75°, and C-Re-C angles are 84.07°, 88.70°, and 88.93°. Re-C bond lengths are 1.916 Å, 1.918 Å, and 1.927 Å, Re-$N_{quinoline}$ bond lengths are 2.216 Å and 2.221 Å, and the Re-$N_{tertiary}$ bond length is 2.230 Å.

2.2.12. 3-[Bis(2-quinolinylmethyl)amino]propan-1-ol (19) [62]

This was obtained from the reaction of quinoline-2-carbaldehyde and 3-aminopropanol in the presence of $NaBH(OAc)_3$ in 1,2-dichloroethane. [62] *Fac*-[Re(**19**)$(CO)_3](PF_6)$ (**WOXMUU**) [62] has the Re(I) ion in a distorted octahedral coordination environment, coordinated to both the quinoline nitrogen atoms (Re-N = 2.216 Å and 2.239 Å) and the tertiary amine (Re-N = 2.228 Å), with the three other sites occupied by CO ligands (Re-C bond lengths lie in the range 1.909 Å – 1.920 Å). The –OH group is not involved in any interactions with the metal ion. *Cis* N-Re-N bond angles are 77.15°, 78.61°, and 80.90°, *cis* N-Re-C angles vary between 92.74° – 103.10°, and the *cis* C-Re-C angles are 83.09°, 84.94°, and 90.82°. The *trans* N-Re-C bond angles are 170.66°, 173.10°, and 178.29°.

2.2.13. 1-[3-[bis(quinolin-2-ylmethyl)amino]propyl]pyrrole-2,5-dione (20) [64,65]

Ligand **20** was obtained from the reaction of bis(quinolylmethyl) aminopropanol and maleimide in THF, in the presence of PPh_3 and DEAD. [64] The Re(I) complex *fac*-[Re(**20**)$(CO)_3$]Br (**MAKZAA**) [65] has the ligand binding to the metal ion in a tridentate fashion through coordination to the two nitrogen donors of the quinoline moieties and the tertiary amine of the ligand. The *trans* N-Re-C bond angles are 170.65°, 171.18° and 176.54°, the *cis* N-Re-N angles are 75.68°, 78.44° and 80.83°, the N-Re-CO angles lie between 92.11° and 103.54°, and the *cis* C-Re-C angles are 83.82°, 87.05° and 87.90°, all indicative of a distorted octahedral geometry. The Re-$N_{quinoline}$ bond distances are 2.220 Å and 2.227 Å, the Re-N_{amine} bond length is 2.217 Å, and the three Re-C bonds are between 1.911 Å and 1.929 Å.

2.2.14. 5-(Bis(quinolin-2-ylmethyl)amino)pentanoic acid (21) [47,49,66,67]

Ligand **21** was synthesised by a reductive amination reaction involving quinoline-2-carbaldehyde, 5-aminopentanoic acid and $NaBH(OAc)_3$. [47,49,66] The X-ray structure of the ligand (**XEGMEC**) shows it to adopt a tripodal conformation, [47] similar to that of ligand **16** in section 2.2.9, with the carboxylic acid proton hydrogen-bonded to a quinoline N atom of a neighbouring molecule ($d_{O\text{-}N}$ = 2.701 Å).

Fac-[Re(**21**)$(CO)_3$]Br (**XEGMIG**) [47] is a six-coordinate Re(I) complex with the N_3C_3 donor set derived from one tertiary amine, two quinoline nitrogen atoms, and three carbonyl C atoms. The Re(I) centre displays a distorted octahedral geometry. *Cis* N-Re-N angles are 77.67°, 78.08°, and 78.34°, *cis* N-Re-C angles range from 93.78° to 102.87°, and *cis* C-Re-C angles are 82.37°, 86.13°, and 88.38°. The *trans* bond angles are 170.38°, 173.69°, and 179.05°. Re-C bond distances are between 1.901 Å and 1.923 Å, the Re-$N_{quinoline}$ bond lengths are 2.233 Å and 2.235 Å, and the Re-$N_{tertiary}$ distance is 2.222 Å[47].

The pyridine analogue of *fac*-[Re(**21**)$(CO)_3$]Br (**BETDIO**) [68] displays a very similar structure, with the Re-$N_{pyridine}$ bond lengths shorter than the Re-$N_{quinoline}$ distances, due to the decrease in steric bulk. [68].

2.2.15. N,N′-bis(2-quinolinylmethyl)amantadine (22) [69–72]

The reaction between 1-adamantanamine hydrochloride and 2-(chloromethyl)quinoline hydrochloride in the presence of Na_2CO_3 gives the ligand **22**, [69,70] the X-ray structure of which has been determined (**XOTNAX**). [69].

Structural data for the five complexes of **22**, all of which are five-coordinate, are summarised in Table 4.

The complex [Cu(**22**)$(H_2O)(ClO_4)](ClO_4)\cdot 2H_2O$ (**SUDTAO**) [70] was originally characterised as four-coordinate, with a distorted planar arrangement of the three nitrogen donor atoms from the ligand and one oxygen from a water ligand. It is perhaps better described as five-coordinate, with a perchlorate oxygen atom occupying the fifth coordination site; the Cu-$O_{perchlorate}$ bond length of 2.406 Å is consistent with literature values. [73–79].

The complexes [Cu(**22***)Cl_2] (**UTAVES**) and [Zn(**22***)Cl_2] (**UTAVIW**) [80] are the pyridyl analogues of [Cu(**22**)Cl_2] (**XOSJAS**) and [Zn(**22**)Cl_2] (**CEDZOD**, Fig. 20). While all complexes are five-coordinate, the τ_5 values for the pyridyl complexes (0.26 and 0.23 for the Cu and Zn complexes, respectively) are significantly smaller than those for the quinoline complexes (0.44 and 0.52). These are further examples of the quinolyl split, where bisection of the Cl-M-Cl angle by the planes of the quinoline moieties causes this angle to be substantially larger in the quinolyl complexes than in the pyridine complexes.

Table 4
Five-coordinate complexes of **22.**

Complex	N-M-N/°	N-M-X /°	X-M-X /°	M-$N_{quinoline}$/Å	M-$N_{tertiary}$/Å	M-X/Å	τ_5	ref
[Co(**22**)Cl_2] (**CEDZUJ**)	80.46 81.32 159.78	89.61 90.09 96.01 100.35 114.70 118.56	126.68	2.134 2.148	2.179	2.287 2.314	0.55	[71]
[Zn(**22**)Cl_2] (**CEDZOD**)	78.79 79.52 155.96	89.42 90.71 97.82 101.74 115.70 119.28	124.99	2.171 2.186	2.232	2.250 2.314	0.52	[71]
[Cu(**22**)Cl_2] (**XOSJAS**)	82.09 82.32 162.30	88.15 89.80 96.67 97.00 111.49 112.50	136.00	2.001 2.006	2.247	2.321 2.334	0.44	[69]
[Cu(**22**)Br_2] (**XOSHUK**)	82.39 82.72 162.92	88.37 89.83 96.66 96.70 112.32 113.17	134.50	1.990 2.005	2.239	2.448 2.483	0.47	[69]
[Cu(**22**)$(H_2O)(ClO_4)$]$(ClO_4)_2{\cdot}2H_2O$ (**SUDTAO**)	85.07 85.07 169.82	92.67 92.67 93.72 93.72 107.58 151.25	101.18	1.973 1.973	2.080	1.979(H_2O) 2.406	0.31	[70]

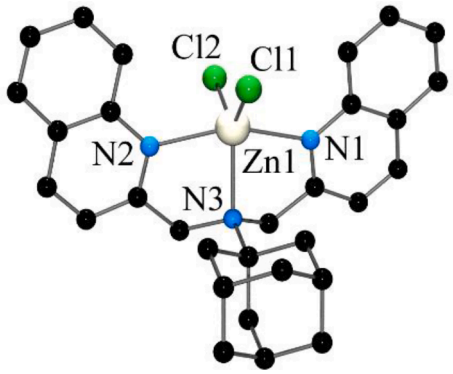

Fig. 20. Structure of the [Zn(**22**)Cl_2] complex. Selected bond lengths (Å) and angles (°): Zn1-N1 2.171, Zn1-N2 2.186, Zn1-N3 2.232, Zn1-Cl1 2.250, Zn1-Cl2 2.314; N1-Zn1-N2 155.96, N1-Zn1-N3 79.52, N2-Zn1-N3 78.79, N1-Zn1-Cl1 101.74, N1-Zn1-Cl2 89.42, N2-Zn1-Cl1 97.82, N2-Zn1-Cl2 90.71, N3-Zn1-Cl1 119.28, N3-Zn1-Cl2 115.70, Cl1-Zn1-Cl2 124.99.

3. Tetradentate ligands

3.1. Tetradentate ligands containing one quinolyl moiety

The structures of these ligands are given in Fig. 21.

3.1.1. 3-(2-methylquinolyl)diethylenetriamine (23) [81,82]

Ligand **23** is prepared from the reaction between 1,5-diphthalimido-3-azapentane and quinoline-2-carbaldehyde in the presence of NaBH$(OAc)_3$ in dichloroethane. Following purification, the 3-(2-quinolinylmethyl)-1,5-diphthalimido-3-azapentane intermediate is deprotected with hydrazine monohydrate in ethanol to yield the desired product. [82] An alternative synthesis uses 2-(chloromethyl)quinoline hydrochloride in place of the aldehyde; 1,5-diphthalimido-3-azapentane and 2-(chloromethyl)quinoline are dissolved in acetonitrile and heated to reflux in the presence of anhydrous K_2CO_3. The intermediate obtained from this step is deprotected as above to yield the ligand. [81].

The pentacoordinate complex, [Cu(**23**)(H_2O)]NDSA·$2H_2O$ (NDSA = 1,5-naphthalenedisulfonate anion) (Fig. 22, **ROYPIH**) [81] adopts a distorted square pyramidal geometry about the copper centre (τ_5 = 0.22) with the three aliphatic nitrogen donor atoms and the aqua oxygen atom forming the equatorial plane, and the quinoline N atom coordinated in the axial position. Bond lengths are 2.213 Å (Cu-$N_{quinoline}$), 2.005 Å (Cu-$N_{aliphatic}$), 2.065 Å (Cu-$N_{tertiary}$), and 1.991 Å (Cu-O). The N-Cu-N bond angles range from 81.31° – 156.77° and N-Cu-O angles range between 92.21° and 169.72°. The Cu(II) ion sits 0.284 Å above the equatorial plane.

3.1.2. N-(quinol-2-ylmethyl)-N′-(pyrid-2-ylmethyl)-1,4-diazepane (24) [83]

The asymmetric ligand **24** was prepared following a two-step procedure, the first being the reaction between 2-(chloromethyl)pyridine hydrochloride and homopiperazine in the presence of triethylamine to give the mono-(N-pyrid-2-ylmethyl) derivative. This was then treated with quinoline-2-carbaldehyde, and following presumed reduction of the resultant imine (no details were provided), the desired ligand was obtained as a yellow oil. [83].

Reaction of the ligand with an equimolar amount of $Mn(ClO_4)_2{\cdot}4H_2O$ gave *trans*-[Mn(**24**)$(OH_2)(OClO_3)$](ClO_4) (Fig. 23, **LIWQUF**), [83] the complex cation of which displays a very distorted (one *cis* N-Mn-N bond angle of 142.49°) octahedral geometry resulting from the coordination of the Mn(II) centre to all four nitrogen donor atoms of the ligand in an *mm* configuration[84] and one oxygen atom each from a perchlorato ligand and a water ligand. The *cis* $O_{perchlorate}$-Mn-$N_{aliphatic}$ angles are 87.42° and 117.96° and the *cis* O_{water}-Mn-$N_{aliphatic}$ angles are 93.40° and 120.57°. The *cis* $O_{perchlorate}$-Mn-$N_{aromatic}$ angles are 81.77° and 84.75° and the *cis* O_{water}-Mn-$N_{aromatic}$ angles are 85.05° and 85.89°. The other N-Mn-N *cis* angles range from 71.32° to 142.49°, with the latter being much greater than the expected cis angle of 90°. The two $N_{aromatic}$-Mn-$N_{aliphatic}$ *trans* angles are 139.00° and 139.74°, and the O-Mn-O angle is 144.31°. The Mn-N bond distances range from 2.207 Å to 2.272 Å,

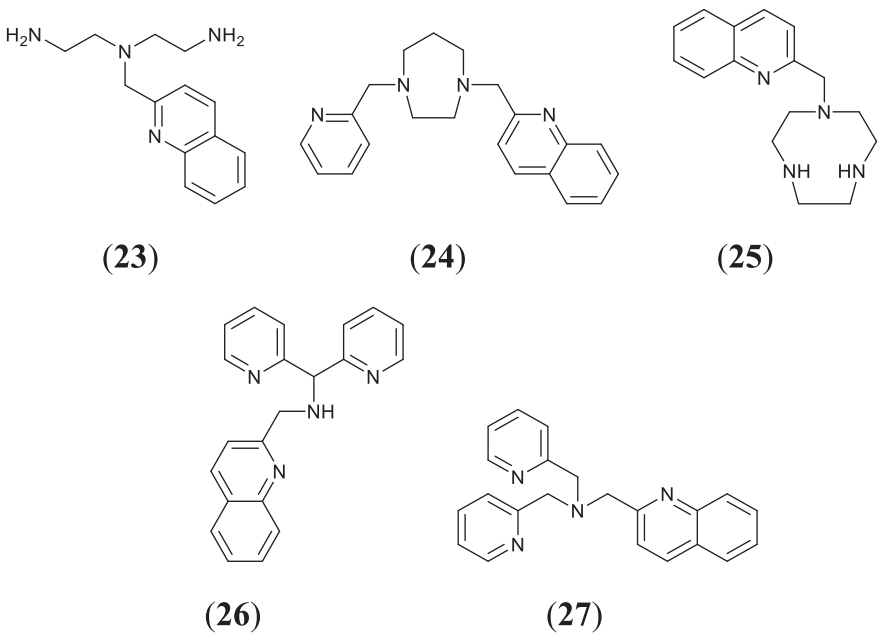

Fig. 21. Structures of the tetradentate ligands containing one quinolyl moiety.

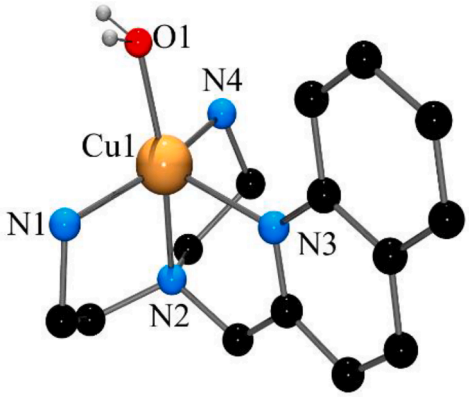

Fig. 22. Structure of the [Cu(**23**)(H_2O)]$^{2+}$cation. Selected bond lengths (Å) and angles (°): Cu1-N1 2.018, Cu1-N2 2.065, Cu1-N3 2.213, Cu1-N4 2.005, Cu1-O1 1.991; N1-Cu1-N2 85.40, N1-Cu1-N3 99.22, N3-Cu1-N4 100.69, N1-Cu1-N4 156.77, N1-Cu1-O1 92.21, N3-Cu1-O1 108.95, N2-Cu1-O1 169.72.

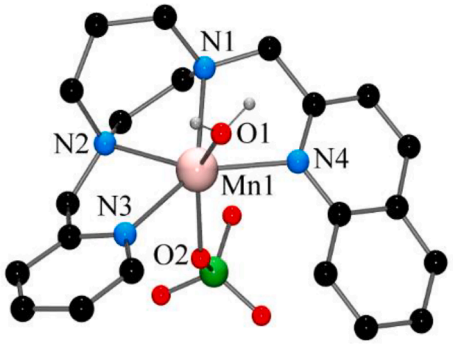

Fig. 23. Structure of the [Mn(**24**)(OH_2)($OClO_3$)]$^{+}$cation. Selected bond lengths (Å) and angles (°): Mn1-N1 2.263, Mn1-N2 2.272, Mn1-N3 2.220, Mn1-N4 2.207, Mn1-O1 2.186, Mn1-O2 2.323; N1-Mn1-N2 71.32, N2-Mn1-N3 74.43, N3-Mn1-N4 142.49, N4-Mn1-N1 77.82, N1-Mn1-N3 139.00, N2-Mn1-N4 139.74, O1-Mn1-O2 144.31.

consistent with HS Mn(II), the water O atom is 2.186 Å from the Mn(II) cation, and the perchlorato ligand is attached via an oxygen atom at a distance of 2.323 Å.

3.1.3. 1-(2-quinolinylmethyl)-1,4,7-triazacyclononane (25) [85,86]

The 1,4,7-tris-(2-quinolinylmethyl)-1,4,7-triazacyclononane ligand was prepared via the reaction of 2-(chloromethyl)quinoline and 1,4,7-triazatricyclo[5.2.1.$0^{4,10}$]decane in MeCN at room temperature to give the ligand as a pale yellow solid. [85].

Potentiometric titration data for **25** in MeCN/H_2O (1:1) gave evidence for protonation of only three of the four N atoms, with pK_a values of 9.8(1), 6.7(1) and 3.1(9). Equilibrium constants (log *K*) measured in MeCN/H_2O (0.1 M NMe_4Cl, 289.1 K) for the reaction of the ligand with Cu^{2+}, Zn^{2+}, Cd^{2+}, and Pb^{2+} are 16.82(4), 14.85(5), 10.4(1), and 11.1 (1), respectively.

Three complexes containing **25** have been structurally characterised; mononuclear [Cu(**25**)CN]BF_4·0.5H_2O (**UNACOC**)[b] and [Cu(**25**)I]I (**UNACUI**), [86] and binuclear [Zn_2Cl_2(**25**)$_2$](BF_4)$_2$·0.5$MeNO_2$·H_2O (**YUHNEV**). [85] The five-coordinate Cu(II) complex cations [Cu(**25**)CN]$^+$ and [Cu(**25**)I]$^+$, despite having τ_5 values of 0.35 and 0.38, respectively, are probably best described as exhibiting distorted trigonal bipyramidal geometries, with one $N_{aliphatic}$-Cu-$N_{aliphatic}$ equatorial angle; ([Cu(**25**)CN]$^+$, 83.49°; [Cu(**25**)I]$^+$, 84.65°) less than 90° as a result of the constraints imposed by the tetradentate ligand. Cu-N bond lengths in the [Cu(**25**)CN]$^+$ cation range from 2.031 Å to 2.146 Å, with Cu-$N_{quinoline}$ = 2.035 Å, while those for the [Cu(**25**)I]$^+$ cation range from 2.008 Å to 2.157 Å, with Cu-$N_{quinoline}$ being the shortest. The crystal structure of [Zn_2Cl_2(**25**)$_2$]$^{2+}$ confirmed the dimeric nature of the cation, with two Zn(II) centres in distorted octahedral environments. Each of the Zn(II) ions coordinate to the four N-donors of the tetradentate ligand, and the remaining two coordination sites are occupied by two bridging Cl^- ligands. Zn-N bond lengths range from 2.126 Å to 2.189 Å, with the Zn-$N_{quinoline}$ bond length being 2.180 Å. π-stacking interactions between neighbouring cations are present, with a centroid–centroid distance of 3.637 Å.

[b] It should be noted that the ORTEP diagram in this paper mistakenly shows the cyanido ligand to be N-bound, and this appears to have been carried through to the CSD.

3.1.4. N-(2-quinolylmethyl)-N-bis(2-pyridyl)methylamine (26) [87]

Ligand **26** was isolated as a by-product from the synthesis of **39** (Section 4.1.1) which involved reaction between 2-(bromomethyl) quinoline and di(pyridine-2-yl)methanamine in THF.

The complex *fac*-[Zn(**26**)$_2$](ClO$_4$)$_2$ (Fig. 24, **TUBHIJ**) [87] exhibits a distorted octahedral geometry about the Zn(II) ion, with the **26** ligands coordinated in a hypodentate fashion via the aliphatic and the two pyridyl nitrogen atoms. The cation has *trans* N-Zn-N angles of 165.92°, 165.92° and 174.34°, and *cis* N-Zn-N bond angles that range between 78.56° and 97.39°. The Zn-N$_{pyridine}$ bond lengths range from 2.150 Å to 2.163 Å, and the two Zn-N$_{aliphatic}$ lengths are 2.202 Å.

The uncoordinated quinoline moieties form weak intramolecular π-π interactions with a pyridine moiety from an adjacent ligand on the zinc centre. This interaction positions the quinoline groups adjacent to the pyridine with a centroid–centroid distance of 3.715 Å.

3.1.5. Bis(2-pyridylmethyl)(2-quinolylmethyl)amine (27) [81,88–107]

The ligand **27** was first synthesised by Wei and co-workers[100] from the reaction of dipicolylamine and 2-(bromomethyl)quinoline in THF, with added triethylamine, at room temperature for 3 days. An alternative synthesis of this ligand involves the reaction of 2-(chloromethyl)quinoline hydrochloride and dipicolylamine in anhydrous acetonitrile in the presence of anhydrous K_2CO_3. [95].

The fluorescent properties of the free ligand **27** and the corresponding [Cd(**27**)(N$_3$)$_2$] complex have been investigated. An emission peak at 550 nm and a shoulder at approximately 435 nm was observed for the free ligand upon excitation of the solid sample at 240 nm at room temperature. Under the same conditions, a distinct enhancement of the fluorescence intensity was observed for [Cd(**27**)(N$_3$)$_2$] which displayed a strong peak at 438 nm and a shoulder at 500 nm. It was proposed that this observed increased fluorescence could be attributed to the conformational rigidity increasing upon the coordination of **27** to the metal centre, or as a result of the CHEF effect. [98].

Twelve complexes of **27**, containing Fe, Co, Cu and Cd, have been structurally characterised. These complexes, with the exception of four-coordinate [Cu(**27**)]B(C$_6$F$_5$)$_4$ [108] are either five- or six-coordinate. In [Cu(**27**)]B(C$_6$F$_5$)$_4$ (Fig. 25, **TUZSOX**), [96] the Cu(I) centre is coordinated to all four nitrogen donor atoms of **27** to give a trigonal pyramidal geometry (τ_4 = 0.83). N-Cu-N bond angles range from 82.57° to 123.63°. The Cu-N$_{pyridine}$ bond lengths are 2.006 Å and 1.988 Å, the Cu-N$_{quinoline}$ bond length is 2.012 Å and the Cu-N$_{tertiary}$ bond length is the longest at 2.185 Å.

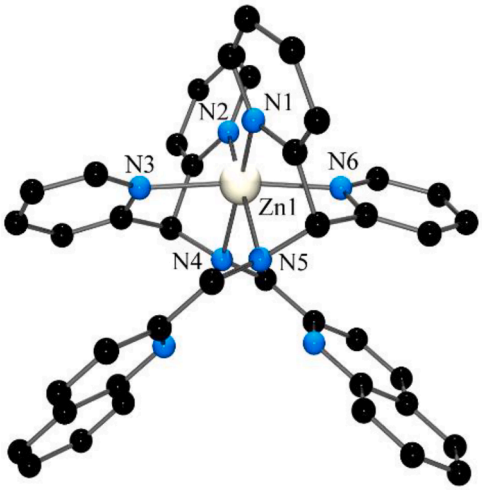

Fig. 24. Structure of the *fac*-[Zn$_2$(**26**)$_2$]$^{2+}$cation. Selected bond lengths (Å) and angles (°): N1-Zn1 2.150, N2-Zn1 2.150, N3-Zn1 2.163, N4-Zn1 2.202, N5-Zn1 2.202, N6-Zn1 2.163; N1-Zn1-N2 116.42, N2-Zn1-N3 85.92, N3-Zn1-N5 97.39, N3-Zn1-N4 78.56, N2-Zn1-N5 165.92.

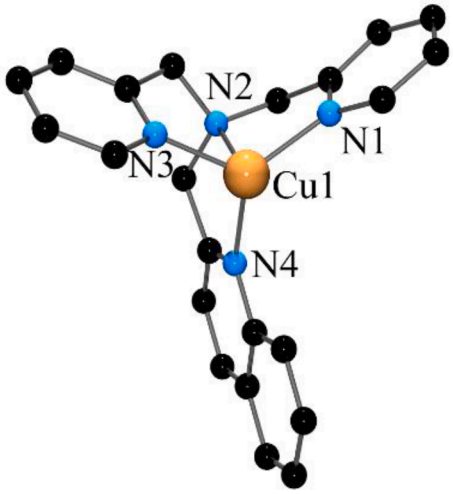

Fig. 25. Structure of the [Cu(**27**)]$^+$cation. Selected bond lengths (Å) and angles (°): Cu1-N1 1.988, Cu10N2 2.185, Cu1-N3 2.006, Cu1-N4 2.012; N1-Cu1-N2 83.11, N2-Cu1-N3 82.57, N3-Cu1-N4 111.70, N1-Cu1-N4 119.95, N1-Cu1-N3 123.63, N2-Cu1-N4 82.58.

Structural data for the remaining structurally characterised complexes containing ligand **27** are summarised in Tables 5 and 6 below. Those complexes containing octahedral metal centres all have the quinoline moiety situated axial relative to the two coordination sites not occupied by **27**. These complexes are also all, by necessity, *cis*.

The complex [(phen)$_2$Fe(CN)$_2$Fe(**27**)]$_2$(PF$_6$)$_4$·H$_2$O(CH$_3$OH)$_2$ (-Fig. 26, **PUCLAB**) [94] (a typographical error in the original paper gave the counterions as PF$_4$) is a self-assembled tetranuclear ferrous cluster. The complex is made up of four Fe(II) centres that are connected via bridging cyanido ligands. Two of the four metal cations are coordinated to two phenanthroline ligands, and the other two are bound to one **27** ligand each.

The structures of the complexes containing the pyridyl congener, namely [Fe(**27***)(OSO$_2$CF$_3$)$_2$] (**NELGAM**) [109], [{Co(**27***)}$_2$(dhbq)](PF$_6$)$_3$ (**RECPAR01**) [110], [Co(**27***)Cl]X (X = $CoCl_4^{2-}$ (**LUXGAM**); X = Cl^- (**PAJSIF**, **QALZOT01**, **QAMBAI**, **QAMBAI01**); X = ClO_4^- (**RITWOH**, **RITWOH01**, **RITWOH02**) [90,111–116], [(phen)$_2$Fe(CN)$_2$Fe(**27***)]$_2$(PF$_6$)$_4$ (**PUCLAB**) [117], and [Fe(**27***)(tcc)]X (X = ClO_4^- (**CAMYAR**, **EQUNAF**); X = SbF_6^- (**REWBAY**, **REWBAY01-07**); X = BPh_4^- (**TAMTAD**); X = PF_6^- (**TAMTEH**, **TAMTEH01-05**); X = NO_3^- (**TAMTIL**, **TAMTIL01**)) [118–121], are very similar to the analogous quinoline complexes. The notable exception is the [Cu(**27***)Cl]$^+$ cation (**AKISIZ**, **AQUFIC**, **BUBCIK**, **GIHWOK**, **ILUVIV**, **ILUVOB**, **YEZGAN**) [122–127], which is trigonal bipyramidal (τ_5 ranges from 0.87 to 1.04) while the quinoline congener [Cu(**27**)Cl]$^+$ is square pyramidal (τ_5 = 0.13 – 0.16, Fig. 27). However, the Cu(I) cation [Cu(**27***)]$^+$ (**ILUTIT**) [123] (τ_4 = 0.88, 0.87) exhibits a very similar geometry to the analogous quinoline complex.

3.2. Tetradentate ligands containing two quinolyl moieties

The structures of these ligands are given in Fig. 28.

3.2.1. Bis(2-quinolinylmethyl)-(R,R)-2,2′ bipyrrolidine (28) [128,129]

Ligand **28** was first prepared in three steps from the synthon N,N-bis (2-quinolinylmethyl)-(R,R)-4,5-diamino-1,7-octadiene. [130 131].

Two structurally characterised metal complexes of this ligand have been reported, *cis*-[Fe(**28**)(OTf)(EtOH)](OTf) (Fig. 29, **GIYDOI**) [128] and *trans*-[Mn(**28**)(OTf)$_2$] (**VOHWIA**). [129] The X-ray structure of *cis*-[Fe(**28**)(OTf)(EtOH)]$^+$ shows a slightly distorted octahedral geometry about the Fe(II) ion, with the ligand coordinating in an *ff* configuration through the four nitrogen donor atoms, and the remaining two

Table 5
Six-coordinate complexes of **27**.

Complex	*Trans* N-M-N/°	*Trans* X-M-N/°	*Cis* N-M-N/°	*Cis* X-M-N/°	*Cis* X-M-X /°	M-$N_{quinoline}$/Å	M-$N_{tertiary}$/Å	M-$N_{pyridine}$/Å	M-X/Å	Ref
cis-[Fe(**27**)$(NCS)_2$] (**CECVUD**)	150.52 169.26	168.97 169.26	74.99 75.73 78.34 82.44 88.45	91.18 91.70 92.19 94.98 96.62 112.02	95.89	2.271	2.236	2.171 2.194	2.048 2.084	[89]
cis-[Fe(**27**)$(OTf)_2$] (**EBORUI**)	149.50	165.15 169.17	74.70 74.81 80.26 83.59 90.75	83.80 93.85 97.84 103.91 104.10 112.26	85.37	2.267	2.207	2.138 2.196	2.056 2.171	[92]
$[(phen)_2Fe(II)(CN)_2Fe(II)$ (**27**)$]_2(PF_6)_4$ (**PUCLAB**)	149.80	165.16 171.98	73.99 76.05 77.62 82.92 87.09	86.56 92.33 92.47 92.47 100.24 116.59	94.76	2.242	2.227	2.194 2.240	2.064 2.084	[94]
[Fe(**27**)(tcc)]ClO_4 (**XENZUL**)	154.91	173.31 176.97	76.01 78.91 81.49 84.38 91.08	91.84 92.63 95.35 98.24 98.42 106.74	85.05	2.153	2.161	2.128 2.190	1.910 1.950	[97]
[{Co(**27**)}$_2$(dhbq)]$(PF_6)_3$ (**POCWOU**)	169.60	173.72 176.64	84.45 85.21 86.68 88.54 91.94	89.27 89.76 90.28 90.60 96.94 99.97	85.95	1.959	1.956	1.948 1.966	1.898 1.906	[93]
cis-[Cd(**27**)$(N_3)_2$] (**XOBCIC**)	142.48	162.32 164.03	70.76 71.72 72.89 75.85 92.55	89.63 93.02 93.19 94.23 101.17 115.01	101.13	2.416	2.405	2.395 2.396	2.215 2.291	[98]

Table 6
Five-coordinate complexes of **27**.

Complex	N-M-N/°	N-M-X /°	M-$N_{quinoline}$/Å	M-$N_{tertiary}$/Å	M-$N_{pyridine}$/Å	M-X/Å	τ_5	ref
[Co(**27**)Cl]ClO_4 (**CIJTUN**)	76.69 76.87 78.05 105.54 115.73 124.11	96.68 100.86 111.18 171.74	2.111	2.219	2.075 2.078	2.301	0.79	[90]
[Cu(**27**)Cl]ClO_4 (**CIXWEO**)	81.12 81.41 83.33 83.90 101.92 162.57	95.87 98.13 106.84 172.00	2.357	2.061	1.993 2.010	2.253	0.157	[91]
[Cu(**27**)Cl]PF_6 (**CIXWIS**)	81.44 81.45 83.60 85.12 100.46 163.03	96.09 97.41 07.72 170.82	2.347	2.060	1.983 2.003	2.245	0.13	[91]
[Co(**27**)Cl]$PF_6{\cdot}H_2O$ (**SOBSOT**)	76.65 77.48 77.66 109.85 116.16 119.74	95.65 99.16 114.06 168.31	2.105	2.197	2.082 2.084	2.298	0.81	[95]
[Cu(**27**)Cl]PF_6.0.5Et_2O (**YEXSEZ**)	80.75 81.58 83.51 88.16 100.16 161.49	96.04 96.99 108.30 170.93	2.344	2.063	1.983 1.999	2.257	0.157	[99]

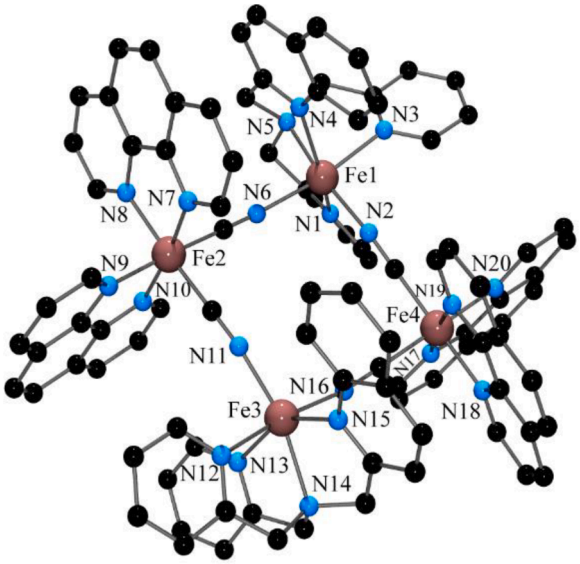

Fig. 26. Structure of the $[(phen)_2Fe(CN)_2Fe(\mathbf{27})]_2^{4+}$ cation. Selected bond lengths (Å) and angles (°):Fe1-N1 2.240, Fe1-N2 2.064, Fe1-N3 2.194, Fe1-N4 2.242, Fe1-N5 2.227, Fe1-N6 2.084, Fe3-N11 2.064, Fe3-N12 2.194, Fe3-N13 2.240, Fe3-N14 2.227, Fe3-N15 2.242, Fe4-N16 2.084; N1-Fe1-N2 92.33, N1-Fe1-N6 100.24, N2-Fe1-N3 92.47, N3-Fe1-N4 87.09, N4-Fe1-N5 73.99, N5-Fe1-N6 95.89, N1-Fe1-N4 149.80, N2-Fe1-N5 165.46, N3-Fe1-N6 171.98, N11-Fe3-N12 92.47, N11-Fe3-N15 94.76, N12-Fe3-N13 82.92, N13-Fe3-N14 76.05, N14-Fe3-N15 73.99, N15-Fe3-N16 85.56, N11-Fe3-N14 165.46, N12-Fe3-N16 171.98, N13-Fe3-N15 149.80.

coordination sites are occupied by a $CF_3SO_3^-$ ligand and an EtOH ligand. The cation has Fe-$N_{quinoline}$ bond lengths of 2.270 Å and 2.272 Å and the Fe-$N_{tertiary}$ distance is 2.188 Å. The triflato and ethanol ligands are coordinated with Fe-O bond lengths of 2.104 Å and 2.138 Å, respectively. The *cis* N-Fe-N angles range between 75.54 and 96.80° and the *trans* N-Fe-N angle is 168.01°. The *cis* N-Fe-$O_{triflate}$ and N-Fe-$O_{ethanol}$ angles are 93.26°, 84.01, 101.74° and 84.69°, 96.69°, 106.18°, respectively. The $O_{triflate}$-Fe-$O_{ethanol}$ angle is 88.12° while the *trans* O-Fe-N angles are 174.66° and 177.91°.

The significantly distorted octahedral Mn complex *trans*-[Mn(**28**)$(OTf)_2$] is coordinated by all four nitrogen donor atoms of the ligand in an *mm* configuration and two oxygen atoms from two triflato ligands. The distortion is most evident in the *cis* N-Mn-N bond angles, which are 73.35°, 74.12°, 76.17° and 136.76°. The *trans* N-Mn-N bond angles are 148.41° and 149.88°, the *cis* N-Mn-O angles range from 79.94° to 102.47° and the *trans* O-Mn-O bond angle is 158.92°. The Mn-$N_{quinoline}$ bond lengths are 2.297 Å and 2.250 Å, the Mn-$N_{bipyrrolidine}$ bond lengths are 2.264 Å and 2.295 Å, and the Mn-O bond lengths are 2.186 Å and 2.217 Å.

The complex *cis*-[Mn(**28***)$(OTf)_2$] (**IQEPEA**), [132] the pyridine analogue of the Mn complex above, exhibits an octahedral geometry, but in this case the triflato ligands are *cis*-disposed and the tetradentate ligand binds in an *ff* configuration.

3.2.2. *N,N'-bis(2-methylquinolyl)dimethyl-1,3-propanediamine (29) [133,134]*

The ligand **29** was prepared from the reaction of 2-(chloromethyl) quinoline hydrochloride and *N,N'*-dimethyl-1,3-propanediamine in refluxing ethanol in the presence of K_2CO_3[133]. The BQDMPN ligand in a solution of 20 % propan-1-ol in H_2O displayed an emission maximum of 388 nm when excited at 271 nm.

The Cu(II) complex *trans*-[Cu(**29**)$(ONO_2)_2$] (**JUJZUL**) [134] is the only structurally characterised complex of **29**. The Cu(II) ion is coordinated to the four nitrogen donor atoms of **29**, which display an *mm* configuration, and an oxygen atom of two NO_3^- ligands to give a distorted octahedral geometry. The Cu-$N_{aliphatic}$ bond lengths are 2.045 Å, the Cu-$N_{quinoline}$ bond lengths are 2.027 Å and the Cu-O bonds are 2.673 Å. The *cis* N-Cu-N bond angles range between 81.38° and 104.12°, and the *cis* N-Cu-O bond angles range from 82.41° to 97.37°. The *trans* N-Cu-N angles are both 171.82°, and the *trans* O-Cu-O angle is 179.61°. The authors deemed the Cu-O distances (2.673 Å) involving the two nitrate ions too long to be coordinated to the metal cation, and described the geometry of the complex as distorted square planar (τ_4 = 0.116). However, Cu-$O_{nitrato}$ bond lengths of > 2.6 Å are not without precedent, [135–141] and a distorted *trans* octahedral geometry appears to be a more appropriate description.

3.2.3. *N,N'-bis(2-quinolylmethyl)-N,N'-dimethylethylenediamine (30) [142–150]*

The reaction of N,N′-diethylethylenediamine, 2-(bromomethyl) quinoline and K_2CO_3 in ethanol gives the ligand **30** as colourless crystals in 73 % yield. [146] An alternative preparation uses 2-(chloromethyl) quinoline hydrochloride in place of the quinoline analogue and acetonitrile as the solvent. [147] In addition, the ligand can be isolated from the reaction of quinoline-2-carbaldehyde and *N,N'*-dimethylethane-1,2-diamine in the presence of $NaBH(OAc)_3$ in anhydrous 1,2-dichloroethane. [148].

Fluorescence titration experiments using **30** in 50 % aqueous DMF at 25 °C showed an increase in fluorescence intensity at 375 nm (λ_{ex} = 317 nm) upon the addition of Zn^{2+} with $K_d = (9.0 \pm 1.00) \times 10^{-6}$ M. Fluorescence studies in the presence of a number of metal ions show that **30** exhibits a selectivity for Zn(II). [149].

A number of complexes containing **30** have been structurally characterised. *Cis*-[Fe(**30**)$(Cl)_2](H_2O)$ (**ZAWTAS**) [146] is a six-coordinate complex where the tetraamine ligand binds via all four nitrogen donor atoms in an *ff* configuration with the methyl substituents *anti*, two chlorido ligands occupy the fifth and sixth positions and the Fe(II) cation exhibits a slightly distorted octahedral environment. The *trans* N-Fe-N angle is 160.95° and the *trans* N-Fe-Cl angles are 168.18° and 173.51°. *Cis* N-Fe-Cl angles range between 89.85° and 104.37°, *cis* N-Fe-N angles

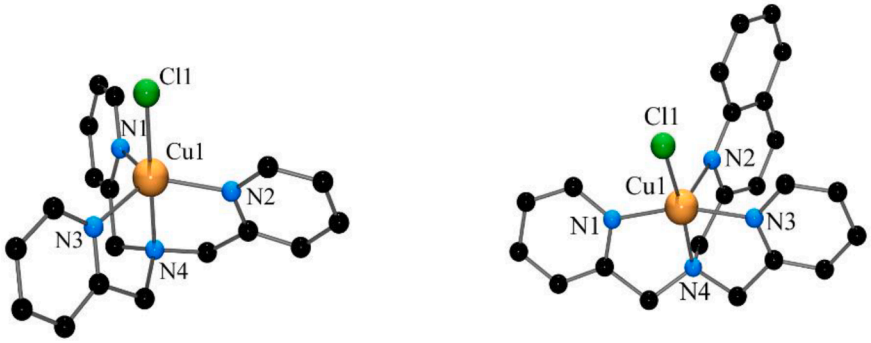

Fig. 27. Structures of the $[Cu(\mathbf{27}^*)Cl]^+$cation in $[Cu(\mathbf{27}^*)Cl]ClO_4$ (left, τ = 0.94) and the $[Cu(\mathbf{27})Cl]^+$ cation in $[Cu(\mathbf{27})Cl]ClO_4$ (right, τ = 0.16).

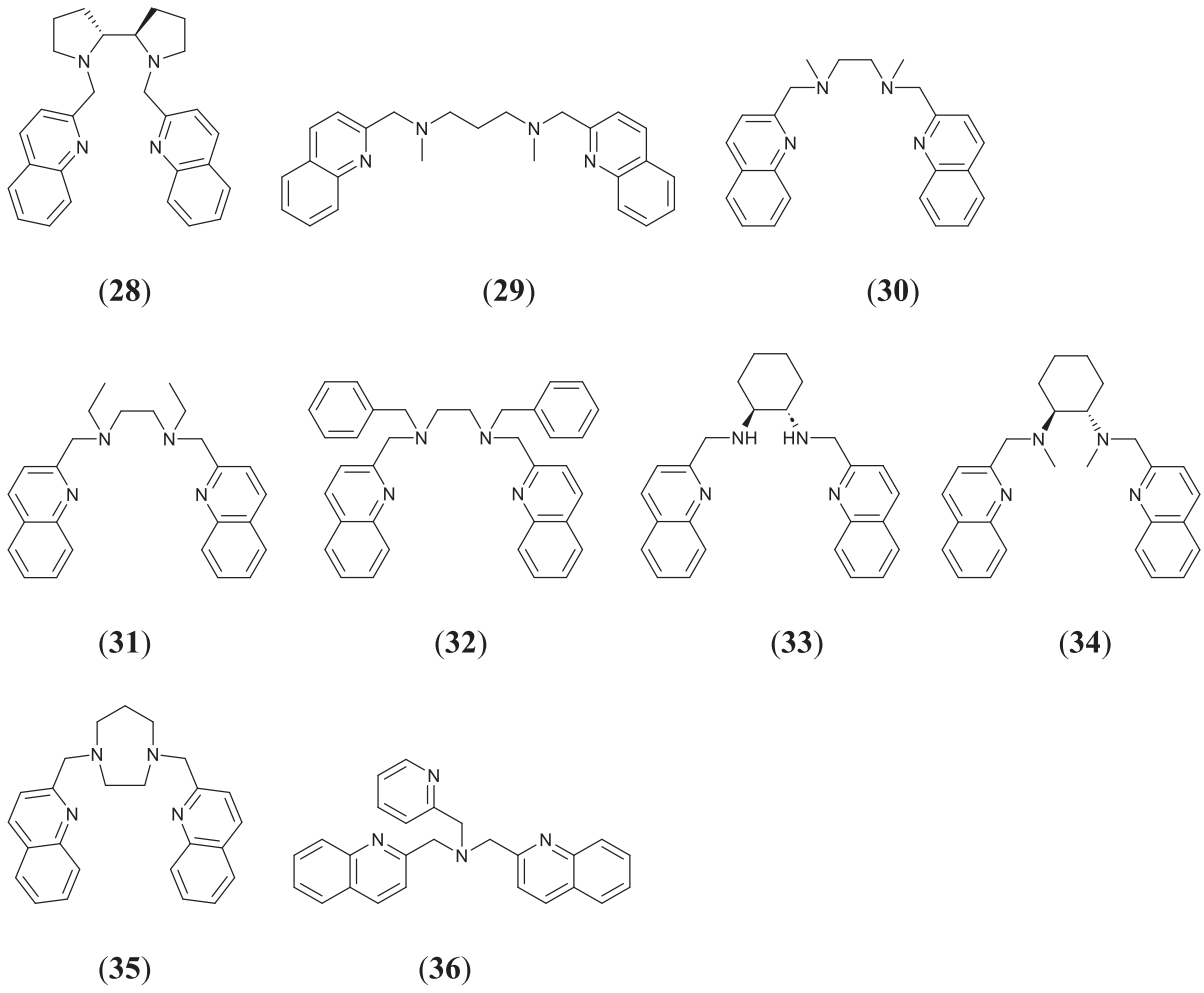

Fig. 28. Structures of the tetradentate ligands containing two quinolyl moieties.

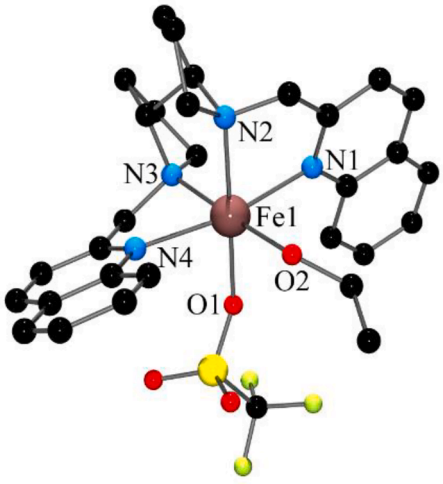

Fig. 29. Structure of the *cis*-[Fe(**28**)(OTf)(EtOH)]$^{+}$ cation. Selected bond lengths (Å) and angles (°): Fe1-N1 2.270, Fe1-N2 2.188, Fe1-N3 2.188, Fe1-N4 2.272, Fe1-O1 2.138, Fe1-O2 2.104; N1-Fe1-N2 76.51, N2-Fe1-N3 81.86, N3-Fe1-N4 75.54, N4-Fe1-O1 84.01, N1-Fe1-O1 101.74, N1-Fe1-O2 84.69, N4-Fe1-O2 106.18, O1-Fe1-O2 88.12, N1-Fe1-N4 168.01, N2-Fe1-O1 174.66.

range from 72.64° to 90.84°, and the unique *cis* Cl-Fe-Cl angle is 95.86°. Fe-N bond lengths lie between 2.258 Å and 2.400 Å, and the Fe-Cl bond lengths are 2.402 Å and 2.459 Å. The *cis*-[Fe(**30**)$(NCS)_2$] (**HOLSIN**), [142] *cis*-[Fe(**30**)$(NCSe)_2$] (**HOLTAG**), [142] *cis*-[Fe(**30**)$(NCBH_3)_2$] (**HOLTIO**), [142] *cis*-[Zn(**30**)$(Cl)_2$] (**RUDMOT**), [149] *cis*-[Fe(**30**)$(OTf)_2$] [148] and *cis*-[Ni(**30**)$(Cl)_2$] [150] complexes all adopt similar geometries to *cis*-[Fe(**30**)$(Cl)_2$] and display similar bond lengths and angles; in all cases, the *cis* isomer is formed and the tetradentate ligand adopts an *ff* configuration with the methyl groups *anti*. X-ray structural data for these complexes are summarised in Table 7. As can be seen in this table, the M-$N_{quinoline}$ bonds are longer than those involving the aliphatic N atoms. The authors ascribed this to the steric bulk of the quinoline groups which leads to the quinoline N atoms being further from the metal centre.

The $Mn(III)_2$ dimer, $[(Mn(\mathbf{30}))_2(\mu\text{-}O)_2](ClO_4)_2.2DMF$ (Fig. 30, **NIKQUU**) [147] comprises two Mn^{III}(**30**) units bridged by a $(\mu\text{-}O)_2$ core; this is unusual as such bis(μ-oxo) complexes are usually mixed-valence Mn(III)-Mn(IV) species. The Mn-$N_{quinoline}$ bonds (2.439 Å and 2.463 Å) are significantly longer than the Mn-$N_{aliphatic}$ bonds (2.144 Å and 2.169 Å), which was attributed to the Jahn-Teller distortion expected for high spin d^4 Mn(III). The Mn-Mn distance of 2.665 Å is the shortest observed for a bis(μ-oxo) $Mn(III)_2$ dimer. This has been proposed to be due to π-π stacking interactions between the two quinoline rings. Room temperature magnetic susceptibility measurements displayed a smaller magnetic moment per molecule (μ_{eff} = 2.8 μ_B) than that expected for a high spin $Mn(III)_2$ system that has no magnetic coupling (6.9 μ_B). Measurements taken at lower temperatures gave even smaller magnetic moments,

Table 7
Six-coordinate complexes of **30.**

Complex cation	*Trans* N-M-N/°	*Trans* X-M-N/°	*Cis* N-M-N/°	*Cis* X-M-N/°	*Cis* X-M-X /°	M-$N_{quinoline}$/Å	M-$N_{aliphatic}$/Å	M-X/Å	Ref
cis-[Fe(**30**)$(NCS)_2$]	162.94	171.68	73.59	89.10	94.67	2.360	2.228	2.075	[142]
(**HOLSIN**)		171.68	73.59	89.10		2.360	2.228	2.075	
			93.21	92.63					
			93.21	92.63					
			80.38	102.52					
				102.52					
cis-[Fe(**30**)$(NCSe)_2$]	162.38	173.47	74.06	89.38	93.33	2.337	2.237	2.058	[142]
(**HOLTAG**)		173.47	74.06	89.38		2.337	2.237	2.058	
			82.15	92.36					
			92.50	92.36					
			92.50	102.78					
				102.78					
cis-[Fe(**30**)$(NCBH_3)_2$]	166.38	172.94	74.14	85.07	94.24	2.321	2.224	2.104	[142]
(**HOLTIO**)		173.27	74.14	86.31		2.327	2.236	2.115	
			81.69	92.02					
			95.32	92.18					
			95.43	103.13					
				104.22					
cis-[Zn(**30**)$(Cl)_2$]	163.19	162.75	73.12	90.87	97.44	2.436	2.209	2.347	[149]
(**RUDMOT**)		169.34	73.12	90.87		2.436	2.209	2.347	
			81.25	91.07					
			93.93	91.07					
			93.93	100.23					
				100.23					
cis-[Fe(**30**)$(Cl)_2$]	160.95	168.18	72.04	87.01	95.86	2.399	2.258	2.402	[146]
(**ZAWTAS**)		173.51	73.20	89.85		2.400	2.259	2.59	
			78.74	90.18					
			90.84	95.40					
			93.81	104.35					
				104.37					
cis-[Ni(**30**)$(Cl)_2$]	169.50	174.70	76.58	85.91	92.99	2.286	2.128	2.377	[150]
		174.70	76.58	91.74		2.286	2.128	2.377	
			83.63	91.74					
			95.50	101.38					
			95.50	101.38					
cis-[Fe(**30**)$(OTf)_2$]	169.56	170.49	75.31	81.25	95.18	2.249	2.207	2.100	[148]
		175.90	75.71	85.35		2.253	2.220	2.155	
			82.58	87.92					
			96.44	94.33					
			96.61	102.48					
				105.15					

X = ancillary ligand donor atom.

indicative of a strong antiferromagnetic interaction present in the complex dimer.

The complexes cis-[Fe(**30***)$(NCCH_3)_2$] (**AHINOX**, **GOTNIM**, **MOPSIT**, **MOPSIT01**), [151–154] *cis*-[Fe(**30***)$(NCBH_3)_2$] (**DUBFOY**, **DUBFOY01**), [155] *cis*-[Fe(**30***)$(NCSe)_2$] (**QUHWAT**), [156] *cis*-[Fe(**30***)$(Cl)_2$] (**LUXFEP**, **LUXFEP01**), [157,158] and $[(Mn(\mathbf{30}^*))_2(\mu\text{-}O)_2](ClO_4)_2{\cdot}5H_2O$ (**HEWJIC**) [159] are the pyridyl analogues of the complexes in Table 7. The pyridyl complexes all show the tetradentate ligand adopting an *ff* configuration, the methyl substituents *anti*, and the remaining two coordination sites in a *cis* disposition, with the usual shorter lengths of the M-$N_{pyridine}$ bonds.

3.2.4. *N,N′-bis(2-quinolylmethyl)-N,N′-diethyl-1,2-ethanediamine (31) [147]*

Ligand **31** was prepared from the reaction of 2-(chloromethyl) quinoline hydrochloride and N,N′-diethylethylenediamine in acetonitrile in the presence of K_2CO_3. The structure of $[(Mn(\mathbf{31}))_2(\mu\text{-}O)_2](ClO_4)_2{\cdot}H_2O$ (**NIKRAB**) [147] is similar to that of $[(Mn(\mathbf{31}))_2(\mu\text{-}O)_2](ClO_4)_2.2DMF$ (Section 3.2.4), comprising two Mn^{III}**31** units bridged by a $(\mu\text{-}O)_2$ core, with the tetradentate ligand binding in an *ff* configuration and the ethyl substituents *anti*. Again, the complex displays significant Jahn-Teller elongation of the Mn-$N_{quinoline}$ bonds, which have lengths between 2.434 Å and 2.445 Å, while the Mn-$N_{aliphatic}$ bond lengths range from 2.145 Å to 2.160 Å. The Mn-O bond lengths are between 1.821 Å and 1.830 Å. The distance between the two Mn(III) centres is again short, at 2.667 Å, similar to the that found for the analogous **30** complex. The magnetic behaviour of the complex is similar to that of $[(Mn(\mathbf{30}))_2(\mu\text{-}O)_2](ClO_4)_2.2DMF$ above.

3.2.5. *N,N′-dibenzyl-N,N′-di(quinoline-2-methyl)-1,2-ethylenediamine (32) [146,160,161]*

The tetradentate ligand **32** was first reported from the reaction between 2-(bromomethyl)quinoline and 1,2-diphenylethylenediamine in ethanol in the presence of K_2CO_3. [146] A more recent synthesis involves the reductive amination reaction of quinoline-2-carbaldehyde and 1,2-diphenylethylenediamine in methanol, using $NaBH_3CN$ to reduce the diamine. [161] The crystal structure of the ligand has been reported (**ZAWSUL**, **ZAWSUL01**). [146,162].

$[Pd(\mathbf{32})](NO_3)_2{\cdot}H_2O$ (**XEQFUU**) [160] is the only complex of ligand **32** to have been structurally characterised. While the structure deposited in the CSD is incomplete, the data in the publication show $[Pd(\mathbf{32})](NO_3)_2{\cdot}H_2O$ to contain a four-coordinate Pd^{2+} ion that is bonded to all four nitrogen atoms of the ligand to give an approximately square planar geometry ($\tau_4 = 0.17$). The Pd-$N_{quinoline}$ bond lengths are 2.020 Å and 2.078 Å, and the Pd-$N_{aliphatic}$ bond lengths are 2.008 Å and 2.026 Å. The N-Pd-N bond angles range from 78.95° to 112.14°.

3.2.6. *Trans N,N′-bis(quinolin-2-ylmethylene)-1,2-cyclohexanediamine (33) [163–166]*

The tetradentate ligand **33** comprises two quinolylmethyl groups bonded to a *trans*-1,2-cyclohexyl bridging group. The synthesis involves reaction of quinoline-2-carbaldehyde with *trans*-1,2-diaminocyclohexane

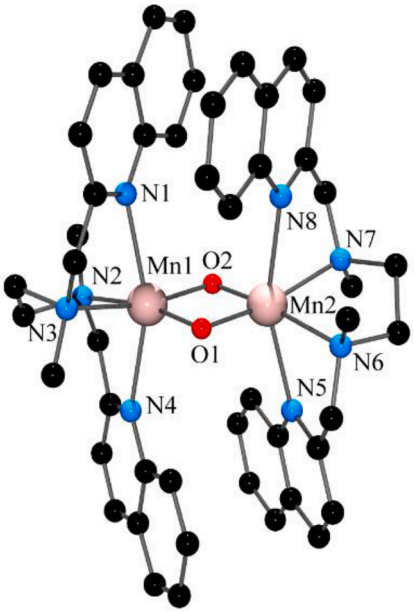

Fig. 30. Structure of the $[Mn(\mathbf{30})_2(\mu\text{-}O)_2]^{2+}$ cation. Selected bond lengths (Å) and angles (°):Mn1-N1 2.463, Mn1-N2 2.144, Mn1-N3 2.169, Mn1-N4 2.439, Mn1-O1 1.824, Mn1-O2 1.825, Mn2-N5 2.439, Mn2-N6 2.144, Mn2-N7 2.169, Mn2-N8 2.463, Mn2-O1 1.825, Mn2-O2 1.824; N1-Mn1-N3 72.22, N2-Mn1-N3 82.78, N1-Mn1-O1 98.20, N1-Mn1-O2 96.99, N3-Mn1-O1 98.12, N2-Mn1-O2 95.22, N5-Mn2-N6 72.41, N6-Mn2-N7 82.78, N7-Mn2-N8 72.22, N8-Mn2-O1 96.99, N8-Mn2-O2 98.20, N6-Mn2-O1 95.22, N7-Mn2-O2 98.12.

in ethanol to give the diimine, the first report of which dates from 1999. [167] This is then reduced with $NaBH_4$ to give the ligand as a white solid. A crystal structure of the diimine is available (**ROHBOF**, **ROHBOF01**). [163,168].

Potentiometric titrations carried out in 4:1 dioxane-water gave evidence for only two protonation steps (formation of $\mathbf{33}H^+$ and $\mathbf{33}H_2^{2+}$) between pH 2 and 14. [166].

The Cu(II) complex, $[Cu(\mathbf{33})Cl]OTf{\cdot}1.5H_2O$ (**IGOMAS**) [166] has the Cu(II) centre coordinated to all four nitrogen donors of **33**, with the fifth site occupied by a chlorido ligand. The Cu^{2+} ion exhibits a distorted square pyramidal environment, with $\tau_5 = 0.21$. The Cu-$N_{quinoline}$ bond lengths are 2.048 Å and 2.269 Å, Cu-$N_{aliphatic}$ are 2.013 Å and 2.022 Å, and the chlorido ligand sits 2.274 Å from the Cu(II) centre. The N-Cu-N bond angles range between 77.27° and 112.37°, and the N-Cu-Cl bond angles range from 92.87° to 151.55°.

The complex *trans*-$[Fe(\mathbf{33})Cl_2].3CHCl_3$ (Fig. 31, **ONOJIL**) [165] displays a significantly distorted octahedral geometry, with the tetradentate ligand coordinating to the Fe(II) centre through all four nitrogen atoms in an *mm* configuration and the two chlorido ligands situated mutually *trans*. The complex cation displays Fe-$N_{quinoline}$ bond lengths of 2.213 Å and 2.187 Å, and Fe-$N_{aliphatic}$ distances of 2.193 Å and 2.197 Å. The Fe-Cl bond lengths appear to be unusually long at 2.495 Å and 2.509 Å, in comparison to typical Fe(II)-tetraamine complexes where Fe-Cl bond lengths are generally shorter (e.g. 2.397 Å[169] and 2.401 Å [146]). The *trans* N-Fe-N angles are 152.18° and 152.74°, and the *trans* Cl-Fe-Cl angle is 172.90°. The *cis* N-Fe-N angles range from 74.53° to 132.71°, the latter being a $N_{quinoline}$-Fe-$N_{quinoline}$ angle. The *cis* Cl-Fe-N angles range from 84.87° to 95.50°.

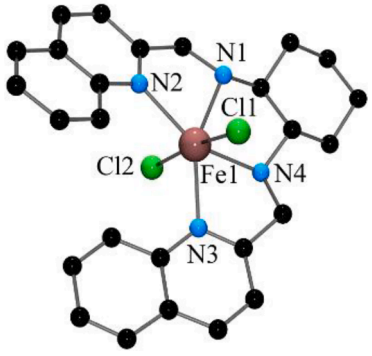

Fig. 31. Structure of the *trans*-$[Fe(\mathbf{33})(Cl)_2]^{2+}$cation. Selected bond lengths (Å) and angles (°): Fe1-N1 2.193, Fe1-N2 2.213, Fe1-N3 2.187, Fe1-N4 2.197, Fe1-Cl1 2.495, Fe1-Cl2 2.509; N1-Fe1-N2 74.53, N2-Fe1-N3 132.71, N3-Fe1-N4 74.80, N4-Fe1-N1 77.96, N1-Fe1-Cl1 95.50, N3-Fe1-Cl1 84.87, N1-Fe1-N3 152.74, N2-Fe1-N4 152.18, Cl1-Fe1-Cl2 172.90.

The complex $[Fe(\mathbf{33})(Cl)(\mu\text{-}O)FeCl_3)]CHCl_3$ (**RECDUB**) [164] is a dimer comprising two Fe(III) centres bridged by a μ-oxido ligand. The six-coordinate Fe(III) centre adopts a very distorted octahedral geometry (one of the *cis* N-Mn-N bond angles is 133.97°) and is coordinated to four nitrogen atoms of ligand **33** in an *mm* configuration, one chlorido ligand, and the bridging oxido ligand, the latter ligands being situated *trans* to each other. The oxido ligand is bound to the second Fe(III) centre (Fe-O-Fe = 150.26°), which is also coordinated to three chlorido ligands and exhibits an almost ideal tetrahedral geometry ($\tau_4 = 0.987$).

Reaction of $Zn(NO_3)_2{\cdot}6H_2O$ with **33** in aqueous methanol, and subsequent crystallisation of the recovered solid from water gives what was purported to be the complex $[Zn(\mathbf{33})O_2NO]NO_3$, and this was studied for use as a fluorescent chemosensor. In fact, the correct formulation of this complex, as evidenced by the crystal structure, is $\{[Zn(\mathbf{33})O_2NO](NO_3)\}_2.[Zn(\mathbf{33})OH_2](NO_3)_2$ (**OZOXEH**), [163] where two octahedral $[Zn(\mathbf{33})NO_3]^+$ and one square pyramidal ($\tau_5 = 0.01$) $[Zn(\mathbf{33})OH_2]^{2+}$ moieties are contained within the asymmetric unit. The octahedral cations feature a Zn(II) metal centre which binds to all four nitrogen atoms of ligand **33** in an *fm* configuration and two oxygen atoms of a bidentate nitrate ligand, while the square pyramidal cation features a Zn (II) ion bonded to all four nitrogen atoms of **33** and the oxygen atom of a monodentate aqua ligand.

Both ligand **33** and its corresponding Zn(II) complex are fluorescent. The ligand alone in HEPES buffer (10 mM, pH 7.4) displayed weak fluorescence at 346 nm ($\lambda_{ex} = 315$ nm) assigned to a PET process. The fluorescence intensity demonstrated no change at 346 nm upon the addition of different +/2+/3 + metal cations to the ligand solution. However, upon addition of Zn(II), there was a noticeable red shift of 30 nm and a significant enhancement in the intensity of the fluorescence observed. It has been suggested that this enhancement may be due to blocking of the PET pathway as a result of complexation of the ligand quinoline nitrogen atoms to the Zn(II) centre.

The pyridyl congener of $[Fe(\mathbf{33})(Cl)_2]$, $[Fe(\mathbf{33}*)(Cl)_2]$ (**COBWEX**), [170] has also been structurally characterised. Interestingly, this displays a *cis* geometry and an *ff* ligand configuration, presumably as a result of the less sterically demanding pyridine rings; a *cis* geometry for $[Fe(\mathbf{33})(Cl)_2]$ would result in unfavourable interactions between the H-8 protons of the quinoline rings and the chlorido ligands.

3.2.7. N,N'-Bis(2-quinolylmethyl)-N,N'-dimethyl-trans-1,2-cyclohexanediamine (34)[144]

The ligand **34**, first reported in 2021, [144] was prepared by the reaction of 2-(chloromethyl)quinoline hydrochloride and *N,N'*-dimethyl-*trans*-1,2-cyclohexanediamine in the presence of K_2CO_3 and KI, in anhydrous MeCN at reflux for two days under N_2. The X-ray structure of the $\bullet HClO_4$ salt (**ONONAJ**) [144] showed protonation of one of the aliphatic nitrogen atoms.

The coordination chemistry of this ligand is limited to the bis(μ-oxo) $Mn_2^{III,III}$ dimer, $[Mn_2(\mu\text{-}O)_2(\mathbf{34})_2](ClO_4)_2$ (**ONOPOZ**)). Both the Mn(III) centres adopt a pseudo octahedral geometry, each coordinated to all four N atoms of one **34** ligand in an *ff* configuration and the two bridging oxido O-atoms. The *trans* $N_{quinoline}$-Mn-$N_{quinoline}$ angles are 161.07° and 162.46°, and the *trans* $N_{aliphatic}$-Mn-O angles range from 166.55° to 168.28°. The *cis* N-Mn-N angles lie between 73.57° and 93.55°, the *cis* N-

Mn-O angles between 93.92° and 99.72°, and the *cis* O-Mn-O angles are 85.57° and 86.05°. The Mn-$N_{quinoline}$ bonds lie along the Jahn-Teller axis and, as a result, are significantly longer (2.438 Å to 2.483 Å) than the Mn-$N_{aliphatic}$ bonds (2.155 Å to 2.164 Å). The Mn-O bond lengths of 1.829 to 1.842 Å give a Mn(III)-Mn(III) separation of 2.691 Å. The crystal structure of the complex cation reveals a π-π stacking interaction between the neighbouring intramolecular quinoline groups from each ligand with a centroid–centroid distance of ~ 3.4 Å.

3.2.8. 1,4-Bis(2-quinolylmethyl)-1,4-diazepane (35) [171–176]

The preparation of **35** from the reaction of 2-(chloromethyl)quinoline and homopiperazine in a basic solution of ethyl acetate was first described in 2007. [171] A subsequently reported method involves the reductive amination reaction between homopiperazine and quinoline-2-carbaldehyde to yield the desired ligand. Similar to the related ligand **24** described above (Section 3.1.2), the paper does not give details of the presumed reduction step. [176].

Two complexes, mononuclear *trans*-[Mn(**35**)$(ClO_4)_2$] (**OMUGOT**) [176] and binuclear [(**35**Ni)$_2$(μ-CO_3)]$(Ph_4B)_2$ (Fig. 32, **FORFOK**) [174] have been structurally characterised. The six-coordinate Mn(II) complex has four coordination sites occupied by N atoms of the ligand **35** in an *mm* configuration and the other two by O atoms of perchlorate ions. The metal ion displays a very distorted octahedral geometry (one N-Mn-N *cis* angle of 139.81°), with *trans* N-Mn-N angles of 138.63° and 142.87°, and 160.33° for the $O_{perchlorate}$-Mn-$O_{perchlorate}$ angle. The *cis* $N_{aromatic}$-Mn-$O_{perchlorate}$ angles range between 82.37° and 95.75°, and the *cis* $N_{aliphatic}$-Mn-$O_{perchlorate}$ angles between 83.31° and 109.57°. The complex displays *cis* N-Mn-N angles of 70.77°, 75.76°, 77.32°, and 139.81°, with the latter deviating significantly from the ideal 90° *cis* angle for an octahedral complex. Mn-N bond lengths range from 2.226 Å to 2.274 Å, and the two Mn-O bonds are 2.209 Å and 2.282 Å in length.

The dimeric complex cation [(**35**Ni)$_2$(μ-CO_3)]$^{2+}$ consists of two Ni(II) centres in distorted octahedral environments that are both coordinated to the N atoms of a **35** ligand in an *mf* configuration and are bridged by all three oxygen atoms of a CO_3^{2-} ligand. The Ni-$N_{aromatic}$ bond distances lie between 2.099 Å and 2.157 Å, the Ni-$N_{aliphatic}$ between 2.080 Å and 2.099 Å, and the Ni-O between 2.010 Å and 2.413 Å. Two of the quinoline ligands bind significantly bent, with the angles between the Ni-$N_{quinoline}$ vector and the aromatic plane around 158°. *Trans* N-Ni-N angles are 158.05° and 158.63° and *trans* N-Ni-O angles lie between 141.16° and 157.78°. The *cis* N-Ni-N angles range from 76.31° to 114.08°, *cis* N-Ni-O angles are from 83.96° to 105.41°, and *cis* O-Ni-O angles are very small, at 58.82° and 59.13°.

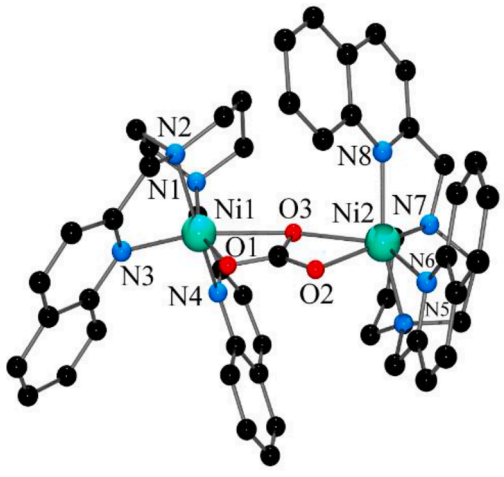

Fig. 32. Structure of the [(**35**Ni)$_2$(μ-CO_3)]$^{2+}$cation. Selected bond lengths (Å) and angles (°): Ni1-N1 2.091, Ni1-N2 2.099, Ni1-N3 2.157, Ni-N4 2.099. Ni1-O1 2.014, Ni1-O3 2.427, Ni2-O2 2.010, Ni2-O3 2.413, Ni2-N5 2.098, Ni2-N6 2.144, Ni2-N7 2.080, Ni2-N8 2.111; N1-Ni1-N2 76.31, N1-Ni1-N3 115.21, N2-Ni-O3 100.52, N4-Ni1-O1 105.06, N2-Ni1-N4 158.05, N1-Ni1-O1 157.78, N3-Ni1-O3 141.16, O1-Ni1-O2 58.82, N5-Ni2-N6 76.60, N6-Ni2-N7 114.08, N6-Ni2-N8 10.56, N8-Ni2-O2 105.41, N5-Ni2-O3 101.10, O2-Ni2-O3 59.13.

The analogous pyridine complex, [(**35***Ni)$_2$(μ-CO_3)]$(ClO_4)_2$·H_2O (**FORGEB**) [174], displays a similar overall geometry.

3.2.9. (2-pyridylmethyl)bis(2-quinolylmethyl)amine) (36) [37,39,91,92,95,99,100,102,103,105–107,177–188]

Ligand **36** was initially synthesised by Karlin and coworkers[99] by reaction of 2-(bromomethyl)quinoline with 2-(aminomethyl)pyridine in THF in the presence of diisopropylethylamine. Purification by column chromatography and recrystallisation afforded the ligand as a white crystalline material. Slight variations of this method have also been reported. [91,177] An alternative approach reported by Das [178] involves the reaction of 2-(aminomethyl)pyridine and 2-(bromomethyl) quinoline in anhydrous DMF in the presence of Cs_2CO_3 in the absence of light.

Six- and five-coordinate complexes of **36** containing Fe, Co, Cu, Zn, and Cd have been structurally characterised, and bond length and angle data for these are summarised in Tables 8 and 9.

Not included in the table above are the four-coordinate Cu^I complexes [Cu(**36**)](BArF), [189] [Cu(**36**)PPh_3]ClO_4 (**PITPUD**) [100] and [Cu(**36**)CO]$B(C_6F_5)_4$ (**SIYTIE**). [180] In [Cu(**36**)](BArF) ligand **36** is tetradentate, with all four N atoms bonded to the Cu(I) ion ($\tau_4 = 0.86$) [189]. However, both the [Cu(**36**-κ^3*N*)PPh_3]$^+$ ($\tau_4 = 0.74$) [100] and [Cu(**36**-κ^3*N*)CO]$^+$ ($\tau_4 = 0.75$)[180] complex ions contain a hypodentate [190,191] **36** ligand, with a quinoline N atom uncoordinated to the metal centre, and the fourth coordination position occupied by the either a PPh_3 or CO ligand. Both complexes display distorted tetrahedral geometries.

The [Zn(**36**)$(H_2O)(ClO_4)$]$^+$ cation (**OZONIB**) [187] adopts a distorted octahedral structure in which the Zn(II) ion is bonded to all four nitrogen atoms of the tetradentate ligand, a water oxygen atom and a perchlorate oxygen atom (Zn–O = 2.58 Å).

The [Cd(**36**-κ^3*N*)$_2$]$^{2+}$ cation (Fig. 33, **SOFGAX**) [186] contains two hypodentate **36** ligands coordinated via the pyridine, aliphatic, and one of the quinoline N atoms, with the dangling quinoline N atoms situated 3.32 Å from the metal centre. The complex displays a pseudo-trigonal prismatic geometry about the Cd(II) ion, with significant interligand π-π interactions.

The bis(μ-fluorido)-bridged complex [Co_2(μ-F)$_2$(**36**)$_2$]$(BF_4)_2$ (**YUJTIJ**) [185] has a distorted octahedral geometry about both metal centres, these being separated by 3.071 Å. The Co(II) oxidation state is confirmed by the Co-N bond lengths, which range from 2.098 Å to 2.178 Å. The quinoline moieties are situated axial with respect to the Co–$(F)_2$-Co plane, and these exhibit intramolecular π-π interactions, with centroid–centroid distances of 3.326 – 3.521 Å.

The complex cations [Fe_2(μ-OH)$_2$(**36***)$_2$]$^{2+}$ (**FEXYEN**, **FEXYIR**), [37] [Co(DBCat)(**36***)]$^+$ (**LIWQUE**), [192] [Co(**36***)Cl]$^+$ (**ALOPOI**, **IGUZUF**, **LUXGAM**, **PAJSIF**, **QALZOT01**, **QAMBAI**, **QAMBAI01**, **RITWOH**, **RITWOH01**, **RITWOH02**), [90,111–116] and [Cu(**36***-κ^3*N*)PPh_3]$^+$ (**ILUVER**, **PEGDEK**) [123,193], which contain the analogous pyridine ligand, are structurally very similar to their quinoline congeners.

The [Cu(**36***)Cl]$^+$ cation (**AKISIZ**, **AQUFIC**, **BUBCIK**, **EBAWIN**, **GIHWOK**, **GIHWOK01**, **ILUVIV**, **ILUVOB**, **YEZGAN**) [122–127] exhibits a similar distorted trigonal bipyramidal geometry about the Cu(II) ion to [Cu(**36**)Cl]$^+$, which itself is interestingly not square pyramidal like the analogous monoquinolyl (ligand **27**) and triquinolyl (ligand **37**) complexes. However, the same is not true of the [Cu(**36***)H_2O]$^+$ (**EJIMOB**, **RABFUV**, **WODYEV**, **WODYEV01**, **WOFPIT**) [194–198] and [Cu(**36**)H_2O]$^+$ cations; the former is trigonal bipyramidal ($\tau_5 = 0.94$–0.99) while the latter approaches a square pyramidal structure ($\tau_5 = 0.07$).

Significant differences are also observed for the pyridine analogues of [Cu(**36**)CO]$B(C_6F_5)_4$ and [Cd(**36**)$_2$]$^{2+}$. In the absence of the two quinoline groups, the tetradentate pyridine ligand **36*** binds via all four

Table 8
Six-coordinate complexes of **36.**

Complex	*Trans* N-M-N/°	*Trans* X-M-N/°	*Cis* N-M-N/°	*Cis* X-M-N/°	*Cis* X-M-X /°	M-$N_{quinoline}$/ Å	M-$N_{tertiary}$/ Å	M-$N_{pyridine}$/ Å	M-X/ Å	Ref
cis-[Fe(**36**)(H_2O)(ClO_4)](ClO_4) (**EBOSAP**)	153.29 170.85	165.37 170.85	75.89 78.39 81.22 89.03 94.06	91.72 107.80 112.58 83.11 89.64 89.66	81.04	2.172 2.202	2.197	2.184	2.094 2.262	[92]
[Fe_2(μ-OH)$_2$(**36**)$_2$] (CF_3SO_3)$_2$.2MeCN (**FEXYOX**)	149.27	174.17 175.66	74.63 74.79 78.39 82.16 88.86	90.05 95.80 95.94 101.89 103.88 108.80	81.89	2.288 2.306	2.242	2.170	1.984 2.101	[37]
[Fe_2(O)(OH)(**36**)$_2$](ClO_4)$_3$.MeCN (**JUQKEL**)	150.21	176.30 177.65	75.18 75.66 80.49 84.15 85.19	94.06 94.86 95.92 101.34 103.46 105.88	82.22	2.204 2.208	2.197	2.143	1.896 1.943	[188]
[{Co(**36**)}$_2$μ-(BP)] (PF_6)$_2$.6CH_3COCH_3 (**IWOCEF**)	168.23	172.48 172.53	82.41 85.82 86.66 89.02 90.25	85.87 89.27 89.92 95.10 96.58 100.79	86.66	1.914 2.027	1.951	1.911	1.869 1.891	[105]
[Cd(**36**-κ^3*N*)$_2$](ClO_4)$_2$.2MeOH (**SOFGAX**)	133.89 153.05 153.70	69.81 69.81 70.01 70.01 80.16 90.12 90.12 103.64 103.64 110.76 110.76 153.70				2.460 2.460	2.446 2.446	2.342 2.342		[186]
[Co_2(μ-F)$_2$(**36**)$_2$](BF_4)$_2$.Et_2O. MeOH (**YUJTIJ**)	157.33	171.34 172.16	78.48 78.93 82.91 87.37 87.99	88.34 89.83 93.47 100.19 102.42 105.69	81.53	2.168 2.178	2.136	2.098	1.977 2.077	[185]
[Co(DBCat)(**36**)]PF_6.2MeOH (**KUGJOO**)	156.08	172.31 175.77	77.65 78.67 82.76 87.01 93.34	84.23 93.32 93.81 99.11 103.96 104.50	79.34	2.139 2.164	2.141	2.166	1.973 2.145	[177]
cis-[Zn(**36**)(H_2O)(ClO_4)]ClO_4. EtOH.Et_2O (**SOFFUQ**)	155.58	163.18 169.47	77.8179.85 84.46 93.09 94.44	82.12 85.08 86.28 98.42 100.13 112.27	78.15	2.101 2.170	2.160	2.114	1.998 2.577	[92]

available nitrogen donors to afford the five-coordinate carbonyl complex, [Cu(**36***)CO]$^+$ (**SIYTOK**). [180] Likewise, the smaller **36*** ligand allows formation of the eight-coordinate Cd(II) complex cation [Cd(**36***)$_2$]$^{2+}$ (**VIQLOW**, **YAQRAL**), [199,200] in which each **36*** ligand binds using four N atoms.

3.3. Tetradentate ligands containing three quinolyl moieties

The structure of this ligand is given in Fig. 34.

3.3.1. Tris(2-quinolylmethyl)amine (37) [37,90,99,100,102,105–107,186,186,186,201–212]

The C_{3v} symmetrical ligand **37** was first reported in 1994[100] alongside the ligands **27** and **36**. These three quinoline-containing ligands and the pyridyl analogue tris(2-pyridylmethyl)amine make up a pseudo-homologous series of ligands that differ only in the number of pyridine and quinoline units. **37** was originally prepared by the reaction of 2-(bromomethyl)quinoline and ammonium hydroxide in THF, and there is a minor adaption of this method available. [212] Ligand **37** has also been synthesised by a reductive amination involving reaction of 2-(aminomethyl)quinoline hydrochloride and quinoline-2-carbaldehyde in dichloromethane in the presence of Na_2CO_3, with $NaBH(OAc)_3$ as the reductant.

Potentiometric titration data in H_2O gave evidence for protonation of three of the four nitrogen atoms, with pK_a values of 6.3(1), 3.0(1), and 2.49(2). Equilibrium constants (log *K*) measured in H_2O (289.1 K), for the reaction of the ligand with Zn^{2+}, Cd^{2+} and Pb^{2+} are 8.7(2), 8.7(2), and 8.6(2) respectively, reflecting a relatively modest affinity of the ligand for these three metal ions.

The free **37** ligand exhibits an emission peak at 390 nm upon

Table 9
Five-coordinate complexes of **36.**

Complex	N-M-N/°	N-M-X /°	M-$N_{quinoline}$/Å	M-$N_{tertiary}$/Å	M-$N_{pyridine}$/Å	M-X/Å	τ_5	ref
[Co(**36**)Cl]ClO_4 (**CIJTOH**)	75.84 76.15 77.93 106.96 116.20 121.07	94.69 103.24 113.36 168.07	2.141 2.145	2.160	2.124	2.284	0.78	[90]
[Cu(**36**)Cl]PF_6 (**CIXWOY**)	79.03 79.61 81.02 103.41 114.50 132.70	94.02 99.31 109.27 171.07	2.111 2.251	2.025	2.073	2.226	0.64	[91]
[Cu(**36**)H_2O]$(ClO_4)_2$·1.5H_2O (**OZONIB**)	81.37 83.18 83.69 91.76 94.36 163.05	92.31 98.80 117.57 159.04	2.011 2.205	2.055	1.977	2.015	0.07	[187]
[Co(**36**)Cl]PF_6 (**SOBSUZ**)	75.97 76.66 78.68 106.64 114.33 124.12	94.25 101.44 114.88 166.15	2.136 2.137	2.163	2.135	2.284	0.70	[95]

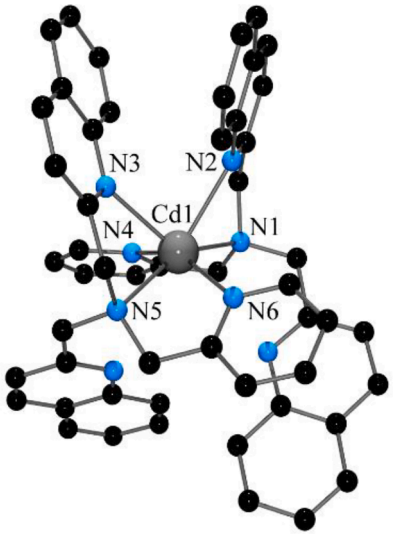

Fig. 33. Structure of the $[Cd(\mathbf{36})_2]^{2+}$cation. Selected bond lengths (Å) and angles (°): Cd1-N1 2.446, Cd1-N2 2.460, Cd1-N3 2.460, Cd1-N4 2.342, Cd1-N5 2.446, Cd1-N6 2.342; N1-Cd1-N2 69.81, N1-Cd1-N4 70.01, N2-Cd1-N3 80.16, N3-Cd1-N4 90.12, N3-Cd1-N6 110.76, N4-Cd1-N5 69.81, N4-Cd1-N5 103.64, N1-Cd1-N6 103.64, N1-Cd1-N5 153.70, N2-Cd1-N5 133.89, N4-Cd1-N6 153.05.

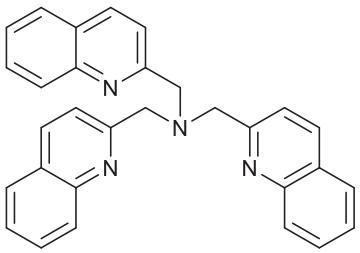

(37)

Fig. 34. Structure of the tetradentate ligand containing three quinolyl moieties.

excitation at 317 nm in a methanol/water mix (1:1). However, in the presence of a number of metal ions, emission peaks were observed at 445 nm for the 1:1 complexes with Cd^{2+} and Zn^{2+}, while negligible fluorescence was observed for the other complexes. The greatest fluorescence intensity was observed for the Zn/**37** complex, followed by the Cd/**37** complex. This observation was rationalised by the idea that distortion of the Zn-N bond length leads to quenching of the CHEF effect in Zn(II) complexes. However, the reported structure of $[Zn(\mathbf{37})H_2O]^{2+}$ reveals no evidence of any such bond length distortion in this complex. [203].

The structurally characterised five- and six-coordinate complexes containing the ligand **37** are summarised in Tables 10 and 11. Not included in this table are the free ligand as the ethanol solvate (**CUBDIN**), [203] four-coordinate [Cu(**37**)]ClO_4 (**PITRAL**), [100] and eight-coordinate [Pb(**37**)$(NO_3)_2$].C_2H_5OH (Fig. 35, **CUBDUZ**). [203] The free ligand adopts a tripodal conformation, albeit with the quinoline donor atoms on the 'wrong' side for preorganised metal binding. The $[Cu(\mathbf{37})]^+$ cation in [Cu(**37**)]ClO_4 displays an approximate trigonal pyramidal geometry about the metal ion (τ_4 = 0.77, 0.83), and intermolecular (or more correctly, interionic) π-π interactions are present (centroid–centroid distances of 3.66 Å). In [Pb(**37**)$(NO_3)_2$].C_2H_5OH, the eight coordination sites are occupied by four nitrogen donors from the **37** ligand and four oxygen atoms from two bidentate nitrato ligands, both of which are bound asymmetrically. The structure provides evidence for the presence of a stereochemically active lone pair.

The $[Ag(\mathbf{37})OClO_3]^+$ cation (**CUBDOT**) [203] stands out in being essentially trigonal bipyramidal while the other five-coordinate complexes tend towards square pyramidal. This appears to be a result of the long Ag-O bond (2.572 Å) in this cation, which minimises interaction of the ancillary ligand with the quinoline moieties. The analogous bonds in the other complexes are 1.982 Å, 2.000 Å, and 2.244 Å.

The $[Mn(CO)_3(\mathbf{37}\text{-}\kappa^3N)]^+$ cation (**KUKQIT**) [208] exhibits hypodentate coordination of the quinoline ligand, which binds in a *fac* configuration. The bis-(μ-chlorido) and bis-(μ-oxido) dimeric cations $[Co_2(\mu\text{-}Cl)_2(\mathbf{37})_2]^{2+}$ (**CIJVAV**) [90] and $[Mn_2(\mathbf{37})_2(\mu\text{-}O)_2]^{2+}$ (**EFUJAT**, **HUJQUB**) [209,210] both feature extensive intramolecular interligand π-π interactions, which results in clefts above and below the bridging ligands (centroid–centroid distances range from 3.611 Å to 3.857 Å). The incorporation of bulkier acetate bridging ligands in the $[Mn_2(\mathbf{37})_2(\mu\text{-}OAc)_2]^{2+}$ cation (**EFUJEX**) [209] disrupts these interactions.

Several pyridyl analogues of the complexes above have been

Table 10
Five-coordinate complexes of **37.**

Complex	N-M-N/^{o}	N-M-X /^{o}	M-$N_{quinoline}$/Å	M-$N_{tertiary}$/Å	M-X /Å	τ_5	Ref
[Ag(**37**)($OClO_3$)] (**CUBDOT**)	69.32 69.86 70.88 103.96 110.84 112.04	104.08 109.04 116.03 172.59	2.396 2.416 2.426	2.484	2.572	0.94	[203]
[Zn(**37**)H_2O](ClO_4)$_2$·0.5H_2O (**CUBFAH**)	77.17 80.50 85.59 86.30 97.99 156.84	93.42 103.14 123.70 150.47	2.082 2.153 2.162	2.132	2.000	0.106	[203]
[Cu(CH_3CN)(**37**)](ClO_4)$_2$ (**NAYPEK**)	80.63 82.94 84.43 89.73 91.14 163.38	94.19 96.63 136.21 139.31	2.028 2.030 2.127	2.075	1.982	0.40	[213]
[Cu(**37**)Cl]PF_6.MeCN.0.5Et_2O (**YEXSID**)	80.41 81.66 83.17 89.45 91.36 161.82	91.91 94.01 118.51 158.24	2.030 2.033 2.103	2.143	2.244	0.06	[99]

structurally characterised. The [Mn_2(**37***)$_2$(μ-O)$_2$]$^{2+}$ cation in [Mn_2(**37***)$_2$(μ-O)$_2$]($Ce_2O_2NO)_{10}$(μ-O)) (**PINXUH**) [215] exhibits π-π interactions comparable to those observed in the analogous quinoline complex, while the same cation in [Mn_2(**37***)$_2$(μ-O)$_2$](BF_4)$_2$ (**NAPYIN**, **NAPYIN01**) [216,217] has the pyridyl rings on the neighbouring ligands bent away from each other. The pyridyl analogue of [Mn_2(**37**)$_2$(μ-OAc)$_2$]$^{2+}$ (**PIFVUV**, **XESVOH**) [218,219] has a similar geometry to the quinoline complex, as do the monomeric [Fe(**37***)(OSO_2CF_3)$_2$] (**NELGAM**), [109] [Mn(**37***)(CO)$_3$]$^{+}$ (**IYERAH02**, **PODQOQ**) [220,221] (the former has the free pyridine situated further from the metal ion though), and [Cu(**37***)]$^{+}$ (**ILUTIT**) [123] complexes. The [Cu(**37***)$NCCH_3$]$^{2+}$ cation (**HEQWEF**, **HEQWEF01**, **XEZXEH**), [222–224] adopts a very different geometry from its quinolyl congener, being essentially trigonal bipyramidal (τ_5 values range from 0.84 to 1.03). This is most likely due to the MeCN ligand being free from destabilising interactions with the quinolyl protons in a trigonal bipyramidal geometry. The same difference, although even more pronounced, is seen in the [Cu(**37***)Cl]$^{+}$ cation (**AKISIZ**, **AQUFIC**, **BUBCIK**, **EBAWIN**, **GIHWOK**, **GIHWOK01**, **ILUVIV**, **ILUVOB**, **YEZGAN**), [122–127,197,225] which is trigonal bipyramidal (τ_5 values range from 0.87 to 1.04), [226] in contrast to the quinolyl analogue (τ_5 = 0.06).

4. Pentadentate ligands

4.1. Pentadentate ligands containing two quinolyl moieties

The structures of these ligands are given in Fig. 36.

4.1.1. N,N-bis(2-quinolylmethyl)-N-bis(2-pyridyl)methylamine (38) [87]

The synthesis of the pentadentate ligand **38** was achieved from the reaction of 2-(bromomethyl)quinoline and di(pyridine-2-yl) methanamine in THF. Following purification on a Dowex cation exchange column, the ligand was isolated as its tetrahydrochloride salt. [87] The complexes of **38** that have been structurally characterised are [Mn(**38**)(OH_2)](OTf)$_2$·2H_2O (**CAWWOP**), [227] [Mn(**38**)(OTf)](OTf).Et_2O (**CAWWUV**), [227] [Fe(O)(**38**)](ClO_4)$_2$·H_2O (**JIKZUB**), [228] [Fe(**38**)(OTf)](OTf)$_2$.C_7H_8 (**OGEKOD**), [229] [Fe(**38**)(Cl)]$FeCl_4$.MeCN (**OGELAQ**), [229] [Fe(**38**)(Br)]$FeBr_4$.MeCN (**OGEKUJ**), [229] [Fe(**38**)(Cl)](ClO_4).2$CHCl_3$ (**OGELUK**), [229] [Fe(**38**)(Br)](ClO_4).2$CHCl_3$ (**OGELOE**), [229] [Cu(**38**)(NO_3)](NO_3)0·.5H_2O (**TUBHEF**), [87] [Cu(**38**)(NO_3)](NO_3) (**WUYQOZ**), [230] [Zn(**38**)($NCCH_3$)](ClO_4)$_2$.CH_3CN (**TUBHOP**), [87] [Cu(**38**-κ^3*N*)($NCCH_3$)]OTf.MeCN (**WUYQUF**), [230] [Fe(**38**)(OH_2)](OTf)$_2$·H_2O0.8C_8H_{10} (**AXUNEP**), [231] [Fe(**38**)(OH_2)](OTf)$_2$·2H_2O (**WAWKEO**), [232] [Fe(**38**)($NCCH_3$)](ClO_4)$_2$ (**WAWPET**), [232] [{Fe(**38**-κ^3*N*)(OH_2)}$_2$(μ-O)](ClO_4)$_4$.0.5MeCN.1.5EtOAc (**WAWPIX**), [232] [{Fe(**38**-Bz)($NCCH_3$)}$_{0.9}${Fe(**38**)($NCCH_3$)}$_{0.1}$](BF_4)$_2$.MeCN (**WAWPOD**), [232] [Fe(**38**)(Cl)]ClO_4.3.5C_6H_6 (**WAWPUJ**)[232]. All of the six-coordinate complexes display a slightly distorted pseudo-octahedral geometry with **38** coordinating through the five nitrogen donors and the metal ion sitting above the plane of the equatorial aromatic N donor atoms. The Cu(I) complex cation [Cu(**38**-κ^3*N*)($NCCH_3$)]$^{+}$ features a hypodentate **38** ligand which binds to the metal ion through 3 N atoms to give what is best described as a distorted trigonal pyramidal geometry (τ_4 = 0.74). [190,191].

The complex [Cu(**38**)(NO_3)](NO_3) (**WUYQOZ**), [230] adopts a distorted octahedral geometry, with a monodentate nitrato ligand bound opposite the aliphatic N atom, and the Cu(II) ion situated 0.434 Å above the equatorial plane. A Jahn-Teller axis involving one quinoline N atom (Cu-N = 2.425 Å) and a pyridine N atom (Cu-N = 2.534 Å) makes these Cu-N bonds significantly longer than the two others in the equatorial plane (2.096 Å and 2.045 Å, respectively). The Cu-O bond length is 1.965 Å. The *cis* N-Cu-N angles range from 73.37° to 100.11° and the *cis* N-Cu-O angles range from 91.06° to 114.94°. The *trans* N-Cu-N angles are 151.15° and 160.53°, and the N-Cu-O angle is 167.15°. The nitrato ligand is oriented such that the unbound O atoms point towards the pyridine rings, owing to steric hindrance from the quinoline H atoms. [87].

The Mn-N bonds in in the [Mn(**38**)(OH_2)]$^{2+}$ (**CAWWOP**), [227] and [Mn(**38**)(OTf)]$^{2+}$ (**CAWWUV**), [227] cations are all > 2.2 Å, consistent with high-spin Mn(II). [227] The metal ions sit 0.577 Å and 0.560 Å respectively, above the mean plane of the of the aromatic nitrogen donor atoms.

The [Fe(**38**)(O)]$^{2+}$ cation (Fig. 37, **JIKZUB**) [228] is a rare example of a crystallographically characterised Fe(IV)-oxo complex. [228] Bond angles within the cation are 161.47° and 160.74° for *trans* N-Fe-N, 170.46° for *trans* O = Fe-N, and between 79.01°-82.36° and 93.47°-105.36° for *cis* N-Fe-N and O = Fe-N, respectively. Fe-N bond lengths range between 2.022 Å and 2.084 Å, and the Fe = O bond has a length of 1.677 Å. The oxo ligand sits ~ 2.15 Å away from the nearest quinoline protons, whereas the closest pyridine protons lie 2.702 Å and 2.731 Å away. As a result, the oxo ligand is slightly tilted towards the pyridine rings, a structural feature which the authors contend assists the

Table 11
Six-coordinate complexes of **37**.

Complex	*Trans* N-M-N/°	*Trans* X-M-N/°	*Cis* N-M-N/°	*Cis* X-M-N/°	*Cis* X-M-X/°	M-$N_{quinoline}$/Å	M-$N_{tertiary}$/Å	M-X/Å	Ref
$[Co_2(\mu\text{-}Cl)_2(\mathbf{37})_2](ClO_4)_2.0.7MeOH{\cdot}0.3H_2O$ (**CIJVAV**)	157.37	165.67 166.92	77.87 79.57 84.14 91.48 94.22	85.29 88.11 88.31 100.45 101.12 111.60	81.69	2.185 2.191 2.236	2.126	2.327 2.602	[90]
$[Mn_2(\mathbf{37})_2(\mu\text{-}O)_2](ClO_4)_2$ (**EFUJAT**)	147.36	172.26 175.60	74.15 74.58 82.44 82.45 84.40	89.88 94.52 94.57 101.91 105.19 106.71	85.75	2.145 2.361 2.383	2.114	1.824 1.829	[209]
$[Mn_2(\mathbf{37})_2(\mu\text{-}OAc)_2](ClO_4)_2{\cdot}4.5H_2O$ (**EFUJEX**)	146.08	164.49 169.26	73.64 76.01 77.01 83.08 90.65	85.61 86.47 92.02 97.83 103.70 112.52	92.79	2.280 2.330 2.373	2.263	2.058 2.148	[209]
cis-$[Mn(\mathbf{37})(MeCN)(ClO_4)]ClO_4.MeCN$ (**EFUJOB**)	150.08	165.69 168.87	74.48 75.79 79.59 83.90 93.90	80.13 82.67 86.27 94.77 103.92 104.60 111.51	82.67	2.254 2.290 2.294	2.239	2.174 2.257	[209]
$[Fe(\mathbf{37})(OTf)_2]$ (**FOXROB**)	153.99	167.65 172.98	75.52 78.55 80.02 82.40 91.12	87.79 87.80 93.24 100.64 105.36 106.12	86.16	2.195 2.215 2.231	2.175	2.045 2.197	[205]
$[Mn_2(\mathbf{37})_2(\mu\text{-}O)_2]MnCl_4.4DMF$ (**HUJQUB**)	147.11	172.92 175.72	74.19 74.77 82.12 83.40 83.89	91.44 93.66 95.67 101.48 105.30 106.23	84.96	2.159 2.328 2.342	2.138	1.828 1.840	[210]
$[Co(\mathbf{37})(DBSQ)]PF_6.2MeOH$ (**KUGJUU**)	155.45	172.03 175.10	77.69 77.82 82.33 88.29 90.26	88.52 90.85 92.77 101.36 102.63 105.62	79.28	2.159 2.206 2.213	2.130	2.042 2.080	[177]
$[Mn(CO)_3(\mathbf{37}\text{-}\kappa^3N)]Br{\cdot}3H_2O$ (**KUKQIT**)		171.60 174.21 176.84	78.01 82.01 87.18	91.22 91.27 92.21 97.11 99.07 104.74	80.99 85.93 90.05	2.093 2.106	2.101	1.793 1.817 1.821	[208]
cis-$[Cd(\mathbf{37})(CH_3CN)(ClO_4)]ClO_4.MeCN$ (**SOFGEB**)	146.82	163.12 168.12	73.18 74.06 77.38 84.09 93.78	77.10 81.92 86.32 95.74 105.38 105.57 114.48	81.92	2.323 2.350 2.356	2.337	2.246 2.433	[186]
cis-$[Co(\mathbf{37})(OIPh)(OH)](CF_3SO_3)_2.2MeCN$ (**SUNZIN**)	166.89	171.70 174.93	81.11 85.20 86.14 88.99 92.97	87.24 89.68 89.83 92.47 99.92 100.47	84.58	1.987 2.013 2.039	1.950	1.877 1.900	[214]
cis-$[Co(\mathbf{37})(CF_3SO_3)(CH_3CN)]CF_3SO_3.2MeCN$ (**SUNZOT**)	156.78	170.89 174.01	77.51 79.34 82.65 85.69 93.15	85.60 88.27 91.90 101.19 101.65 103.29	85.80	2.181 2.195 2.197	2.123	2.077 2.184	[214]
$[Co_2(BP)(\mathbf{37})_2](PF_6)_2.6Me_2CO$ (**IWOCAB**)	156.43	170.37 173.72	78.13 78.54 82.58 86.74 93.54	83.14 91.50 94.18 100.19 102.25 107.03	78.87	2.148 2.202 2.237	2.121	1.983 2.150	[105]

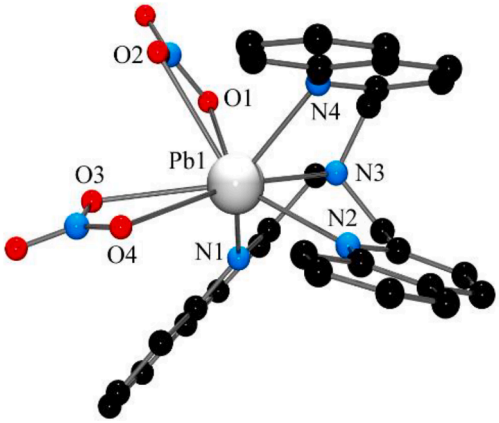

Fig. 35. Structure of the $[Pb(\mathbf{37})(NO_2)_2]^{2+}$cation. Selected bond lengths (Å) and angles (°): Pb1-N1 2.642, Pb1-N2 2.681, Pb1-N3 2.550, Pb1-N4 2.621, Pb1-O1 2.467, Pb1-O2 2.914, Pb1-O3 2.882, Pb1-O4 3.047; N1-Pb1-N2 94.42, N1-Pb1-N3 63.54, N2-Pb1-N4 69.84, N1-Pb1-O4 114.75, N4-Pb1-O1 86.75, O2-Pb1-O3 63.33.

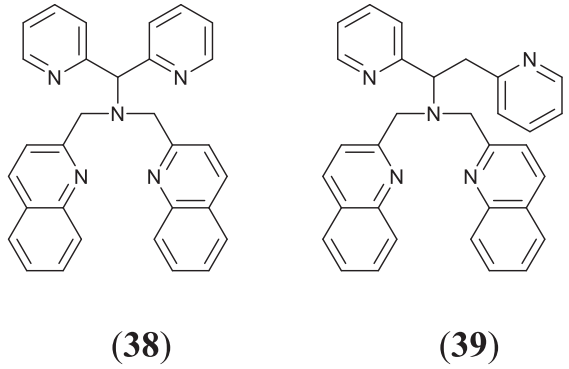

(38) **(39)**

Fig. 36. Structures of the pentadentate ligands containing two quinolyl moieties.

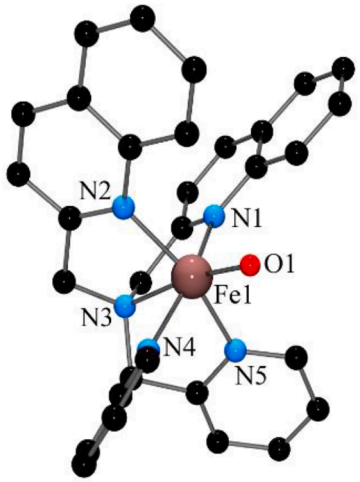

Fig. 37. Structure of the $[Fe(\mathbf{38})(O)]^{2+}$ cation. Selected bond lengths (Å) and angles (°) Fe1-N1 2.073, Fe1-N2 2.067, Fe1-N3 2.084, Fe1-N4 2.002, Fe1-N5 2.023, Fe1-O1 1.677; N1-Fe1-O1 105.36, N2-Fe1-O1 103.89.

oxidative reactivity of the complex.

A similar structural situation is seen in the $[Zn(\mathbf{38})(CH_3CN)]^{2+}$ cation (**TUBHOP**), [87] where the CH_3CN ligand is bent away from the two quinoline groups towards the less bulky pyridines (Zn-N-C = 164.97°). [87] In contrast, the CH_3CN ligand in the hypodentate complex $[Cu(\mathbf{38}\text{-}\kappa^3N)(CH_3CN)]^+$ (Fig. 38, **WUYQUF**), [230] where ligand **38** binds in a tridentate fashion through the quinoline and aliphatic N atoms, experiences no such steric effects and binds essentially linear (Cu-N-C = 177.31°). [108] This complex also exhibits an interesting π-π interaction between the coordinated acetonitrile and one of the free pyridines of the hypodentate **38** ligand; these align almost parallel, with the acetonitrile ligand at a distance of ~ 3.4 Å from the plane of the pyridine (Fig. 38).

Several complexes of the analogous tetrapyridine ligand **38*** have been structurally characterised. The cations of both [Mn(**38***)(OTf)] $(OTf)_{0.5}(ClO_4)_{0.5}$ (**KICGAG**) [233] and [Mn(**38***)(OTf)](OTf) (**TIWMIX**) [234] exhibit very similar geometries to that of $[Mn(\mathbf{38})(OTf)]^+$.

The structure of $[Fe(O)(\mathbf{38}^*)](ClO_4).CH_3CN$ (**PASREH**) [235] is also similar to the analogous quinoline complex, with the major difference being that the oxo ligand coordinates in a linear, rather than tilted, fashion, owing to the absence of the sterically hindering quinoline H atoms (*trans* O = Fe-N = 179.40°).

The corresponding pyridine complex of $[Cu(\mathbf{38})(NO_3)](NO_3)$ (**TUBHAB**) [87] also has the Cu(II) ion positioned in a distorted octahedral geometry, and the overall structures of both cations are again similar, the major difference being the orientation of the monodentate nitrato ligand.

However, the analogous pyridine complex of $[Cu(\mathbf{38})(NCCH_3)]OTf.CH_3CN$ (**HICYIE**) [236] adopts a completely different structure. In the absence of the sterically imposing quinoline groups, the pyridine ligand can coordinate to the metal cation via all five available nitrogen donor atoms. As a result, the $[Cu(\mathbf{38}^*)(NCCH_3)]^+$ cation exhibits a distorted octahedral geometry, with essentially linear coordination of the acetonitrile ligand (Cu-N-C = 175.42°).

4.1.2. *N,N-bis(2-quinolylmethyl)-1,2-di(2-pyridyl)ethylamine (39)* [237]

The asymmetric ligand **39** was prepared from the reaction of *N,N*-bis (2-pyridylmethyl)-1,2-di(2-pyridyl)ethylamine, itself prepared by reduction of 1-(2-quinolyl)-2-(2-pyridyl)ethanone oxime, with 2-(chloromethyl)quinoline in refluxing MeCN for 20 h, in the presence of a 20-fold excess of K_2CO_3. The ligand was isolated as a light brown solid. [237].

Two complexes containing this ligand have been structurally characterised. In $[Fe(\mathbf{39})(Cl)]ClO_4.CH_3COCH_3.CH_3CO_2CH_2CH_3$ (**NIMFAT**), [237] the Fe^{2+} ion displays an octahedral geometry, coordinating to all five nitrogen atoms of the L ligand with the sixth coordination site occupied by a Cl^- ligand. *Trans* N-Fe-N angles range from 167.09° to 169.66°, and values of *cis* N-Fe-N angles lie between 79.25° and 104.48°.

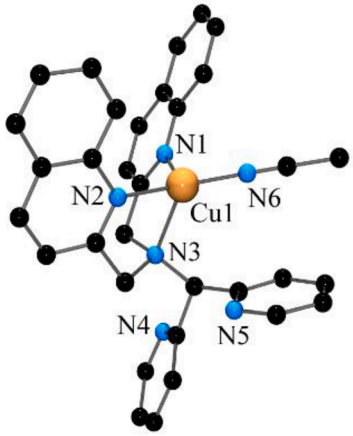

Fig. 38. Structure of the $[Cu(\mathbf{38}\text{-}\kappa^3\mathbf{N})(CH_3CN)]^+$ cation showing the MeCN and pyridyl π-π interaction. Selected bond lengths (Å) and angles (°) Cu1-N1 2.055, Cu1-N2 2.046, Cu1-N3 2.213, Cu1-N6 1.903; N1-Cu1-N6 119.11, N2-Cu1-N6 127.93, N3-Cu1-N6 127.65, N1-Cu1-N2 107.39.

Fe-N bond lengths lie in the range 2.203 Å to 2.292 Å, and the Fe(II) cation is positioned 0.438 Å above the plane of the of the aromatic nitrogen donor atoms. The complex [Mn(**39**)OSO_2CF_3](CF_3SO_3).Et_2O (**GEBPEM**) [238] also has the metal ion in an octahedral geometry and sitting out of the plane of the equatorial donor atoms. Both structures are very similar to those of their analogues in Section 4.1.1.

5. Hexadentate ligands

5.1. Hexadentate ligands containing one quinolyl moiety

The structure of this ligand is given in Fig. 39.

5.1.1. N,N,N' -tris(2-pyridylmethyl)-N'-(2-quinolylmethyl)ethane1,2-diamine (40) [239]

Although the synthesis of **40** has not been reported, the complex [Zn(**40**)]$(ClO_4)_2$ (Fig. 40, **BIZHAU**) [239] has been structurally characterised. The Zn(II) cation displays a highly distorted octahedral geometry with *trans* N-Zn-N angles ranging from 156.04° to 170.80°, and values of *cis* N-Zn-N angles between 77.09° and 125.00°. Zn-N bond distances range from 2.130 Å to 2.229 Å, with the Zn-$N_{quinoline}$ bond being 2.138 Å.

5.2. Hexadentate ligands containing two quinolyl moieties

The structure of this ligand is given in Fig. 41.

5.2.1. N,N' -bis(2-pyridylmethyl)-N,N'-bis(2-quinolylmethyl)ethane-1,2-diamine (41) [239]

Ligand **41** was prepared from the reaction of 2-(chloromethyl) quinoline hydrochloride and *N,N'*-bis(2-pyridylmethyl)ethylenediamine in anhydrous MeCN in the presence of K_2CO_3 and KI. [240] Like **40**, there is only a single structurally characterised complex of **41**, namely [Zn(**41**)]$(ClO_4)_2{\cdot}H_2O$ (**BIZHEY**). [239] This displays a distorted octahedral geometry, very similar to that of [Zn(**40**)]$(ClO_4)_2$; *trans* N-Zn-N angles range from 153.5° to 173.98°, and *cis* N-Zn-N angles lie between 75.40° and 129.83°. Zn-N bond lengths range from 2.120 Å to 2.217 Å, with the Zn-$N_{quinoline}$ bonds both being 2.217 Å.

5.3. Hexadentate ligands containing three quinolyl moieties

The structures of these ligands are given in Fig. 42.

5.3.1. 1,4,7-tris-(2-quinolinylmethyl)-1,4,7-triazacyclononane (42) [85,241]

1,4,7-tris-(2-quinolinylmethyl)-1,4,7-triazacyclononane (**42**) can be prepared by reaction of 2-(chloromethyl)quinoline and 1,4,7-triazacyclononane in anhydrous toluene in the presence of KOH, [85] or alternatively from the reaction of 1,4,7-triazacyclononane with 2-(bromomethyl)quinoline in THF, in the presence of triethylamine. [242].

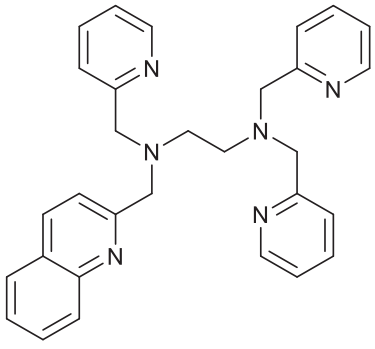

(40)

Fig. 39. The structure of the hexadentate ligand containing one quinolyl moiety.

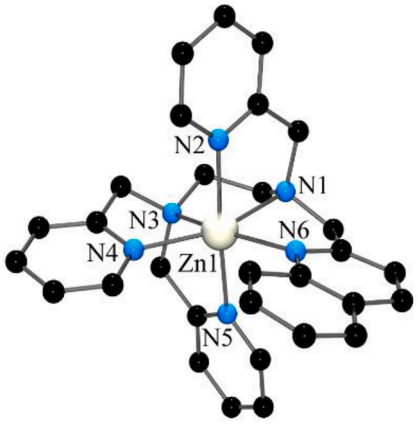

Fig. 40. Structure of the $[Zn(\mathbf{40})]^{2+}$ cation. Selected bond lengths (Å) and angles (°)Zn1-N1 2.229, Zn1-N2 2.130, Zn1-N3 2.190, Zn1-N4 2.181, Zn1-N5 2.182, Zn1-N6 2.138; N1-Zn1-N3 81.95, N3-Zn1-N4 77.09, N4-Zn1-N6 125.00, N3-Zn1-N6 156.04, N1-Zn1-N4 157.41.

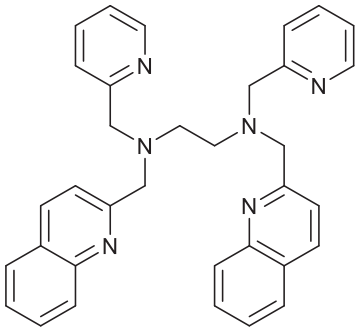

(41)

Fig. 41. The structure of the hexadentate ligand containing two quinolyl moieties.

Potentiometric titration data in MeCN/H_2O (1:1) gave evidence for protonation of only four of the six nitrogen atoms, with pK_a values of 9.94(4), 4.07(7), 2.99(7) and 1.8(1). This mirrors the behaviour of the analogous trispyridyl ligand, **42***, which also exhibits only four pK_a values (11.07(2), 5.07(2), 3.55(2), and 1.78(3)), suggesting this to be the more basic of the two ligands. [243] Equilibrium constants (log *K*) measured in MeCN/H_2O (0.1 M NMe_4Cl, 289.1 K), for the reaction of the ligand with Cu^{2+}, Zn^{2+}, Cd^{2+}, Hg^{2+} and Pb^{2+} are > 17, 14.2(1), 12.5(1), 13.9(1), and 11.8(2) respectively. The authors contended that the trend in these values appears to contradict what might be expected on the basis of metal ion size, as the larger metal cations should be better accommodated by the relatively large ligand with less steric crowding. However, the potentiometric data show that the Zn(II) complex is over 5 orders of magnitude more stable than the complex of the larger Pb(II) ion (>17 vs. 11.8(2)). Therefore, the authors concluded that steric crowding is not the main contributing factor contributing to the stability of complexes containing this ligand. However, log *K* values for the less sterically demanding trispyridyl ligand with Cu^{2+} and Zn^{2+} are 27.4(1) and 17.25(4) respectively. [243].

Selected bond lengths and angles for the structurally characterised

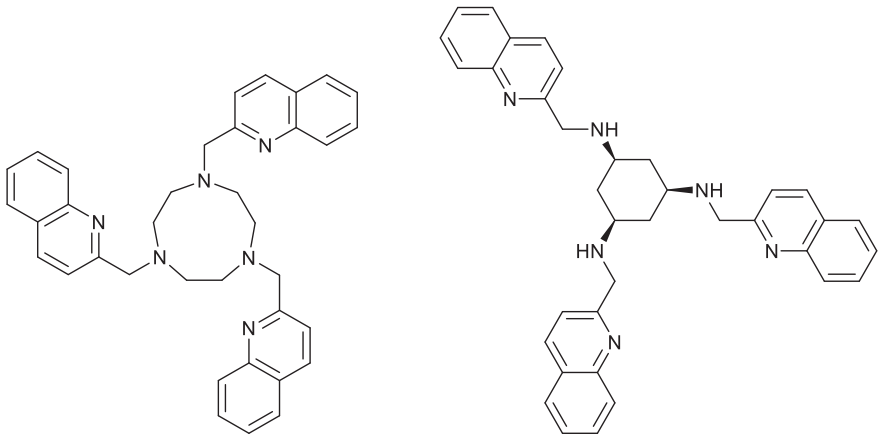

(42) (43)

Fig. 42. The structures of the hexadentate ligands containing three quinolyl moieties.

mononuclear complexes [M(**42**)]X_2 are given in Table 12.

In all the complexes, **42** binds in a hexadentate fashion, coordinating to the metal ion through all six nitrogen atoms. The complex cations range in geometry from pseudo-octahedral ([Cu(**42**)]$^{2+}$ (**YUHMEU**), [85] [Zn(**42**)]$^{2+}$ (**YUHNIZ**), [85] and [Fe(**42**)]$^{2+}$ (**IQIWOW**), [241] through pseudo-trigonal prismatic ([Cd(**42**)]$^{2+}$ (**YUHLUJ**)[85] and [Hg(**42**)]$^{2+}$ (**YUHMOE**), [85] Fig. 43)), to highly trigonally distorted pseudo-octahedral [Pb(**42**)]$^{2+}$ (Fig. 44, **YUHNAR**), [85] with *trans* N-M-N angles being significantly smaller than 180° in all cases. The M-N bond lengths increase as the metal ion radius increases, and, as expected, the [Cu(**42**)]$^{2+}$ complex cation displays the expected Jahn-Teller effect; the *trans*-disposed Cu-$N_{quinolyl}$ (2.527 Å) and Cu-$N_{tertiary}$ (2.207 Å) bonds are noticeably longer than the other Cu-N distances (2.028–2.170 Å).

The free **42** ligand exhibits very weak fluorescence ($\phi = 0.0007$) at 380 nm on excitation at 316 nm. Investigations of the 1:1 Cu(II), Zn(II), Cd(II), Hg(II) and Pb(II) complexes in MeCN/H_2O (1:1) showed that only the Zn(II) complex exhibited the CHEF effect over the pH range 3.0 – 10.0, with the maximum occurring at pH 7.0. This was attributed, at least in part, to the relatively small size of the Zn(II) ion. [85].

The complexes [Cu(**42***)]$(ClO_4)_2$ (**ACADIS**), [244] [Zn(**42***)]$(ClO_4)_2$ (**ACADOY**), [244] and [Fe(**42***)]$(ClO_4)_2$ (**DUCFOW**), [245] containing the corresponding pyridine ligand, have been structurally characterised.

The [Cu(**42***)]$^{2+}$ cation (**ACADIS**), [244] also exhibits an octahedral N_6 environment about the Cu(II) centre like the quinoline cation [Cu(**42**)]$^{2+}$, although a *cis* N-Cu-N angle of 118.85° and a *trans* angle of

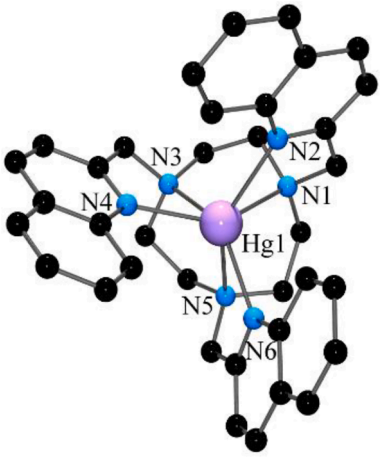

Fig. 43. Structure of the [Hg(**42**)]$^{2+}$ cation. Selected bond lengths (Å) and angles (°) Hg1-N1 2.455, Hg1-N2 2.377, Ag1-N3 2.402, Ag1-N4 2.474, Hg1-N5 2.450, Ag1-N6 2.340; N1-Hg1-N 70.67, N2-Hg1-N3 109.72, N3-Hg1-N4 70.21, N4-Hg1-N6 103.12, N6-Hg1-N1 113.07, N2-Hg1-N5 140.94.

Table 12
Six-coordinate complexes of **42.**

Complex	*trans* N-M-N/°	*cis* N-M-N/°	M-$N_{quinoline}$/Å	M-$N_{aliphatic}$/ Å	Ref
[Zn(**42**)]$(BF_4)_2$ (**YUHNIZ**)	154.69–160.95	77.97–105.96	2.270 2.234 2.190	2.233 2.207 2.144	[85]
[Pb(**42**)]$(ClO_4)_2$.MeCN (**YUHNAR**)	132.30–134.58	62.92–120.01	2.833 2.799 2.712	2.535 2.509 2.504	[85]
[Hg(**42**)]$(NO_3)_2$ (**YUHMOE**)	140.72– 142.01	70.21–113.07	2.424 2.377 2.340	2.455 2.450 2.402	[85]
[Cu(**42**)]$(BF_4)_2$ (**YUHMEU**)	152.25–163.18	72.42–103.37	2.527 2.170 2.073	2.207 2.196 2.028	[85]
[Cd(**42**)]$(ClO_4)_2$ (**YUHLUJ**)	142.79–144.89	71.17–111.61	2.396 2.371 2.350	2.366 2.389 2.392	[85]
[Fe(**42**)]$(BF_4)_2$ (**IQIWOW**)	153.51–159.17	75.94–107.20	2.262 2.235 2.212	2.239 2.218 2.174	[241]

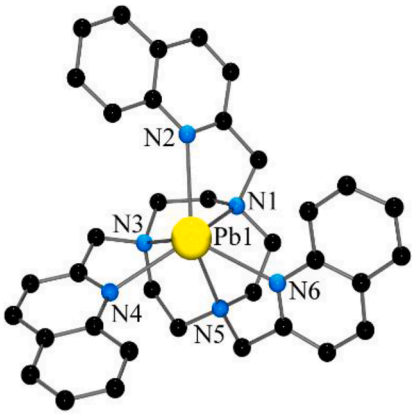

Fig. 44. Structure of the $[Pb(\mathbf{42})]^{2+}$ cation. Selected bond lengths (Å) and angles (°) Hg1-N1 2.455, Hg1-N2 2.377, Ag1-N3 2.402, Ag1-N4 2.474, Hg1-N5 2.450, Ag1-N6 2.340; N1-Hg1-N 70.67, N2-Hg1-N3 109.72, N3-Hg1-N4 70.21, N4-Hg1-N6 103.12, N6-Hg1-N1 113.07, N2-Hg1-N5 140.94.

146.47° are evidence of a significant distortion. The Cu-N bond distances in the pyridine complex are shorter than those in the quinoline analogue, but there is no obvious Jahn-Teller axis in the former. Overall, while it appears that the shorter Cu-$N_{pyridine}$ bond lengths lead to greater structural distortions in this complex relative to the quinoline congener, it is difficult to ascribe the difference in bond lengths to one particular factor, as this may be due to the expected lengthening of the Cu-$N_{quinoline}$ bonds in comparison to the Cu-$N_{pyridine}$ bonds, or the Jahn-Teller effect, or a combination of both. [244].

The octahedral Zn(II) complex of the pyridyl analogue (**ACADOY**), [244] is, like the Cu(II) complex, more distorted than the quinoline complex, with all three *trans* N-Zn-N bond angles being ~ 150°, and one *cis* N-Zn-N angle of 115.55°. As expected, the Zn-$N_{pyridine}$ bond lengths are shorter than the Zn-$N_{quinoline}$ bond distances. [244].

By contrast, the $[Fe(\mathbf{42}^*)]^{2+}$ cation (**DUCFOW**) [245] appears significantly less distorted than its quinoline congener. All Fe-N bond lengths lie around 2 Å in the former, and 2.2 Å in the latter, and this very strongly suggests that the pyridine complex is low-spin and the quinoline complex is high-spin. Unfortunately, the spin state of the quinoline complex was not investigated in the original publication. [245].

5.3.2. *N,N',N''-tris(2-quinolinylmethyl)-cis,cis-1,3,5-triaminocyclohexane) (43) [246]*

This ligand was prepared through the reaction of quinoline-2-carbaldehyde with *cis,cis*-1,3,5-triaminocyclohexane[247] to form the tris imine, followed by reduction with borohydride. [246] Mononuclear $[Zn(\mathbf{43})](ClO_4)_2{\cdot}H_2O$ (Fig. 45, **JEMTEB**) [246] is the only structurally characterised complex of this ligand; the Zn(II) ion is six-coordinate and displays a distorted octahedral geometry, with *trans* N-Zn-N angles ranging from 167.09° to 169.66°, and *cis* N-Zn-N angles lying between 79.25° and 104.48°. The Zn-$N_{aliphatic}$ bond lengths (2.124 Å, 2.135 Å and 2.171 Å) are all shorter than the Zn-$N_{quinoline}$ bond lengths (2.296 Å, 2.255 Å and 2.198 Å).

There are three analogous pyridyl Zn(II) complexes $[Zn(\mathbf{43}^*)](ClO_4)_2.CH_3OH$ (**DOSVAI**) [248], $[Zn(\mathbf{43}^*)]Cl.ClO_4$ (**PAWXAP**) [249] and $[Zn(\mathbf{43}^*)](ClO_4)_2{\cdot}H_2O$ (**PAWWUI**) [249] to which $[Zn(\mathbf{43})](ClO_4)_2{\cdot}H_2O$ may be compared. All three pyridyl congeners display a similar octahedral geometry about the metal centre to the quinolyl complex, and the Zn-N bond lengths are only slightly longer in the latter. Interestingly, the pyridine and quinoline complexes all exhibit bent coordination of the aromatic N atoms, being most pronounced in the quinoline complex (an angle of 149.45° between the Zn-N bond and the plane of the aromatic ring). This presumably indicates significant chelate ring strain owing to the constrained nature of the ligand.

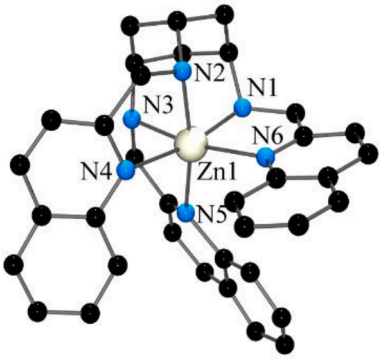

Fig. 45. Structure of the $[Zn(\mathbf{43})]^{2+}$ cation. Bond lengths Zn1-N1 2.136 Å, Zn1-N2 2.124 Å, Zn1-N3 2.170 Å, Zn1-N4 2.296 Å, Zn1-N5 2.198 Å, Zn1-N6 2.256 Å. Selected bond angles N1-Zn1-N3 88.21°, N3-Zn1-N4 85.61°, N4-Zn1-N6 105.97°, N3-Zn1-N4 79.25°, N1-Zn1-N4 169.66°, N3-Zn1-N6 167.09°, N2-Zn1-N5 168.89°.

5.4. *Hexadentate ligands containing four quinolyl moieties*

The structures of these ligands are given in Fig. 46.

5.4.1. *(N,N,N',N'-tetrakis(2-quinolylmethyl)-1,2-phenylenediamine (44) [250]*

The preparation of **44** was achieved from the reaction of 2-(bromomethyl)quinoline with 1,2-phenylenediamine. **44** coordinates to both Cd^{2+} and Zn^{2+} to give the structurally characterised mononuclear complexes $[Cd(\mathbf{44})](ClO_4)_2$ (Fig. 47, **ROMKIP**) [250] and $[Zn(\mathbf{44})](ClO_4)_2$ (**ROMKOV**). [250] X-ray structural data for these complexes are given in Table 13. The ligand imposes significant constraints on the geometry of these complexes, and they therefore adopt extremely distorted octahedral geometries about the metal ion, with both containing a *cis*-N-M-N angle of over 130°. The constraints are further exemplified by the very bent coordination of two of the quinolyl units; the putative sp^2 electron pair on the N atom lies significantly out of the plane of the pyridine ring, with the angles between the M-$N_{quinoline}$ vectors and the aromatic planes ranging from 136° to 143°. Not surprisingly, these are the longest M-N bonds in both complex cations.

Fluorescence studies with $\lambda_{ex} = 317$ nm showed that **44** in DMF-H_2O at 25 °C exhibits faint fluorescence. When reacted with Na^+, K^+, Ag^+, Mg^{2+}, Ca^{2+}, Mn^{2+}, Co^{2+}, Ni^{2+}, Cu^{2+}, Zn^{2+}, Cd^{2+} Hg^{2+}, Pb^{2+}, Fe^{2+}, and Fe^{3+}, only in the presence of Cd^{2+} is a 6-fold enhancement in fluorescence observed (λ_{em} = 392 nm). Although log K values were not measured, it was shown that addition of Cd(II) to solutions of the Cu(II), Ag(I) and Hg(II) complexes did not give rise to the expected fluorescence, implying that the log K values for these three metal ions are significantly larger than that of Cd(II).

5.4.2. *N,N,N',N'-tetrakis(2-quinolylmethyl)ethylenediamine (45) [251,252]*

Ligand **45** was prepared from the reaction of 2-(chloromethyl) quinoline hydrochloride and ethylenediamine in the presence of K_2CO_3 in MeCN. [251] The crystal structure of **45**.4$CHCl_3$ (**FICHOP**) [251] shows offset π-π interactions between neighbouring pyridine rings (centroid–centroid distance = 3.685 Å) and two different types of C-H-N hydrogen bonds involving the quinoline N atom and a C-H bond from a chloroform solvate molecule.

Excitation of **45** in DMF or aqueous DMF (1:1) at 317 nm resulted in very weak fluorescence. However, a 23-fold fluorescence enhancement was observed upon the addition of an equimolar amount of Zn^{2+} to the ligand solution (λ_{em} = 383 nm). The PET and CHEF mechanisms in the ligand **45** have been attributed as the cause the observed significant increase in fluorescence. Of a variety of other metal cations (Na^+, K^+, Ag^+, Zn^{2+}, Mg^{2+}, Ca^{2+}, Cu^{2+}, Ni^{2+}, Mn^{2+}, Co^{2+}, Cd^{2+}, Fe^{3+}), only Cd^{2+}

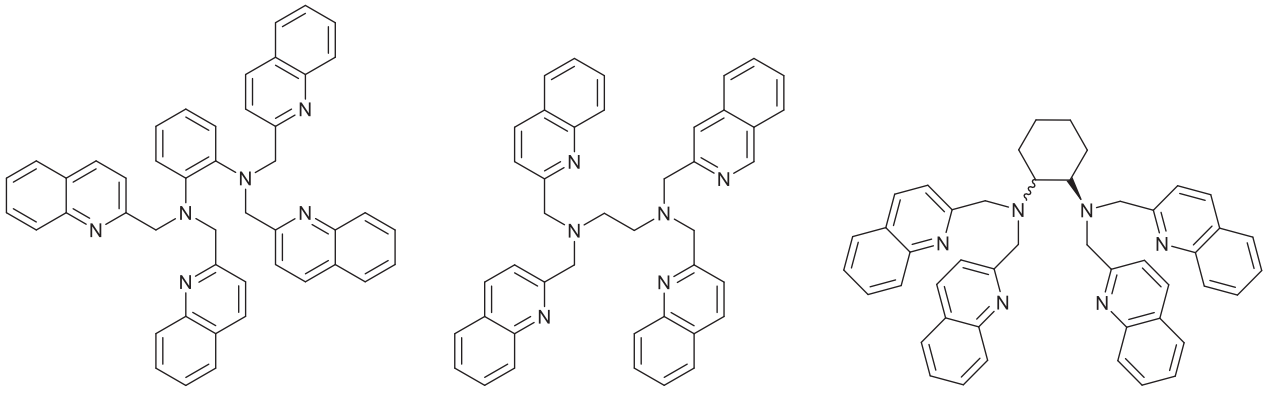

(44) (45) (46)

Fig. 46. The structures of the hexadentate ligands containing four quinolyl moieties.

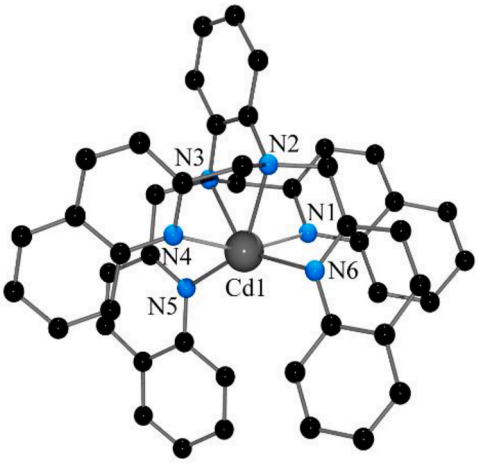

Fig. 47. Structure of the $[Cd(\mathbf{44})]^{2+}$ cation. Selected bond lengths (Å) and angles (°) Cd1-N1 2.461, Cd1-N2 2.393, Cd1-N3 2.377, Cd1-N4 2.286, Cd1-N5 2.536, Cd1-N6 2.259; Selected bond angles N2-Cd1-N3 73.98, N4-Cd1-N6 144.61.

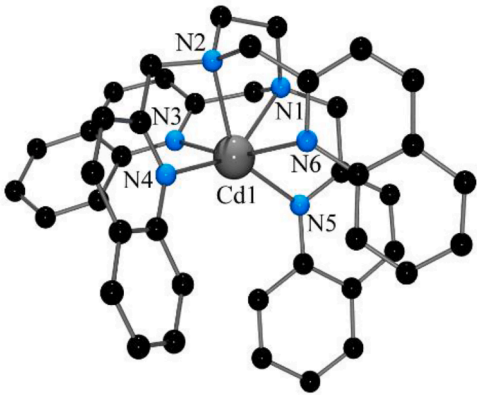

Fig. 48. Structure of the $[Cd(\mathbf{45})]^{2+}$ cation. Selected bond lengths (Å) and angles (°) Cd1-N1 2.377, Cd1-N2 2.401, Cd1-N3 2.435, Cd1-N4 2.354, Cd1-N5 2.375, Cd1-N6 2.370; N1-Cd1-N2 74.69, N4-Cd1-N6 141.80, N5-Cd1-N6 100.55.

gave substantial fluorescence enhancement, with an observed fluorescence intensity approximately 60 % that of Zn^{2+}.

The Zn^{2+} and Cd^{2+} complexes of **45**, $[Zn(\mathbf{45})](ClO_4)_2.2.5MeCN$ (**FICHUV**) [251] and $[Cd(\mathbf{45})](ClO_4)_2.2CHCl_3$ (Fig. 48, **VICWIP**), [252] have been structurally characterised. The former displays a distorted octahedral geometry very similar to the Zn^{2+} complexes of **40** (Section 5.1.1) and **41** (Section 5.2.1), while the Cd^{2+} complex displays a remarkable geometry around the metal ion which could be described as approaching a square plane with two *cis* pseudo-axial donor atoms. The crystal data for both complexes are summarised in Table 14.

The ligands **40**, **41**, and **45** form a homologous series with an increasing number of quinoline moieties. Therefore, there is only a single pyridine congener of these ligands. While the analogous pyridine Zn(II) complexes (**BOBCOL**, **DECDAR**, **FICJAD**) [239,251,253] exhibit no significant structural differences to the corresponding Zn(II) quinoline complexes, this is not so for the larger Cd(II) ion. The quinoline-containing cation $[Cd(\mathbf{45})]^{2+}$ is six-coordinate, whereas the reduced steric bulk of the multidentate ligand in the pyridine congener results in the seven-coordinate species, $[Cd(\mathbf{45}^*)H_2O](ClO_4)_2$ (**VICWAH**) [252] and $[Cd(\mathbf{45}^*)ONO_2]NO_3.CH_3COOH$ (**MUDZEQ**). [254].

5.4.3. *N,N,N′,N′-tetrakis(2-quinolylmethyl)-trans/cis-1,2-cyclohexanediamine (46)* [252,255]

The *trans* and *cis* isomeric versions of this cyclohexanediamine-based

Table 13
Six-coordinate complexes of **44**.

Complex	*trans* N-M-N/°	*cis* N-M-N/°	M-$N_{quinoline}$/Å	M-$N_{aliphatic}$/ Å	Ref
$[Cd(\mathbf{44})](ClO_4)_2.MeOH$	141.20–160.82	72.09–144.61	2.259 2.286 2.461 2.536	2.377 2.393	[250]
$[Zn(\mathbf{44})](ClO_4)_2.MeOH$	148.74–168.85	76.10–130.62	2.110 2.124 2.321 2.561	2.191 2.199	[250]

Table 14
Six-coordinate complexes of **45.**

Complex	*trans* N-M-N/°	*cis* N-M-N/°	M-$N_{quinoline}$/Å	M-$N_{aliphatic}$/ Å	Ref
[Zn(**45**)]$(ClO_4)_2$.2.5MeCN	157.73–165.94	76.21–124.25	2.127 2.154 2.371 2.401	2.150 2.168	[251]
[Cd(**45**)]$(ClO_4)_2$.2$CHCl_3$)	142.12–161.57	70.73–141.80	2.354 2.370 2.375 2.435	2.377 2.402	[252]

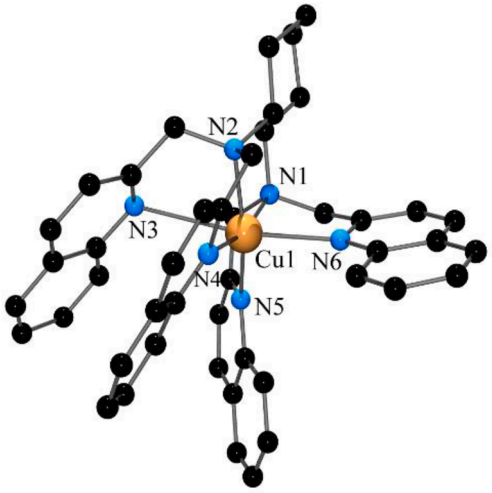

Fig. 49. Structure of the [Cu(*trans*-**46**)]$^{2+}$ cation. Selected bond lengths (Å) and angles (°) Cu1-N1 2.039, Cu1-N2 2.048, Cu1-N3 2.348, Cu1-N4 2.033, Cu1-N5 2.073, Cu1-N6 2.825; N1-Cu1-N6 76.01, N2-Cu1-N5 165.28, N3-Cu1-N6 169.73, N1-Cu-N4 159.25.

ligand can be prepared from the reaction of *trans/cis*-1,2-cyclohexanediamine and 2-(chloromethyl)quinoline hydrochloride[252] or 2-(bromomethyl)quinoline[255] in the presence of K_2CO_3. The crystal structure of the diequatorial *trans* isomer is available (**VICXOW**). [252].

Both *cis*- and *trans*-**46** show negligible fluorescence upon excitation at 317 nm in aqueous DMF at 25 °C. Addition of either Zn^{2+} or Cd^{2+} resulted in a significant increase in emission intensity at 455 nm, and, as found for ligand **45**, these were the only cations to display such a response.

One structurally characterised complex of *cis*-**46** ([Zn(*cis*-**46**)]$(ClO_4)_2$) (**GUFBER**)[255] and four of *trans*-**46** ([M(*trans*-**46**)]$(ClO_4)_2$, M = Fe^{2+} (**UTUTIP**), [256] Zn^{2+} (**VICXIQ**), [252] Cu^{2+} (Fig. 49, **VICXAI**), [252] and Cd^{2+} (**VICWUB**)[252]) have been reported. The *cis*-ligand coordinates to the central zinc ion through all six of the nitrogen atoms, albeit it with one very long (2.533 Å) 'bent' Zn-$N_{quinoline}$ bond (the angle between the Zn-$N_{quinoline}$ vector and the aromatic plane is 139°). The remaining Zn-N bond lengths range from 2.127 Å to 2.271 Å. The bond lengths and angles for complexes of the *trans* ligand are summarised in Table 15. The Cu(II) complex exhibits an extremely long Cu-$N_{quinoline}$ bond (2.825 Å) which is also significantly bent (the angle between the Cu-$N_{quinoline}$ vector and the aromatic plane is 116°, Fig. 49). The Cu-$N_{quinoline}$ bond trans to this is also elongated (2.348 Å) compared to the other two Cu-$N_{quinoline}$ bonds (2.073 and 2.033 Å) and such long bonds can be ascribed to the Jahn-Teller effect.

6. Conclusions

The data outlined above show that the incorporation of quinoline moieties in multidentate amine ligands leads to a wide variety of geometries about the metal ions in the resulting transition metal complexes. The majority of the four-coordinate complexes exhibit near tetrahedral geometries, with the only exception being, unsurprisingly, a square planar geometry in a Pd(II) complex (Section 3.2.5). It is in the five-coordinate complexes where the presence of a quinoline moiety in the ligand appears to have the most significant effect, when compared to the corresponding pyridine congener. The τ_5 values collected herein show conclusively that the quinoline-containing ligands give complexes whose geometry tends significantly towards square pyramidal, the exceptions generally being complexes of Co(II). This appears to be the result of destabilising interactions between the quinoline H-8 proton(s) and an axial ligand that occur in a trigonal bipyramidal geometry. Avoidance of such interactions also appears to be the reason behind the quinolyl split in five-coordinate complexes containing tridentate ligands. Complexes displaying this feature have the three N atoms from the tridentate ligand arranged essentially coplanar, with the remaining two ligands bisected by the plane(s) of the quinolyl ring(s). In all cases,

Table 15
Six-coordinate complexes of **46.**

Complex	*trans* N-M-N/°	*cis* N-M-N/°	M-$N_{quinoline}$/Å	M-$N_{aliphatic}$/ Å	Ref
[Zn(**46**)]$(ClO_4)_2$.MeOH (**VICXIQ**)	152.98–166.78	76.42–126.39	2.485 2.289 2.142 2.127	2.204 2.180	[252]
[Cu(**46**)]$(ClO_4)_2$.3MeOH (**VICXAI**)	159.25–169.73	76.01–105.07	2.825 2.348 2.073 2.033	2.073 2.039	[252]
[Cd(**46**)]$(ClO_4)_2$ (**VICWUB**)	137.70–175.65	74.40–102.01	2.472 2.472 2.290 2.290	2.386 2.386	[252]
[Fe(**46**)]$(CF_3SO_3)_2$.MeCN (**UTUTIP**)	151.07–168.92	74.12–134.64	2.252 2.252 2.194 2.194	2.238 2.238	[256]

the pyridyl analogues have one of these ligands close to coplanar with a pyridine ring. The six-coordinate complexes generally display close to octahedral geometries, but significant distortion is observed in some cases, particularly in complexes of Mn(II). Such distortions are probably due to a combination of factors, including the size of the metal ion, geometric constraints imposed by the multidentate ligand, and destabilising interactions involving the quinoline moiety. One surprising feature of a small, but significant number of complexes outlined above is the 'bent' coordination of the quinoline moiety. This is not unique to quinoline-containing ligands (see Section 5.3.2) but it appears that the steric bulk of the quinoline moiety is important in enforcing such coordination.

We hope that the ligands and complexes outlined herein may pique the interest of coordination chemists and lead to the synthesis of yet more fascinating quinolyl-containing species.

Declaration of competing interest

The authors declare that they have no known competing financial interests or personal relationships that could have appeared to influence the work reported in this paper.

Data availability

No data were used for the research described in the article.

References

[1] W. Xu, Y. Nagata, N. Kumagai, TEtraQuinolines: A Missing Link in the Family of Porphyrinoid Macrocycles, J. Am. Chem. Soc. 145 (2023) 2609–2618, https://doi.org/10.1021/jacs.2c12582.

[2] R.L. Ray, Alkaloids—The world's pain killers, J. Chem. Educ. 37 (1960) 451, https://doi.org/10.1021/ed037p451.

[3] P.H. Walker, On the use of organic bases in the preparation of barium and calcium ferrocyanides, J. Am. Chem. Soc. 17 (1895) 927, https://doi.org/10.1021/ja02167a005.

[4] W. Staronka, Additive Compounds of Mercury Salts with Aromatic Bases, Bull. Int. Acad. Pol. Sci. Lett. Cl. Sci. Math. Nat. (1910) 372.

[5] U. Pomilio, New Metalloquinolides. I. Metalloquinolides of Silver Nitrate, Rend Accad Sci Fis Mat Napoli. 17 (1912) 326.

[6] T. Ratho, M. Mrs, Krishnaswamy, Structure of complex silver quinoline perchlorate, Indian J. Phys. 41 (1967) 511.

[7] A.R. Joaquim, M.P. Gionbelli, G. Gosmann, A.M. Fuentefria, M.S. Lopes, S. Fernandes de Andrade, Novel Antimicrobial 8-Hydroxyquinoline-Based Agents: Current Development, Structure-Activity Relationships, and Perspectives, J. Med. Chem. 64 (2021) 16349–16379, https://doi.org/10.1021/acs.jmedchem.1c01318.

[8] R. Gupta, V. Luxami, K. Paul, Insights of 8-hydroxyquinolines: A novel target in medicinal chemistry, Bioorganic Chem. 108 (2021), 104633, https://doi.org/10.1016/j.bioorg.2021.104633.

[9] C. Sonkar, S. Sarkar, S. Mukhopadhyay, Ruthenium(II)-arene complexes as anti-metastatic agents, and related techniques, RSC Med. Chem. 13 (2022) 22–38, https://doi.org/10.1039/d1md00220a.

[10] C. Bissani Gasparin, D.A. Pilger, 8-Hydroxyquinoline, Derivatives and Metal-Complexes: A Review of Antileukemia Activities, ChemistrySelect 8 (2023), https://doi.org/10.1002/slct.202204219 e202204219.

[11] L. Southcott, C. Orvig, Inorganic radiopharmaceutical chemistry of oxine, Dalton Trans. 50 (2021) 16451–16458, https://doi.org/10.1039/d1dt02685b.

[12] C.W. Tang, S.A. Vanslyke, Organic electroluminescent diodes, Appl. Phys. Lett. 51 (1987) 913–915, https://doi.org/10.1063/1.98799.

[13] Y. Kurebayashi, P.L. Choyke, N. Sato, Imaging of cell-based therapy using ^{89}Zr-oxine ex vivo cell labeling for positron emission tomography, Nanotheranostics. 5 (2021) 27–35, https://doi.org/10.7150/ntno.51391.

[14] F. Valach, P. Sivý, B. Koreň, Structure of bis(isothiocyanato)tetrakis(pyridine) nickel(II), $C_{22}H_{20}N_6NiS_2$, a redetermination, Acta Crystallogr. Sect. c. 40 (1984) 957–959, https://doi.org/10.1107/S0108270184006405.

[15] D. Soldatov, J. Lipkowski, X-Ray Diffraction Study of a Clathrate with the Quinoline-Containing Werner Complex ($[NiQ_4(NCS)_2].2Q$), J. Struct. Chem. 38 (1997) 811–818.

[16] G. Zhu, J.M. Tanski, D.G. Churchill, K.E. Janak, G. Parkin, The Reactivity of Mo$(PMe_3)_6$ towards Heterocyclic Nitrogen Compounds: Transformations Relevant to Hydrodenitrogenation, J. Am. Chem. Soc. 124 (2002) 13658–13659, https://doi.org/10.1021/ja028512w.

[17] R. Kumar, A. Thakur, D. Sachin, A.K. Chandra, P.K. Dhiman, U.S. Verma, Quinoline-based metal complexes: Synthesis and applications, Coord. Chem. Rev. 499 (2024), 215453, https://doi.org/10.1016/j.ccr.2023.215453.

[18] W. Luo, K. Huang, Z. Zhang, C. Hong, C.-J. Wang, Design, synthesis and cholinesterase inhibitory activity of quinoline-polyamine conjugates, Yao Xue Xue Bao 48 (2013) 269–275.

[19] P. Häfliger, S. Mundwiler, G. Andócs, L. Balogh, K. Bodo, K. Ortner, B. Spingler, R. Alberto, Structure, Stability, and Biodistribution of Cationic $[M(CO)_3]^+$ (M = Re, ^{99}Tc, ^{99m}Tc) Complexes with Tridentate Amine Ligands, Synth. React. Inorg. Met.-Org. Nano-Met. Chem. 35 (2005) 27–34, https://doi.org/10.1081/SIM-200047534.

[20] D.G. Gusev, Dehydrogenative Coupling of Ethanol and Ester Hydrogenation Catalyzed by Pincer-Type YNP Complexes, ACS Catal. 6 (2016) 6967–6981, https://doi.org/10.1021/acscatal.6b02324.

[21] I. Mallinckrodt, R. Alberto, R. Schibli, Molecules for the treatment and diagnosis of tumors, WO0050086A1. https://worldwide.espacenet.com/patent/search/family/026153277/publication/WO0050086A1?q=WO0050086A1 (accessed June 21, 2023).

[22] V. Egger, M. Gude, C. Hubschwerlen, G. Rueedi, J.-P. Surivet, C. Zumbrunn, 2-Benzothiophenyl and 2-naphthyl-oxazolidinones and their azaisostere analogues as antibacterial agents, WO2010041219A1, 2010.

[23] S.S. Massoud, A.E. Guilbeau, H.T. Luong, R. Vicente, J.H. Albering, R.C. Fischer, F.A. Mautner, Mononuclear, dinuclear and polymeric 1D thiocyanato- and dicyanamido–copper(II) complexes based on tridentate coligands, Polyhedron 54 (2013) 26–33, https://doi.org/10.1016/j.poly.2013.01.033.

[24] T. Dhanalakshmi, E. Suresh, H. Stoeckli-Evans, M. Palaniandavar, New Copper(II) Complexes as Efficient Catalysts for Olefin Aziridination: The Effect of Ligand Steric Hindrance on Reactivity, Eur. J. Inorg. Chem. 2006 (2006) 4687–4695, https://doi.org/10.1002/ejic.200600490.

[25] H. Timmerman, M. Zang, K. Onogi, M. Tamura, T. Tohma, Y. Wada, Diamine derivatives and pharmaceutical containing the same, WO9902520A1, 1999.

[26] M. Du, Y.-M. Guo, X.-H. Bu, J. Ribas, M. Monfort, Ferromagnetic coupling in a unique Cu(II) metallacyclophane with functionalized diazamesocyclic ligands formed by Cu(II)-directed self-assembly: magneto-structural correlations for dichloro-bridged Cu(II) dinuclear complexes, New J. Chem. 26 (2002) 645–650, https://doi.org/10.1039/B110465A.

[27] T. Dhanalakshmi, R. Loganathan, E. Suresh, H. Stoeckli-Evans, M. Palaniandavar, Interaction of copper(II) complexes with bis(p-nitrophenyl)phosphate: Structural and spectral studies, Inorganica Chim. Acta. 372 (2011) 237–242, https://doi.org/10.1016/j.ica.2011.02.030.

[28] S. Muthuramalingam, M. Velusamy, R. Mayilmurugan, Fixation of atmospheric CO_2 as C1-feedstock by nickel(II) complexes, Dalton Trans. 50 (2021) 7984–7994, https://doi.org/10.1039/D0DT03887C.

[29] T. Dhanalakshmi, E. Suresh, M. Palaniandavar, Olefin aziridination by copper(II) complexes: Effect of redox potential on catalytic activity, Inorganica Chim. Acta. 365 (2011) 143–151, https://doi.org/10.1016/j.ica.2010.08.051.

[30] E.M. Prokopchuk, R.J. Puddephatt, Methyl(hydrido)platinum(IV) Complexes with Flexible Tridentate Nitrogen-Donor Ligands, Organometallics 22 (2003) 787–796, https://doi.org/10.1021/om0206352.

[31] F.A. Mautner, F.R. Louka, J. Hofer, M. Spell, A. Lefèvre, A.E. Guilbeau, S. S. Massoud, One-Dimensional Cadmium Polymers with Alternative di(EO/EE) and di(EO/EO/EO/EE) Bridged Azide Bonding Modes, Cryst. Growth Des. 13 (2013) 4518–4525, https://doi.org/10.1021/cg400998r.

[32] L.J. Raszeja, D. Siegmund, A.L. Cordes, J. Güldenhaupt, K. Gerwert, S. Hahn, N. Metzler-Nolte, Asymmetric rhenium tricarbonyl complexes show superior luminescence properties in live cell imaging, Chem. Commun. 53 (2017) 905–908, https://doi.org/10.1039/C6CC07553C.

[33] A. Kunishita, T. Osako, Y. Tachi, J. Teraoka, S. Itoh, Syntheses, Structures, and O2-Reactivities of Copper(I) Complexes with Bis(2-pyridylmethyl)amine and Bis(2-quinolylmethyl)amine Tridentate Ligands, Bull. Chem. Soc. Jpn. 79 (2006) 1729–1741, https://doi.org/10.1246/bcsj.79.1729.

[34] J.-L. Li, L. Jiang, S.-T. Li, J.-L. Tian, W. Gu, X. Liu, S.-P. Yan, Self-activated DNA cleavage of a water-soluble mononuclear Cu(II) complex with polyquinolinyl ligand, J. Coord. Chem. 67 (2014) 3598–3612, https://doi.org/10.1080/00958972.2014.973867.

[35] S. Kakuda, C.J. Rolle, K. Ohkubo, M.A. Siegler, K.D. Karlin, S. Fukuzumi, Lewis Acid-Induced Change from Four- to Two-Electron Reduction of Dioxygen Catalyzed by Copper Complexes Using Scandium Triflate, J. Am. Chem. Soc. 137 (2015) 3330–3337, https://doi.org/10.1021/ja512584r.

[36] J.-L. Li, L. Jiang, B.-W. Wang, J.-L. Tian, W. Gu, X. Liu, S.-P. Yan, Significant differences in the biological activity of mononuclear Cu(II) and Ni(II) complexes with the polyquinolinyl ligand, New J. Chem. 39 (2014) 529–538, https://doi.org/10.1039/C4NJ00876F.

[37] S.V. Kryatov, S. Taktak, I.V. Korendovych, E.V. Rybak-Akimova, J. Kaizer, S. Torelli, X. Shan, S. Mandal, V.L. MacMurdo, A. Mairata i Payeras, L. Que, Dioxygen Binding to Complexes with FeII2(μ-OH)2 Cores: Steric Control of Activation Barriers and O2-Adduct Formation, Inorg. Chem. 44 (2005) 85–99, https://doi.org/10.1021/ic0485312.

[38] T.K. Paine, J. England, L. Que Jr., Iron-Catalyzed C2–C3 Bond Cleavage of Phenylpyruvate with O_2: Insight into Aliphatic C-C Bond-Cleaving Dioxygenases, Chem. – Eur. J. 13 (2007) 6073–6081, https://doi.org/10.1002/chem.200601844.

[39] H. Kim, J. Kang, K.B. Kim, E.J. Song, C. Kim, A highly selective quinoline-based fluorescent sensor for Zn(II), Spectrochim. Acta. A. Mol. Biomol, Spectrosc. 118 (2014) 883–887, https://doi.org/10.1016/j.saa.2013.09.118.

[40] L.A. Hunter, S. Naidoo, A. Mambanda, N, N-bis(2-quinolinylmethyl)benzylamine, Molbank. 2021 (2021) M1208, https://doi.org/10.3390/M1208.

[41] J. Manzur, A. Vega, A.M. García, C. Acuña, M. Sieger, B. Sarkar, M. Niemeyer, F. Lissner, T. Schleid, W. Kaim, Coordination Alternatives in Dinuclear Bis

(pyridin-2-ylalkyl)benzylaminecopper(II) Complexes with OH^-, RO^-, F^-, or Cl^- Bridges: Experimental Structures and DFT Preferences, Eur. J. Inorg. Chem. 2007 (2007) 5500–5510, https://doi.org/10.1002/ejic.200700637.
[42] A. Bhattacharyya, A. Dixit, S. Banerjee, B. Roy, A. Kumar, A.A. Karande, A. R. Chakravarty, BODIPY appended copper(II) complexes for cellular imaging and singlet oxygen mediated anticancer activity in visible light, RSC Adv. 6 (2016) 104474–104482, https://doi.org/10.1039/C6RA23118G.
[43] J. Zhang, A.E. Holmes, A. Sharma, N.R. Brooks, R.S. Rarig, J. Zubieta, J. W. Canary, Derivatization, complexation, and absolute configurational assignment of chiral primary amines: Application of exciton-coupled circular dichroism, Chirality 15 (2003) 180–189, https://doi.org/10.1002/chir.10158.
[44] Đ. Škalamera, E. Sanders, R. Vianello, A. Maršavelski, A. Pevec, I. Turel, S.I. Kirin, Synthesis and characterization of ML and ML_2 metal complexes with amino acid substituted bis(2-picolyl)amine ligands, Dalton Trans. 45 (2016) 2845–2858, https://doi.org/10.1039/C5DT03387J.
[45] S. Zahn, J.W. Canary, Absolute Configurations of N, N-Dialkyl α-Amino Acids and β-Amino Alcohols from Exciton-Coupled Circular Dichroism Spectra of Cu(II) Complexes, Org. Lett. 1 (1999) 861–864, https://doi.org/10.1021/ol990715a.
[46] J.C. Slootweg, H.B. Albada, D. Siegmund, N. Metzler-Nolte, Efficient Reagent-Saving Method for the N-Terminal Labeling of Bioactive Peptides with Organometallic Carboxylic Acids by Solid-Phase Synthesis, Organometallics 35 (2016) 3192–3196, https://doi.org/10.1021/acs.organomet.6b00544.
[47] S.R. Banerjee, J.W. Babich, J. Zubieta, A new bifunctional amino acid chelator targeting the glucose transporter, Inorganica Chim. Acta. 359 (2006) 1603–1612, https://doi.org/10.1016/j.ica.2005.11.022.
[48] L. Raszeja, A. Maghnouj, S. Hahn, N. Metzler-Nolte, A Novel Organometallic ReI Complex with Favourable Properties for Bioimaging and Applicability in Solid-Phase Peptide Synthesis, Chembiochem 12 (2011) 371–376, https://doi.org/10.1002/cbic.201000576.
[49] L. Wei, J. Babich, W.C. Eckelman, J. Zubieta, Rhenium Tricarbonyl Core Complexes of Thymidine and Uridine Derivatives, Inorg. Chem. 44 (2005) 2198–2209, https://doi.org/10.1021/ic048301n.
[50] L. Wei, S.R. Banerjee, M.K. Levadala, J. Babich, J. Zubieta, Complexes of the *fac*-$\{Re(CO)_3\}^+$ core with tridentate ligands derived from arylpiperazines, Inorganica Chim. Acta. 357 (2004) 1499–1516, https://doi.org/10.1016/j.ica.2003.11.027.
[51] S.A. Moya, J. Guerrero, R. Pastene, R. Sartori, R. Schmidt, R. Sariego, J. Sanz-Aparicio, I. Fonseca, M. Martinez-Ripoll, Metallic Carbonyl Complexes Containing Heterocycle Nitrogen Ligands. 2. Tricarbonylbromo(3,3'-*R*-2,2'-biquinoline)Rhenium(I) Compounds, Inorg. Chem. 33 (1994) 2341–2346, https://doi.org/10.1021/ic00089a007.
[52] S.R. Banerjee, M.K. Levadala, N. Lazarova, L. Wei, J.F. Valliant, K.A. Stephenson, J.W. Babich, K.P. Maresca, J. Zubieta, Bifunctional Single Amino Acid Chelates for Labeling of Biomolecules with the $\{Tc(CO)_3\}^+$ and $\{Re(CO)_3\}^+$ Cores. Crystal and Molecular Structures of $[ReBr(CO)_3(H_2NCH_2C_5H_4N)]$, $[Re(CO)_3\{(C_5H_4NCH_2)_2NH\}]Br$, $[Re(CO)_3\{(C_5H_4NCH_2)_2NCH_2CO_2H\}]Br$, $[Re(CO)_3\{X(Y)NCH_2CO_2CH_2CH_3\}]Br$ (X = Y = 2-pyridylmethyl; X = 2-pyridylmethyl, Y = 2-(1-methylimidazolyl)methyl; X = Y = 2-(1-methylimidazolyl) methyl), $[ReBr(CO)_3\{(C_5H_4NCH_2)NH(CH_2C_4H_3S)\}]$, and $[Re(CO)_3\{(C_5H_4NCH_2)N(CH_2C_4H_3S)(CH_2CO_2)\}]$, Inorg. Chem. 41 (2002) 6417–6425. https://doi.org/10.1021/ic020476e.
[53] T. Osako, S. Nagatomo, T. Kitagawa, C.J. Cramer, S. Itoh, Kinetics and DFT studies on the reaction of copper(II) complexes and H_2O_2, JBIC J. Biol. Inorg. Chem. 10 (2005) 581–590, https://doi.org/10.1007/s00775-005-0005-5.
[54] T. Osako, Y. Ueno, Y. Tachi, S. Itoh, Structures and Redox Reactivities of Copper Complexes of (2-Pyridyl)alkylamine Ligands. Effects of the Alkyl Linker Chain Length, Inorg. Chem. 42 (2003) 8087–8097, https://doi.org/10.1021/ic034958h.
[55] L. Wei, J.W. Babich, W. Ouellette, J. Zubieta, Developing the $\{M(CO)_3\}^+$ Core for Fluorescence Applications: Rhenium Tricarbonyl Core Complexes with Benzimidazole, Quinoline, and Tryptophan Derivatives, Inorg. Chem. 45 (2006) 3057–3066, https://doi.org/10.1021/ic0517319.
[56] T. Ahmad, A. Waheed, S. Abdel-Azeim, S. Khan, N. Ullah, Three new turn-on fluorescent sensors for the selective detection of Zn^{2+}: Synthesis, properties and DFT studies, Arab. J. Chem. 15 (2022), 104002, https://doi.org/10.1016/j.arabjc.2022.104002.
[57] G. Gasser, A. Pinto, S. Neumann, A.M. Sosniak, M. Seitz, K. Merz, R. Heumann, N. Metzler-Nolte, Synthesis, characterisation and bioimaging of a fluorescent rhenium-containing PNA bioconjugate, Dalton Trans. 41 (2012) 2304–2313, https://doi.org/10.1039/C2DT12114J.
[58] I. Kitanovic, S. Can, H. Alborzinia, A. Kitanovic, V. Pierroz, A. Leonidova, A. Pinto, B. Spingler, S. Ferrari, R. Molteni, A. Steffen, N. Metzler-Nolte, S. Wölfl, G. Gasser, A Deadly Organometallic Luminescent Probe: Anticancer Activity of a Re^I Bisquinoline Complex, Chem. – Eur. J. 20 (2014) 2496–2507, https://doi.org/10.1002/chem.201304012.
[59] M.K. Levadala, S.R. Banerjee, K.P. Maresca, J.W. Babich, J. Zubieta, Direct Reductive Alkylation of Amino Acids: Synthesis of Bifunctional Chelates for Nuclear Imaging, Synthesis 2004 (2004) 1759–1766, https://doi.org/10.1055/s-2004-829120.
[60] E. Benoist, Y. Coulais, M. Almant, J. Kovensky, V. Moreau, D. Lesur, M. Artigau, C. Picard, C. Galaup, S.G. Gouin, A Click procedure with heterogeneous copper to tether technetium-99m chelating agents and rhenium complexes. Evaluation of the chelating properties and biodistribution of the new radiolabelled glucose conjugates, Carbohydr. Res. 346 (2011) 26–34, https://doi.org/10.1016/j.carres.2010.10.011.
[61] A. Frei, M. Amado, M.A. Cooper, M.A.T. Blaskovich, Light-Activated Rhenium Complexes with Dual Mode of Action against Bacteria, Chem. – Eur. J. 26 (2020) 2852–2858, https://doi.org/10.1002/chem.201904689.
[62] M.A. Wuillemin, M.J. Reber, T. Fox, B. Spingler, D. Brühwiler, R. Alberto, H. Braband, Towards ^{99m}Tc- and Re-Based Multifunctional Silica Platforms for Theranostic Applications, Inorganics. 7 (2019) 134, https://doi.org/10.3390/inorganics7110134.
[63] T.R. Hayes, P.A. Lyon, E. Silva-Lopez, B. Twamley, P.D. Benny, Photo-initiated Thiol-ene Click Reactions as a Potential Strategy for Incorporation of $[M^I(CO)_3]^+$ (M = Re, ^{99m}Tc) Complexes, Inorg. Chem. 52 (2013) 3259–3267, https://doi.org/10.1021/ic302771f.
[64] S.R. Banerjee, P. Schaffer, J.W. Babich, J.F. Valliant, J. Zubieta, Design and synthesis of site directed maleimide bifunctional chelators for technetium and rhenium, Dalton Trans. (2005) 3886–3897, https://doi.org/10.1039/B507096A.
[65] S.R. Banerjee, J.W. Babich, J. Zubieta, Site directed maleimide bifunctional chelators for the $M(CO)_3^+$ core (M = ^{99m}Tc, Re), Chem. Commun. (2005) 1784–1786, https://doi.org/10.1039/B417588C.
[66] N. Viola-Villegas, A.E. Rabideau, J. Cesnavicious, J. Zubieta, R.P. Doyle, Targeting the Folate Receptor (FR): Imaging and Cytotoxicity of Re^I Conjugates in FR-Overexpressing Cancer Cells, ChemMedChem 3 (2008) 1387–1394, https://doi.org/10.1002/cmdc.200800125.
[67] E. Gabano, L. Do Quental, E. Perin, F. Silva, P. Raposinho, A. Paulo, M. Ravera, Pt (IV)/Re(I) Chitosan Conjugates as a Flexible Platform for the Transport of Therapeutic and/or Diagnostic Anticancer Agents, Inorganics. 6 (2018) 4, https://doi.org/10.3390/inorganics6010004.
[68] S.R. Banerjee, J.W. Babich, J. Zubieta, Bifunctional chelates with aliphatic amine donors for labeling of biomolecules with the $\{Tc(CO)_3\}^+$ and $\{Re(CO)_3\}^+$ cores: the crystal and molecular structure of $[Re(CO)_3\{(H_2NCH_2CH_2)_2N(CH_2)_4CO_2Me\}]Br$, Inorg. Chem. Commun. 7 (2004) 481–484, https://doi.org/10.1016/j.inoche.2004.01.008.
[69] Y.-H. Zhou, J. Tao, D.-L. Sun, L.-Q. Chen, W.-G. Jia, Y. Cheng, Synthesis, structure and superoxide dismutase-like activity of copper(II) complexes based on N, N′-bis (2-quinolinylmethyl)amantadine, Polyhedron 85 (2015) 849–856, https://doi.org/10.1016/j.poly.2014.10.010.
[70] Y.-H. Zhou, L.-Q. Chen, Q.-C. Lv, J. Tao, X.-W. Liu, Y. Cheng, Synthesis, Structure, and Bio-activity of a Copper(II)-OH_2 Complex based on N, N′-Bis(2-quinolinylmethyl)amantadine, Z. Für Anorg. Allg. Chem. 641 (2015) 483–489, https://doi.org/10.1002/zaac.201400393.
[71] Y.-H. Zhou, X.-W. Liu, J. Tao, S.-Q. Wang, P. Ren, P. Ni, Y. Cheng, p-Nitrophenyl acetate hydrolysis promoted by Zn(II) and Co(II) complexes with the tripodal ligand of N, N′-bis(2-quinolinylmethyl)amantadine, J. Coord. Chem. 70 (2017) 177–188, https://doi.org/10.1080/00958972.2016.1247954.
[72] Y.-H. Zhou, S.-Q. Wang, L.-Q. Chen, D.-Y. Gong, P. Ni, Y. Cheng, Effective reduction of p-nitrophenol catalyzed by nickel(II) adamantane complexes, Transit. Met. Chem. 42 (2017) 175–180, https://doi.org/10.1007/s11243-017-0122-3.
[73] L. Martínez, C. Bazzicalupi, A. Bianchi, F. Lloret, R. González, C. Kremer, R. Chiozzone, Structural and magnetic properties of polynuclear oximate copper complexes with different topologies, Polyhedron 138 (2017) 125–132, https://doi.org/10.1016/j.poly.2017.09.017.
[74] A.M. Schuitema, P.G. Aubel, I.A. Koval, M. Engelen, W.L. Driessen, J. Reedijk, M. Lutz, A.L. Spek, Dinuclear copper(II) complexes of four new pyrazole-containing macrocyclic ligands are active catalysts in the oxidative coupling of 2,6-dimethylphenol, Inorganica Chim. Acta. 355 (2003) 374–385, https://doi.org/10.1016/S0020-1693(03)00362-1.
[75] W. Zhang, N. Saraei, H. Nie, J.R. Vaughn, A.S. Jones, M.S. Mashuta, R. M. Buchanan, C.A. Grapperhaus, Reversible methanol addition to copper Schiff base complexes: a kinetic, structural and spectroscopic study of reactions at azomethine CN bonds, Dalton Trans. 45 (2016) 15791–15799, https://doi.org/10.1039/C6DT01955B.
[76] A.K. Patra, M. Nethaji, A.R. Chakravarty, Red-light photosensitized cleavage of DNA by (L-lysine) (phenanthroline base)copper(II) complexes, Dalton Trans. (2005) 2798–2804, https://doi.org/10.1039/B506310H.
[77] A. Adamski, M. Osińska, M. Kubicki, Z. Hnatejko, G. Consiglio, V. Patroniak, Molecular Switching of Copper Complexes with Quaterpyridine, Eur. J. Inorg. Chem. 2017 (2017) 859–872, https://doi.org/10.1002/ejic.201601148.
[78] S.A. Shaikh, S.S. Bhat, V.K. Revankar, B.D. Kulkarni, K. Kumara, N.K. Lokanath, V. Kumbar, K. Bhat, R.J. Butcher, Fluorophore Tagged Mixed Ligand Copper(II) Complexes: Synthesis, Structural Characterization, Protein Binding, DNA Cleavage and Anticancer Activity, ChemistrySelect. 6 (2021) 12666–12676, https://doi.org/10.1002/slct.202103314.
[79] C. Gérard, A. Mohamadou, J. Marrot, S. Brandes, A. Tabard, Synthesis and Characterization of Copper Complexes Containing the Tripodal N7 Ligand Tris2-[(pyridin-2-ylmethyl)amino]ethylamine (=N′-(Pyridin-2-ylmethyl)-N, N-bis2-[(pyridin-2-ylmethyl)amino]ethylethane-1,2-diamine): Equilibrium, Spectroscopic Data, and Crystal Structures of Mono- and Trinuclear Copper(II) Complexes, Helv. Chim. Acta. 88 (2005) 2397–2412, https://doi.org/10.1002/hlca.200590176.
[80] Y.-H. Zhou, L.-Q. Chen, J. Tao, J.-L. Shen, D.-Y. Gong, R.-R. Yun, Y. Cheng, Effective cleavage of phosphodiester promoted by the zinc(II) and copper(II) inclusion complexes of β-cyclodextrin, J. Inorg. Biochem. 163 (2016) 176–184, https://doi.org/10.1016/j.jinorgbio.2016.07.011.
[81] M. Saga, G. Sakane, S. Yamazaki, K. Saito, Fluorescent ligand design for mononuclear copper(I) complex fluorescence in aqueous solution, Inorganica Chim. Acta. 502 (2020), 119368, https://doi.org/10.1016/j.ica.2019.119368.
[82] L.M. Mesquita, V. André, C.V. Esteves, T. Palmeira, M.N. Berberan-Santos, P. Mateus, R. Delgado, Dinuclear Zinc(II) Macrocyclic Complex as Receptor for Selective Fluorescence Sensing of Pyrophosphate, Inorg. Chem. 55 (2016) 2212–2219, https://doi.org/10.1021/acs.inorgchem.5b02596.

[83] N. Saravanan, M. Sankaralingam, M. Palaniandavar, Manganese(II) complexes of tetradentate 4N ligands with diazepane backbones for catalytic olefin epoxidation: effect of nucleophilicity of peroxo complexes on reactivity, RSC Adv. 4 (2014) 12000–12011, https://doi.org/10.1039/C3RA44729D.

[84] R.M. Hartshorn, D.A. House, A simple method for identifying and distinguishing between the diastereoisomers that result from wrapping polydentate ligands around octahedral metal ions., J. Chem. Soc. Dalton Trans, Inorg. Chem. (1998) 2577–2588.

[85] M. Mameli, M.C. Aragoni, M. Arca, M. Atzori, A. Bencini, C. Bazzicalupi, A. J. Blake, C. Caltagirone, F.A. Devillanova, A. Garau, M.B. Hursthouse, F. Isaia, V. Lippolis, B. Valtancoli, Synthesis and Coordination Properties of Quinoline Pendant Arm Derivatives of [9]aneN$_3$ and [9]aneN$_2$S as Fluorescent Zinc Sensors, Inorg. Chem. 48 (2009) 9236–9249, https://doi.org/10.1021/ic901012w.

[86] M.A. Tetilla, M.C. Aragoni, M. Arca, C. Caltagirone, C. Bazzicalupi, A. Bencini, A. Garau, F. Isaia, A. Laguna, V. Lippolis, V. Meli, Colorimetric response to anions by a "robust" copper(II) complex of a [9]aneN$_3$ pendant arm derivative: CN^- and I^- selective sensing, Chem. Commun. 47 (2011) 3805–3807, https://doi.org/10.1039/C0CC04500D.

[87] W.K.C. Lo, C.J. McAdam, A.G. Blackman, J.D. Crowley, D.A. McMorran, The pentadentate ligands 2PyN2Q and N4Py, and their Cu(II) and Zn(II) complexes: A synthetic, spectroscopic and crystallographic structural study, Inorganica Chim. Acta. 426 (2015) 183–194, https://doi.org/10.1016/j.ica.2014.11.036.

[88] Y. Su, W. Yang, X. Yang, R. Zhang, J. Zhao, Visible Light-Induced CO-Release Reactivity of a Series of ZnII–Flavonolate Complexes, Aust. J. Chem. 71 (2018) 549–558, https://doi.org/10.1071/CH18192.

[89] F. Yu, Magnetic properties of a mononuclear iron(II) complex with a typical FeN$_6$ coordination octahedron, Acta Crystallogr. C. 68 (2012) m287–m290. https://doi.org/10.1107/S010827011203209X.

[90] J.-W. Wang, H.-H. Huang, J.-K. Sun, T. Ouyang, D.-C. Zhong, T.-B. Lu, Electrocatalytic and Photocatalytic Reduction of CO_2 to CO by Cobalt(II) Tripodal Complexes: Low Overpotentials, High Efficiency and Selectivity, ChemSusChem 11 (2018) 1025–1031, https://doi.org/10.1002/cssc.201702280.

[91] S.S. Massoud, F.R. Louka, A.F. Tusa, N.E. Bordelon, R.C. Fischer, F.A. Mautner, J. Vančo, J. Hošek, Z. Dvořák, Z. Trávníček, Copper(II) complexes based on tripodal pyridyl amine derivatives as efficient anticancer agents, New J. Chem. 43 (2019) 6186–6196, https://doi.org/10.1039/C9NJ00061E.

[92] K. Chen, L. Que, Stereospecific Alkane Hydroxylation by Non-Heme Iron Catalysts: Mechanistic Evidence for an $Fe^{V}O$ Active Species, J. Am. Chem. Soc. 123 (2001) 6327–6337, https://doi.org/10.1021/ja010310x.

[93] B. Li, J. Tao, H.-L. Sun, O. Sato, R.-B. Huang, L.-S. Zheng, Side-effect of ancillary ligand on electron transfer and photodynamics of a dinuclear valence tautomeric complex, Chem. Commun. (2008) 2269–2271, https://doi.org/10.1039/B801171K.

[94] D.-Y. Wu, O. Sato, C.-Y. Duan, A mixed-spin Fe(II) tetranuclear cluster: Preparation, structure and magnetic property, Inorg. Chem. Commun. 12 (2009) 325–327, https://doi.org/10.1016/j.inoche.2009.02.007.

[95] S.S. Massoud, R.S. Perkins, F.R. Louka, W. Xu, A.L. Roux, Q. Dutercq, R. C. Fischer, F.A. Mautner, M. Handa, Y. Hiraoka, G.L. Kreft, T. Bortolotto, H. Terenzi, Efficient hydrolytic cleavage of plasmid DNA by chloro-cobalt(II) complexes based on sterically hindered pyridyl tripod tetraamine ligands: synthesis, crystal structure and DNA cleavage, Dalton Trans. 43 (2014) 10086–10103, https://doi.org/10.1039/C4DT00615A.

[96] H.R. Lucas, G.J. Meyer, K.D. Karlin, CO and O_2 Binding to Pseudo-tetradentate Ligand−Copper(I) Complexes with a Variable N-Donor Moiety: Kinetic/Thermodynamic Investigation Reveals Ligand-Induced Changes in Reaction Mechanism, J. Am. Chem. Soc. 132 (2010) 12927–12940, https://doi.org/10.1021/ja104107q.

[97] M. Pascaly, M. Duda, F. Schweppe, K. Zurlinden, F.K. Müller, B. Krebs, The systematic influence of tripodal ligands on the catechol cleavingactivity of iron (III) containing model compounds for catechol 1,2-dioxygenases, J. Chem. Soc. Dalton Trans. (2001) 828–837, https://doi.org/10.1039/B008511L.

[98] F.A. Mautner, C. Berger, M.J. Dartez, Q.L. Nguyen, J. Favreau, S.S. Massoud, Cadmium(II) and zinc(II) azido complexes with different nuclearity and dimensionality, Polyhedron 69 (2014) 48–54, https://doi.org/10.1016/j.poly.2013.11.019.

[99] N. Wei, N.N. Murthy, K.D. Karlin, Chemistry of Pentacoordinate $[LCu^{II}\text{-}Cl]^+$ Complexes with Quinolyl Containing Tripodal Tetradentate Ligands L, Inorg. Chem. 33 (1994) 6093–6100, https://doi.org/10.1021/ic00104a018.

[100] N. Wei, N.N. Murthy, Q. Chen, J. Zubieta, K.D. Karlin, Copper(I)/Dioxygen Reactivity of Mononuclear Complexes with Pyridyl and Quinolyl Tripodal Tetradentate Ligands: Reversible Formation of $Cu:O_2$ = 1:1 and 2:1 Adducts, Inorg. Chem. 33 (1994) 1953–1965, https://doi.org/10.1021/ic00087a036.

[101] M.E. Masaki, D. Paul, R. Nakamura, Y. Kataoka, S. Shinoda, H. Tsukube, Chiral tripode approach toward multiple anion sensing with lanthanide complexes, Tetrahedron 65 (2009) 2525–2530, https://doi.org/10.1016/j.tet.2009.01.061.

[102] H. Park, D. Lee, Ligand Taxonomy for Bioinorganic Modeling of Dioxygen-Activating Non-Heme Iron Enzymes, Chem. – Eur. J. 26 (2020) 5916–5926, https://doi.org/10.1002/chem.201904975.

[103] Y. Suenaga, T. Mibu, T. Okubo, M. Maekawa, T. Kuroda-Sowa, Syntheses, structure and properties of dinuclear Co complexes with bis(catecholate) ligands – Effect of a quinoline ring in the terminal group, Polyhedron 171 (2019) 480–485, https://doi.org/10.1016/j.poly.2019.07.035.

[104] X. Guo, C. Li, W. Wang, Y. Hou, B. Zhang, X. Wang, Q. Zhou, Polypyridyl Co complex-based water reduction catalysts: why replace a pyridine group with isoquinoline rather than quinoline? Dalton Trans. 50 (2021) 2042–2049, https://doi.org/10.1039/C9DT04767K.

[105] Y. Suenaga, T. Mibu, T. Okubo, M. Maekawa, T. Kuroda-Sowa, K. Sugimoto, Dinuclear cobalt complexes with a redox active biphenyl bridging ligand $[Co_2(BP)(tqa)_2](PF_6)_2$ (H_4BP = 4,4′-bis(3- tert -butyl-1,2-catechol), tqa = tris(2-quinolylmethyl)amine): structure and magnetic properties, Dalton Trans. 50 (2021) 9833–9841, https://doi.org/10.1039/D1DT00995H.

[106] T. Mibu, A. Iba, Y. Suenaga, T. Okubo, M. Maekawa, T. Kuroda-Sowa, K. Sugimoto, Syntheses and properties of mononuclear cobalt-dioxolene complexes with the ancillary ligand containing bulky quinoline rings – Electronic state manipulation of the complexes by steric effect, Inorganica Chim. Acta. 527 (2021), 120538, https://doi.org/10.1016/j.ica.2021.120538.

[107] N. Takahashi, T. Nishiyama, T. Mibu, Y. Suenaga, T. Okubo, M. Maekawa, T. Kuroda-Sowa, Dinuclear cobalt complexes with an asymmetric biphenyl bridging ligand, $[Co_2(LFtBu)(bpqa)_2](PF_6)_2$ (H_4LFtBu = 5-fluoro-5′-tert-butyl-3,3′,4,4′-tetrahydroxybiphenyl, bpqa = bis(2-pyridylmethyl)(2-quinolylmethyl) amine): Spectroscopic, electrochemical and magnetic characterization, Inorganica Chim. Acta. 541 (2022), 121095, https://doi.org/10.1016/j.ica.2022.121095.

[108] L. Yang, D.R. Powell, R.P. Houser, Structural variation in copper(I) complexes with pyridylmethylamide ligands: structural analysis with a new four-coordinate geometry index, τ_4, Dalton Trans. (2007) 955–964. https://doi.org/10.1039/B617136B.

[109] A. Diebold, K.S. Hagen, Iron(II) Polyamine Chemistry: Variation of Spin State and Coordination Number in Solid State and Solution with Iron(II) Tris(2-pyridylmethyl)amine Complexes, Inorg. Chem. 37 (1998) 215–223, https://doi.org/10.1021/ic971105e.

[110] G.-L. Li, S. Kanegawa, Z.-S. Yao, S.-Q. Su, S.-Q. Wu, Y.-G. Huang, S. Kang, O. Sato, Influence of Intermolecular Interactions on Valence Tautomeric Behaviors in Two Polymorphic Dinuclear Cobalt Complexes, Chem. – Eur. J. 22 (2016) 17130–17135, https://doi.org/10.1002/chem.201603817.

[111] A.K. Mondal, J. Jover, E. Ruiz, S. Konar, Quantitative Estimation of Ising-Type Magnetic Anisotropy in a Family of C_3-Symmetric Co^{II} Complexes, Chem. – Eur. J. 23 (2017) 12550–12558, https://doi.org/10.1002/chem.201702108.

[112] S.S. Massoud, K.T. Broussard, F.A. Mautner, R. Vicente, M.K. Saha, I. Bernal, Five-coordinate cobalt(II) complexes of tris(2-pyridylmethyl)amine (TPA): Synthesis, structural and magnetic characterization of a terephthalato-bridged dinuclear cobalt(II) complex, Inorganica Chim. Acta. 361 (2008) 123–131, https://doi.org/10.1016/j.ica.2007.06.021.

[113] C.J. Davies, G.A. Solan, J. Fawcett, Synthesis and structural characterisation of cobalt(II) and iron(II) chloride complexes containing bis(2-pyridylmethyl)amine and tris(2-pyridylmethyl)amine ligands, Polyhedron 23 (2004) 3105–3114, https://doi.org/10.1016/j.poly.2004.09.011.

[114] S.-L.-F. Chan, T.L. Lam, C. Yang, S.-C. Yan, N.M. Cheng, A robust and efficient cobalt molecular catalyst for CO_2 reduction, Chem. Commun. 51 (2015) 7799–7801, https://doi.org/10.1039/C5CC00566C.

[115] T.J. Woods, M.F. Ballesteros-Rivas, S. Gómez-Coca, E. Ruiz, K.R. Dunbar, Relaxation Dynamics of Identical Trigonal Bipyramidal Cobalt Molecules with Different Local Symmetries and Packing Arrangements: Magnetostructural Correlations and ab inito Calculations, J. Am. Chem. Soc. 138 (2016) 16407–16416, https://doi.org/10.1021/jacs.6b10154.

[116] T.M. Kooistra, K.F.W. Hekking, Q. Knijnenburg, B. de Bruin, P.H.M. Budzelaar, R. de Gelder, J.M.M. Smits, A.W. Gal, Cobalt Chloride Complexes of N3 and N4 Donor Ligands, Eur. J. Inorg. Chem. 2003 (2003) 648–655, https://doi.org/10.1002/ejic.200390090.

[117] I. Boldog, F.J. Muñoz-Lara, A.B. Gaspar, M.C. Muñoz, M. Seredyuk, J.A. Real, Polynuclear Spin Crossover Complexes: Synthesis, Structure, and Magnetic Behavior of $[Fe_4(\mu\text{-}CN)_4(phen)_4(L)_2)]^{4+}$ Squares, Inorg. Chem. 48 (2009) 3710–3719, https://doi.org/10.1021/ic802306r.

[118] S. Floquet, A.J. Simaan, E. Rivière, M. Nierlich, P. Thuéry, J. Ensling, P. Gütlich, J.-J. Girerd, M.-L. Boillot, Spin crossover of ferric complexes with catecholate derivatives. Single-crystal X-ray structure, Magnetic and Mössbauer investigations, Dalton Trans. (2005) 1734–1742, https://doi.org/10.1039/B418294D.

[119] M. Merkel, M. Pascaly, M. Wieting, M. Duda, A.R. Privatdozentin, Synthesis and characterization of the first (1,2-benzenedithiolato)iron(III) complexes with tripodal ligands., Z, Fuer Anorg. Allg. Chem. 629 (2003) 2216–2221, https://doi.org/10.1002/zaac.200300212.

[120] A. Tissot, H.J. Shepherd, L. Toupet, E. Collet, J. Sainton, G. Molnár, P. Guionneau, M.-L. Boillot, Temperature- and Pressure-Induced Switching of the Molecular Spin State of an Orthorhombic Iron(III) Spin-Crossover Salt, Eur. J. Inorg. Chem. 2013 (2013) 1001–1008, https://doi.org/10.1002/ejic.201201059.

[121] E. Collet, M.-L. Boillot, J. Hebert, N. Moisan, M. Servol, M. Lorenc, L. Toupet, M. Buron-Le Cointe, A. Tissot, J. Sainton, Polymorphism in the spin-crossover ferric complexes $[(TPA)Fe^{III}(TCC)]PF_6$, Acta Crystallogr, Sect. b. 65 (2009) 474–480, https://doi.org/10.1107/S0108768109021508.

[122] S. Hematian, M.A. Siegler, K.D. Karlin, Heme/Copper Assembly Mediated Nitrite and Nitric Oxide Interconversion, J. Am. Chem. Soc. 134 (2012) 18912–18915, https://doi.org/10.1021/ja3083818.

[123] W.T. Eckenhoff, T. Pintauer, Structural Comparison of Copper(I) and Copper(II) Complexes with Tris(2-pyridylmethyl)amine Ligand, Inorg. Chem. 49 (2010) 10617–10626, https://doi.org/10.1021/ic1016142.

[124] W.T. Eckenhoff, T. Pintauer, Atom Transfer Radical Addition in the Presence of Catalytic Amounts of Copper(I/II) Complexes with Tris(2-pyridylmethyl)amine, Inorg. Chem. 46 (2007) 5844–5846, https://doi.org/10.1021/ic700908m.

[125] K.D. Karlin, J.C. Hayes, S. Juen, J.P. Hutchinson, J. Zubieta, Tetragonal vs. trigonal coordination in copper(II) complexes with tripod ligands: structures and

properties of $[Cu(C_{21}H_{24}N_4)Cl]PF_6$ and $[Cu(C_{18}H_{18}N_4)Cl]PF_6$, Inorg. Chem. 21 (1982) 4106–4108, https://doi.org/10.1021/ic00141a049.
[126] W. Xu, J.A. Craft, P.R. Fontenot, M. Barens, K.D. Knierim, J.H. Albering, F. A. Mautner, S.S. Massoud, Effect of the central metal ion on the cleavage of DNA by $[M(TPA)Cl]ClO_4$ complexes (M=Co^{II}, Cu^{II} and Zn^{II}, TPA=tris(2-pyridylmethyl) amine): An efficient artificial nuclease for DNA cleavage, Inorganica Chim. Acta. 373 (2011) 159–166, https://doi.org/10.1016/j.ica.2011.04.012.
[127] J.G.D. Elsberg, S.N. Anderson, D.L. Tierney, E.W. Reinheimer, L.M. Berreau, Tris-(2-pyridylmethyl)amine-ligated Cu(II) 1,3-diketonate complexes: anaerobic retro-Claisen and dehalogenation reactivity of 2-chloro-1,3-diketonate derivatives, Dalton Trans. 50 (2021) 1712–1720, https://doi.org/10.1039/D0DT04074F.
[128] K. Suzuki, P.D. Oldenburg, L. Que Jr., Iron-Catalyzed Asymmetric Olefin cis-Dihydroxylation with 97 % Enantiomeric Excess, Angew. Chem. Int. Ed. 47 (2008) 1887–1889, https://doi.org/10.1002/anie.200705061.
[129] R.V. Ottenbacher, D.G. Samsonenko, E.P. Talsi, K.P. Bryliakov, Highly Enantioselective Bioinspired Epoxidation of Electron-Deficient Olefins with H_2O_2 on Aminopyridine Mn Catalysts, ACS Catal. 4 (2014) 1599–1606, https://doi.org/10.1021/cs500333c.
[130] G. Alvaro, F. Grepioni, D. Savoia, Synthesis and X-ray Crystal Structure of N, N-Bis [(*S*)-1-phenylethyl]-(*R*, *R*)-4,5- diamino-1,7-octadiene, J. Org. Chem. 62 (1997) 4180–4182, https://doi.org/10.1021/jo962219v.
[131] A. Alexakis, A. Tomassini, C. Chouillet, S. Roland, P. Mangeney, G. Bernardinelli, A New Efficient Synthesis of (*R*, *R*)-2,2'-Bipyrrolidine: An Interesting Chiral 1,2-Diamine with C(2) Symmetry, Angew. Chem. Int. Ed Engl. 39 (2000) 4093–4095, https://doi.org/10.1002/1521-3773(20001117)39:22<4093::aid-anie4093>3.0.co;2-r.
[132] R.V. Ottenbacher, K.P. Bryliakov, E.P. Talsi, Non-Heme Manganese Complexes Catalyzed Asymmetric Epoxidation of Olefins by Peracetic Acid and Hydrogen Peroxide, Adv. Synth. Catal. 353 (2011) 885–889, https://doi.org/10.1002/adsc.201100030.
[133] M. Saga, T. Anamushi, W. Miyahara, S. Yamazaki, K. Saito, Fluorescent Character of Cu(I/II) Complexes with Bisquinoline-based Ligands and Fluorometric Detection of Reductants, Anal. Sci. 31 (2015) 185–189, https://doi.org/10.2116/analsci.31.185.
[134] M. Saga, G. Sakane, S. Yamazaki, K. Saito, Crystal Structure of a Copper(II) Complex with N, N';-Bis(2-methylquinolyl)-dimethyl-1,3-propanediamine, X-Ray Struct. Anal, Online 31 (2015) 41–42, https://doi.org/10.2116/xraystruct.31.41.
[135] M. Usman, M. Zaki, R.A. Khan, A. Alsalme, M. Ahmad, S. Tabassum, Coumarin centered copper(II) complex with appended-imidazole as cancer chemotherapeutic agents against lung cancer: molecular insight via DFT-based vibrational analysis, RSC Adv. 7 (2017) 36056–36071, https://doi.org/10.1039/C7RA05874H.
[136] A. Richaud, F. Méndez, N. Barba-Behrens, P. Florian, O.N. Medina-Campos, J. Pedraza-Chaverri, Electrophilic Modulation of the Superoxide Anion Radical Scavenging Ability of Copper(II) Complexes with 4-Methyl Imidazole, J. Phys. Chem. a. 125 (2021) 2394–2401, https://doi.org/10.1021/acs.jpca.0c10654.
[137] J.S. Derrick, Y. Kim, H. Tak, K. Park, J. Cho, S.H. Kim, M.H. Lim, Stereochemistry of metal tetramethylcyclam complexes directed by an unexpected anion effect, Dalton Trans. 46 (2017) 13166–13170, https://doi.org/10.1039/C7DT01489A.
[138] N. Marino, D. Armentano, G. De Munno, J. Cano, F. Lloret, M. Julve, Synthesis, Structure, and Magnetic Properties of Regular Alternating μ-bpm/di-μ-X Copper (II) Chains (bpm = 2,2′-bipyrimidine; X = OH, F), Inorg. Chem. 51 (2012) 4323–4334, https://doi.org/10.1021/ic202740b.
[139] D. Inci, R. Aydin, Y. Zorlu, Affinity of a new copper(II) complex to DNA/BSA and antioxidant/radical scavenging activities: crystal structure of [Cu(4,7-diphenyl-1,10-phenanthroline)(leucine)$(NO_3)(H_2O)$], J. Coord. Chem. 69 (2016) 2677–2696, https://doi.org/10.1080/00958972.2016.1213390.
[140] A. Chatterjee, M.M. Seikh, S. Chowdhury, R. Ghosh, Catecholase and catechol cleavage activities of a dinuclear phenoxobridged Cu(II) complex: Synthesis, structure and magnetostructural studies, Inorganica Chim. Acta. 521 (2021), 120345, https://doi.org/10.1016/j.ica.2021.120345.
[141] E.V. Govor, A.B. Lysenko, E.B. Rusanov, A.N. Chernega, H. Krautscheid, K. V. Domasevitch, Anion Tuning of Cu(II)/4,4′-Bi-1,2,4-Triazole Coordination Polymers, Z. Für Anorg. Allg. Chem. 636 (2010) 209–217, https://doi.org/10.1002/zaac.200900121.
[142] X.-Q. Chen, Y.-D. Cai, Y.-S. Ye, M.-L. Tong, X. Bao, Investigation of SCO property–structural relationships in a family of mononuclear Fe(II) complexes, Inorg. Chem. Front. 6 (2019) 2194–2199, https://doi.org/10.1039/C9QI00577C.
[143] Y. Mikata, A. Yamanaka, A. Yamashita, S. Yano, Isoquinoline-Based TQEN Family as TPEN-Derived Fluorescent Zinc Sensors, Inorg. Chem. 47 (2008) 7295–7301, https://doi.org/10.1021/ic8002614.
[144] Y. Mikata, Y. Kuroda, K. Naito, K. Murakami, C. Yamamoto, S. Yabe, S. Yonemura, A. Matsumoto, H. Katano, Structure and electrochemical properties of $(\mu\text{-}O)_2Mn_2$(III, III) and $(\mu\text{-}O)_2Mn_2$(III, IV) complexes supported by pyridine-, quinoline-, isoquinoline- and quinoxaline-based tetranitrogen ligands, Dalton Trans. 50 (2021) 4133–4144, https://doi.org/10.1039/D1DT00184A.
[145] J. Chen, R.J.M. Klein Gebbink, Deuterated N_2Py_2 Ligands: Building More Robust Non-Heme Iron Oxidation Catalysts, ACS Catal. 9 (2019) 3564–3575, https://doi.org/10.1021/acscatal.8b04463.
[146] B. Rieger, A.S. Abu-Surrah, R. Fawzi, M. Steiman, Synthesis of chiral and C_2-symmetric iron(II) and cobalt(II) complexes bearing a new tetradentate amine ligand system, J. Organomet. Chem. 497 (1995) 73–79, https://doi.org/10.1016/0022-328X(95)00119-B.
[147] Y. Mikata, H. So, A. Yamashita, A. Kawamura, M. Mikuriya, K. Fukui, A. Ichimura, S. Yano, Quinoline-based tetradendate nitrogen ligands stabilize the bis(μ-oxo) dinuclear manganese(III, III) core, Dalton Trans. (2007) 3330–3334, https://doi.org/10.1039/B705080A.
[148] L.S. Morris, M.P. Girouard, M.H. Everhart, W.E. McClain, J.A. van Paridon, R. D. Pike, C. Goh, Epoxidation of alkenes bearing a carboxylic acid group by iron complexes of the tetradentate ligand N, N′-dimethyl-N, N′-bis(2-pyridylmethyl)-1,2-diaminoethane and its derivatives, Inorganica Chim. Acta. 413 (2014) 149–159, https://doi.org/10.1016/j.ica.2013.12.029.
[149] Y. Mikata, A. Yamashita, A. Kawamura, H. Konno, Y. Miyamoto, S. Tamotsu, Bisquinoline-based fluorescent zinc sensors, Dalton Trans. (2009) 3800–3806, https://doi.org/10.1039/B820763A.
[150] N. Singh, J. Niklas, O. Poluektov, K.M. Van Heuvelen, A. Mukherjee, Mononuclear nickel (II) and copper (II) coordination complexes supported by bispicen ligand derivatives: Experimental and computational studies, Inorganica Chim. Acta. 455 (2017) 221–230, https://doi.org/10.1016/j.ica.2016.09.001.
[151] K. Chen, L.Q. Jr, Evidence for the participation of a high-valent iron–oxo species in stereospecific alkane hydroxylation by a non-heme iron catalyst, Chem. Commun. (1999) 1375–1376, https://doi.org/10.1039/A901678C.
[152] M.C. White, A.G. Doyle, E.N. Jacobsen, A Synthetically Useful, Self-Assembling MMO Mimic System for Catalytic Alkene Epoxidation with Aqueous H_2O_2, J. Am. Chem. Soc. 123 (2001) 7194–7195, https://doi.org/10.1021/ja015884g.
[153] A. Bohn, K. Sénéchal-David, J. Vanoutryve, R. Guillot, E. Rivière, F. Banse, Synthesis and Characterization of Iron(II) Complexes with a BPMEN-Type Ligand Bearing π-Accepting Nitro Groups, Eur. J. Inorg. Chem. 2017 (2017) 3057–3063, https://doi.org/10.1002/ejic.201700226.
[154] Y. Roux, W. Ghattas, F. Avenier, R. Guillot, A.J. Simaan, J.-P. Mahy, Synthesis and characterization of $[Fe(BPMEN)ACC]SbF_6$: a structural and functional mimic of ACC-oxidase, Dalton Trans. 44 (2015) 5966–5968, https://doi.org/10.1039/C5DT00347D.
[155] Y.S. Ye, X.Q. Chen, Y. De Cai, B. Fei, P. Dechambenoit, M. Rouzières, C. Mathonière, R. Clérac, X. Bao, Slow Dynamics of the Spin-Crossover Process in an Apparent High-Spin Mononuclear Fe^{II} Complex, Angew. Chem. Int. Ed. 58 (2019) 18888–18891, https://doi.org/10.1002/anie.201911538.
[156] J. Luan, J. Zhou, Z. Liu, B. Zhu, H. Wang, X. Bao, W. Liu, M.-L. Tong, G. Peng, H. Peng, L. Salmon, A. Bousseksou, Polymorphism-Dependent Spin-Crossover: Hysteretic Two-Step Spin Transition with an Ordered [HS–HS–*LS*] Intermediate Phase, Inorg. Chem. 54 (2015) 5145–5147, https://doi.org/10.1021/acs.inorgchem.5b00629.
[157] N. Raffard, V. Balland, J. Simaan, S. Létard, M. Nierlich, K. Miki, F. Banse, E. Anxolabéhère-Mallart, J.-J. Girerd, Bio-inspired iron catalysts for degradation of aromatic pollutants and alkane hydroxylation, Comptes Rendus Chim. 5 (2002) 99–109, https://doi.org/10.1016/S1631-0748(02)01359-0.
[158] S. Resa, A. Millán, N. Fuentes, L. Crovetto, M. Luisa Marcos, L. Lezama, D. Choquesillo-Lazarte, V. Blanco, A.G. Campaña, D.J. Cárdenas, J.M. Cuerva, O-H and (CO)N–H bond weakening by coordination to Fe(II), Dalton Trans. 48 (2019) 2179–2189, https://doi.org/10.1039/C8DT04689A.
[159] J. Glerup, P.A. Goodson, A. Hazell, R. Hazell, D.J. Hodgson, C.J. McKenzie, K. Michelsen, U. Rychlewska, H. Toftlund, Synthesis and Characterization of Bis(.mu.-oxo)dimanganese(III,III), -(III,IV), and -(IV,IV) Complexes with Ligands Related to N,N'-Bis(2-pyridylmethyl)-1,2-ethanediamine (Bispicen), Inorg. Chem. 33 (1994) 4105–4111. https://doi.org/10.1021/ic00096a040.
[160] A.S. Abu-Surrah, U. Thewalt, B. Rieger, Chiral palladium(II) complexes bearing tetradentate nitrogen ligands: synthesis, crystal structure and reactivity towards the polymerization of norbornene, J. Organomet. Chem. 587 (1999) 58–66, https://doi.org/10.1016/S0022-328X(99)00273-9.
[161] S. Sheykhi, L. Mosca, J.M. Durgala, P. Anzenbacher, An indicator displacement assay recognizes enantiomers of chiral carboxylates, Chem. Commun. 55 (2019) 7183–7186, https://doi.org/10.1039/C9CC03352A.
[162] R.E. Marsh, M. Kapon, S. Hu, F.H. Herbstein, Some 60 new space-group corrections, Acta Crystallogr. b. 58 (2002) 62–77, https://doi.org/10.1107/S0108768101017128.
[163] I. Ravikumar, P. Ghosh, Zinc(II) and PPi Selective Fluorescence OFF–ON–OFF Functionality of a Chemosensor in Physiological Conditions, Inorg. Chem. 50 (2011) 4229–4231, https://doi.org/10.1021/ic200314t.
[164] H. Swift, M.W. Carrig, K.D. Oshin, A.I. Vinokur, J.A. Desper, C.J. Levy, Crystal structure of {{(1*R*,2*R*)-N, N′-bis-[(quino-lin-2-yl)methyl]cyclo-hexane-1,2-di-amine}-chlorido-iron(III))-μ-oxido-[tri-chlorido-ferrate(III)] chloroform monosolvate, Acta Crystallogr. Sect. E Crystallogr. Commun. 73 (2017) 936–940, https://doi.org/10.1107/S2056989017007952.
[165] J.E. Dengler, M.W. Lehenmeier, S. Klaus, C.E. Anderson, E. Herdtweck, B. Rieger, A One-Component Iron Catalyst for Cyclic Propylene Carbonate Synthesis, Eur. J. Inorg. Chem. 2011 (2011) 336–343, https://doi.org/10.1002/ejic.201000861.
[166] P. Pallavicini, V. Amendola, C. Massera, E. Mundum, A. Taglietti, 'On–off–on' fluorescent indicators of pH windows based on three separated components, Chem. Commun. (2002) 2452–2453, https://doi.org/10.1039/B205951G.
[167] V. Amendola, L. Fabbrizzi, L. Linati, C. Mangano, P. Pallavicini, V. Pedrazzini, M. Zema, Electrochemically Controlled Assembling/Disassembling Processes with a Bis-imine Bis-quinoline Ligand and the Cu^{II}/Cu^{I} Couple, Chem. – Eur. J. 5 (1999) 3679–3688, https://doi.org/10.1002/(SICI)1521-3765(19991203)5:12<3679::AID-CHEM3679>3.0.CO;2-J.
[168] A.S. Abu-Surrah, T.V. Laine, T. Repo, R. Fawzi, M. Steimann, B. Rieger, An Enantiomerically Pure Schiff Base Ligand, Acta Crystallogr. Sect. c. 53 (1997) 1458–1459, https://doi.org/10.1107/S0108270197006148.
[169] C. Vedder, F. Schaper, H.-H. Brintzinger, M. Kettunen, S. Babik, G. Fink, Chiral Iron(II) and Cobalt(II) Complexes with Biphenyl-Bridged Bis(pyridylimine) Ligands – Syntheses, Structures and Reactivities, Eur. J. Inorg. Chem. 2005 (2005) 1071–1080, https://doi.org/10.1002/ejic.200400912.

[170] X. Sheng, L. Qiao, Y. Qin, X. Wang, F. Wang, Highly efficient and quantitative synthesis of a cyclic carbonate by iron complex catalysts, Polyhedron 74 (2014) 129–133, https://doi.org/10.1016/j.poly.2014.02.047.

[171] R. Mayilmurugan, H. Stoeckli-Evans, M. Palaniandavar, Novel Iron(III) Complexes of Sterically Hindered 4N Ligands: Regioselectivity in Biomimetic Extradiol Cleavage of Catechols, Inorg. Chem. 47 (2008) 6645–6658, https://doi.org/10.1021/ic702410d.

[172] S. Muthuramalingam, K. Anandababu, M. Velusamy, R. Mayilmurugan, One step phenol synthesis from benzene catalysed by nickel(II) complexes, Catal, Sci. Technol. 9 (2019) 5991–6001, https://doi.org/10.1039/C9CY01471C.

[173] S. Muthuramalingam, K. Anandababu, M. Velusamy, R. Mayilmurugan, Benzene Hydroxylation by Bioinspired Copper(II) Complexes: Coordination Geometry versus Reactivity, Inorg. Chem. 59 (2020) 5918–5928, https://doi.org/10.1021/acs.inorgchem.9b03676.

[174] S. Muthuramalingam, M. Sankaralingam, M. Velusamy, R. Mayilmurugan, Catalytic Conversion of Atmospheric CO_2 into Organic Carbonates by Nickel(II) Complexes of Diazepane-Based N4 Ligands, Inorg. Chem. 58 (2019) 12975–12985, https://doi.org/10.1021/acs.inorgchem.9b01908.

[175] H. MiKata, Preparation of diazacycloalkane compounds as metal ion fluorescent probes, (2014). https://worldwide.espacenet.com/patent/search/family/051414400/publication/JP2014136675A?q=pn%3DJP2014136675A (accessed June 20, 2023).

[176] R.A. Geiger, S. Chattopadhyay, V.W. Day, T.A. Jackson, Nucleophilic reactivity of a series of peroxomanganese(III) complexes supported by tetradentate aminopyridyl ligands, Dalton Trans. 40 (2011) 1707–1715, https://doi.org/10.1039/C0DT01570A.

[177] T. Mibu, Y. Suenaga, T. Okubo, M. Maekawa, T. Kuroda-Sowa, Spectroscopic characterization of valence tautomeric behavior in a cobalt-dioxolene complex using an ancillary ligand containing quinoline groups, Inorg. Chem. Commun. 114 (2020), 107826, https://doi.org/10.1016/j.inoche.2020.107826.

[178] S. Adhikari, S. Mandal, A. Ghosh, P. Das, D. Das, Strategically Modified Rhodamine-Quinoline Conjugate as a CHEF-Assisted FRET Probe for Au^{3+}: DFT and Living Cell Imaging Studies, J. Org. Chem. 80 (2015) 8530–8538, https://doi.org/10.1021/acs.joc.5b01141.

[179] M.T. Kieber-Emmons, J.W. Ginsbach, P.K. Wick, H.R. Lucas, M.E. Helton, B. Lucchese, M. Suzuki, A.D. Zuberbühler, K.D. Karlin, E.I. Solomon, Observation of a Cu^{II}_2(μ-1,2-peroxo)/Cu^{III}_2(μ-oxo)$_2$ Equilibrium and its Implications for Copper-Dioxygen Reactivity, Angew. Chem. Int. Ed. 53 (2014) 4935–4939, https://doi.org/10.1002/anie.201402166.

[180] H.C. Fry, H.R. Lucas, A.A. Narducci Sarjeant, K.D. Karlin, G.J. Meyer, Carbon Monoxide Coordination and Reversible Photodissociation in Copper(I) Pyridylalkylamine Compounds, Inorg. Chem. 47 (2008) 241–256, https://doi.org/10.1021/ic701903h.

[181] Y. Kataoka, D. Paul, H. Miyake, S. Shinoda, H. Tsukube, A Cl- anion-responsive luminescent Eu^{3+} complex with a chiral tripod: ligand substituent effects on ternary complex stoichiometry and anion sensing selectivity, Dalton Trans. (2007) 2784, https://doi.org/10.1039/b703944a.

[182] W. Gan, S.B. Jones, J.H. Reibenspies, R.D. Hancock, A fluorescent ligand rationally designed to be selective for zinc(II) over larger metal ions. The structures of the zinc(II) and cadmium(II) complexes of N, N-bis(2-methylquinoline)-2-(2-aminoethyl)pyridine, Inorganica Chim. Acta. 358 (2005) 3958–3966, https://doi.org/10.1016/j.ica.2005.06.043.

[183] T. Tzedakis, Electrochemical study of binuclear manganese complexes as catalysts in Kraft pulp bleaching, Electrochim. Acta 46 (2000) 99–109, https://doi.org/10.1016/S0013-4686(00)00529-6.

[184] P. Mialane, L. Tchertanov, F. Banse, J. Sainton, J.-J. Girerd, Aminopyridine Iron Catecholate Complexes as Models for Intradiol Catechol Dioxygenases. Synthesis, Structure, Reactivity, and Spectroscopic Studies, Inorg. Chem. 39 (2000) 2440–2444, https://doi.org/10.1021/ic981236v.

[185] T. Mibu, Y. Suenaga, T. Okubo, M. Maekawa, T. Kuroda-Sowa, Crystal Structure of a Dinuclear Co Complex with Doubly Bridged Fluorides: Di-μ-fluoride Bis{(2-pyridylmethyl)bis(2-quinolylmethyl)amine} Dicobalt(II) Bis(tetrafluoroborate), $[Co_2(\mu\text{-}F)_2(pbqa)_2](BF_4)_2$, X-Ray Struct. Anal. Online 35 (2019) 61–62, https://doi.org/10.2116/xraystruct.35.61.

[186] Y. Mikata, K. Kawata, S. Takeuchi, K. Nakanishi, H. Konno, S. Itami, K. Yasuda, S. Tamotsu, S.C. Burdette, Isoquinoline-derivatized tris(2-pyridylmethyl)amines as fluorescent zinc sensors with strict Zn^{2+}/Cd^{2+} selectivity, Dalton Trans. 43 (2014) 10751–10759, https://doi.org/10.1039/C4DT01054J.

[187] L.A. Joyce, M.S. Maynor, J.M. Dragna, G.M. da Cruz, V.M. Lynch, J.W. Canary, E. V. Anslyn, A Simple Method for the Determination of Enantiomeric Excess and Identity of Chiral Carboxylic Acids, J. Am. Chem. Soc. 133 (2011) 13746–13752, https://doi.org/10.1021/ja205775g.

[188] H. Zheng, Y. Zang, Y. Dong, V.G. Young, L. Que, Complexes with FeIII2(μ-O)(μ-OH), $Fe^{III}_2(\mu\text{-}O)_2$, and [$Fe^{III}_3(\mu_2\text{-}O)_3$] Cores: Structures, Spectroscopy, and Core Interconversions, J. Am. Chem. Soc. 121 (1999) 2226–2235, https://doi.org/10.1021/ja983615t.

[189] B. Lucchese, Recognizing and Predicting General Trends in the Reactivity and Chemistry of a Series of Related Copper Complexes, Johns Hopkins University, 2003.

[190] E.C. Constable, Higher Oligopyridines as a Structural Motif in Metallosupramolecular Chemistry, Prog. Inorg. Chem., John Wiley & Sons Ltd, in, 1994, pp. 67–138.

[191] A.G. Blackman, Overcoming the chelate effect: hypodentate coordination of common multidentate amine ligands, Comptes Rendus Chim. 8 (2005) 107–119, https://doi.org/10.1016/j.crci.2004.09.002.

[192] A. Beni, A. Dei, S. Laschi, M. Rizzitano, L. Sorace, Tuning the Charge Distribution and Photoswitchable Properties of Cobalt-Dioxolene Complexes by Using Molecular Techniques, Chem. – Eur. J. 14 (2008) 1804–1813, https://doi.org/10.1002/chem.200701163.

[193] Z. Tyeklar, R.R. Jacobson, N. Wei, N.N. Murthy, J. Zubieta, K.D. Karlin, Reversible reaction of dioxygen (and carbon monoxide) with a copper(I) complex. X-ray structures of relevant mononuclear Cu(I) precursor adducts and the trans-(μ-1,2-peroxo)dicopper(II) product, J. Am. Chem. Soc. 115 (1993) 2677–2689, https://doi.org/10.1021/ja00060a017.

[194] S.S. Massoud, F.R. Louka, M.A. Gazzaz, M.M. Henary, R.C. Fischer, F.A. Mautner, Polynuclear copper(II) complexes bridged by polycarboxylates of aromatic and N-heterocyclic compounds, Polyhedron 111 (2016) 45–52, https://doi.org/10.1016/j.poly.2016.03.013.

[195] H. Nagao, N. Komeda, M. Mukaida, M. Suzuki, K. Tanaka, Structural and Electrochemical Comparison of Copper(II) Complexes with Tripodal Ligands, Inorg. Chem. 35 (1996) 6809–6815, https://doi.org/10.1021/ic960303n.

[196] A.G.P. Gutiérrez, J. Zeitouny, A. Gomila, B. Douziech, N. Cosquer, F. Conan, O. Reinaud, P. Hapiot, Y.L. Mest, C. Lagrost, N.L. Poul, Insights into water coordination associated with the Cu^{II}/Cu^{I} electron transfer at a biomimetic Cu centre, Dalton Trans. 43 (2014) 6436–6445, https://doi.org/10.1039/C3DT53548G.

[197] I.J. Bazley, E.A. Erie, G.M. Feiereisel, C.J. LeWarne, J.M. Peterson, K.L. Sandquist, K.D. Oshin, M. Zeller, X-ray Crystallography Analysis of Complexes Synthesized with Tris(2-pyridylmethyl)amine: A Laboratory Experiment for Undergraduate Students Integrating Interdisciplinary Concepts and Techniques, J. Chem. Educ. 95 (2018) 876–881, https://doi.org/10.1021/acs.jchemed.7b00685.

[198] H. Guo, C. Gong, X. Zeng, H. Xu, Q. Zeng, J. Zhang, Z. Zhong, J. Xie, Isopolymolybdate-based inorganic–organic hybrid compounds constructed by multidentate N-donor ligands: syntheses, structures and properties, Dalton Trans. 48 (2019) 5541–5550, https://doi.org/10.1039/C9DT00119K.

[199] D.C. Bebout, S.W. Stokes, R.J. Butcher, Comparison of Heteronuclear Coupling Constants for Isostructural Nitrogen Coordination Compounds of $^{111/113}$Cd and ^{199}Hg, Inorg. Chem. 38 (1999) 1126–1133, https://doi.org/10.1021/ic980825y.

[200] N.G. Spiropulos, E.A. Standley, I.R. Shaw, B.L. Ingalls, B. Diebels, S.V. Krawczyk, B.F. Gherman, A.M. Arif, E.C. Brown, Synthesis of zinc and cadmium O-alkyl thiocarbonate and dithiocarbonate complexes and a cationic zinc hydrosulfide complex, Inorganica Chim. Acta. 386 (2012) 83–92, https://doi.org/10.1016/j.ica.2012.01.040.

[201] J. Zhang, K. Siu, C.H. Lin, J.W. Canary, Conformational dynamics of Cu(I) complexes of tripodal ligands: steric control of molecular motion, New J. Chem. 29 (2005) 1147, https://doi.org/10.1039/b509050d.

[202] M. Yamaguchi, H. Kousaka, S. Izawa, Y. Ichii, T. Kumano, D. Masui, T. Yamagishi, Syntheses, Characterization, and Catalytic Ability in Alkane Oxygenation of Chloro(dimethyl sulfoxide)ruthenium(II) Complexes with Tris(2-pyridylmethyl) amine and Its Derivatives, Inorg. Chem. 45 (2006) 8342–8354, https://doi.org/10.1021/ic060722c.

[203] N.J. Williams, W. Gan, J.H. Reibenspies, R.D. Hancock, Possible Steric Control of the Relative Strength of Chelation Enhanced Fluorescence for Zinc(II) Compared to Cadmium(II): Metal Ion Complexing Properties of Tris(2-quinolylmethyl) amine, a Crystallographic, UV−Visible, and Fluorometric Study, Inorg. Chem. 48 (2009) 1407–1415, https://doi.org/10.1021/ic801403s.

[204] Y. Mikata, Y. Nodomi, R. Ohnishi, A. Kizu, H. Konno, Tris(8-methoxy-2-quinolylmethyl)amine (8-MeOTQA) as a highly fluorescent Zn^{2+} probe prepared by convenient C_3-symmetric tripodal amine synthesis, Dalton Trans. 44 (2015) 8021–8030, https://doi.org/10.1039/C5DT00514K.

[205] A.N. Biswas, M. Puri, K.K. Meier, W.N. Oloo, G.T. Rohde, E.L. Bominaar, E. Münck, L. Que, Modeling TauD-J: A High-Spin Nonheme Oxoiron(IV) Complex with High Reactivity toward C-H Bonds, J. Am. Chem. Soc. 137 (2015) 2428–2431, https://doi.org/10.1021/ja511757j.

[206] S.H. Bae, M.S. Seo, Y.-M. Lee, K.-B. Cho, W.-S. Kim, W. Nam, Mononuclear Nonheme High-Spin (S=2) versus Intermediate-Spin (S=1) Iron(IV)–Oxo Complexes in Oxidation Reactions, Angew. Chem. Int. Ed. 55 (2016) 8027–8031, https://doi.org/10.1002/anie.201603978.

[207] N.Y. Lee, D. Mandal, S.H. Bae, M.S. Seo, Y.-M. Lee, S. Shaik, K.-B. Cho, W. Nam, Structure and spin state of nonheme $Fe^{IV}O$ complexes depending on temperature: predictive insights from DFT calculations and experiments, Chem. Sci. 8 (2017) 5460–5467, https://doi.org/10.1039/C7SC01738C.

[208] P. Güntzel, C. Nagel, J. Weigelt, J.W. Betts, C.A. Pattrick, H.M. Southam, R.M. La Ragione, R.K. Poole, U. Schatzschneider, Biological activity of manganese(I) tricarbonyl complexes on multidrug-resistant Gram-negative bacteria: From functional studies to in vivo activity in Galleria mellonella, Metallomics 11 (2019) 2033–2042, https://doi.org/10.1039/c9mt00224c.

[209] S. Biswas, P. Das, S. Rasaily, A. Pariyar, A.N. Biswas, Synthesis, structures and catalase activities of bis(μ-oxo)diMn$^{III, III}$ and bis(μ-acetato)diMn$^{II, II}$ complexes bearing a quinolyl donor tripod ligand, Inorganica Chim. Acta. 492 (2019) 76–82, https://doi.org/10.1016/j.ica.2019.04.015.

[210] Y. Mikata, K. Murakami, A. Ochi, F. Nakagaki, K. Naito, A. Matsumoto, R. Mitsuhashi, M. Mikuriya, Conversion of $(\mu\text{-}OH)_2Mn_2$(II, II) complex to $(\mu\text{-}O)_2Mn_2$(III, III) core supported by a quinoxaline-based tetranitrogen ligand, Inorganica Chim. Acta. 509 (2020), 119688, https://doi.org/10.1016/j.ica.2020.119688.

[211] Y. Mikata, Quinoline- and isoquinoline-derived ligand design on TQEN (N, N, N′, N′-tetrakis(2-quinolylmethyl)ethylenediamine) platform for fluorescent sensing of specific metal ions and phosphate species, Dalton Trans. 49 (2020) 17494–17504, https://doi.org/10.1039/D0DT03024D.

[212] M. Fbnyi, Ligands Designed To Provide Highly Active Catalyst Complexes, WO2013126745A2 (2013).
[213] C.M. Moore, N.K. Szymczak, A tris(2-quinolylmethyl)amine scaffold that promotes hydrogen bonding within the secondary coordination sphere, Dalton Trans. 41 (2012) 7886, https://doi.org/10.1039/c2dt30406f.
[214] J. Yang, M.S. Seo, K.H. Kim, Y.-M. Lee, S. Fukuzumi, J. Shearer, W. Nam, Structure and Unprecedented Reactivity of a Mononuclear Nonheme Cobalt(III) Iodosylbenzene Complex, Angew. Chem. Int. Ed. 59 (2020) 13581–13585, https://doi.org/10.1002/anie.202005091.
[215] T. Yatabe, M. Kikkawa, T. Matsumoto, H. Nakai, K. Kaneko, S. Ogo, A model for the water-oxidation and recovery systems of the oxygen-evolving complex, Dalton Trans. 43 (2014) 3063–3071, https://doi.org/10.1039/C3DT52846D.
[216] Y. Hitomi, A. Ando, H. Matsui, T. Ito, T. Tanaka, S. Ogo, T. Funabiki, Aerobic Catechol Oxidation Catalyzed by a Bis(μ-oxo)dimanganese(III, III) Complex via a Manganese(II)−Semiquinonate Complex, Inorg. Chem. 44 (2005) 3473–3478, https://doi.org/10.1021/ic050109d.
[217] L. Dubois, J. Pécaut, M.-F. Charlot, C. Baffert, M.-N. Collomb, A. Deronzier, J.-M. Latour, Carboxylate Ligands Drastically Enhance the Rates of Oxo Exchange and Hydrogen Peroxide Disproportionation by Oxo Manganese Compounds of Potential Biological Significance, Chem. – Eur. J. 14 (2008) 3013–3025, https://doi.org/10.1002/chem.200701253.
[218] H. Oshio, E. Ino, I. Mogi, T. Ito, A weak antiferromagnetic interaction between manganese(2+) centers through a TCNQ column: crystal structures and magnetic properties of $[Mn^{II}(tpa)(TCNQ)(CH_3OH)](TCNQ)_2{\bullet}CH_3CN$, $[Mn^{II}(tpa)(\mu\text{-}O_2CCH_3)]_2(TCNQ)_2{\bullet}2CH_3CN$, and $[Mn^{II}(tpa)(NCS)_2]{\bullet}CH_3CN$ (tpa = tris(2-pyridylmethyl)amine), Inorg. Chem. 32 (1993) 5697–5703, https://doi.org/10.1021/ic00077a009.
[219] T. Nagataki, Y. Tachi, S. Itoh, NiII(TPA) as an efficient catalyst for alkane hydroxylation with m-CPBA, Chem. Commun. (2006) 4016–4018, https://doi.org/10.1039/B608311K.
[220] U. Sachs, G. Schaper, D. Winkler, D. Kratzert, P. Kurz, Light- or oxidation-triggered CO release from $[Mn^{I}(CO)_3(\kappa^3\text{-}L)]$ complexes: reaction intermediates and a new synthetic route to $[Mn_2^{III/IV}(\mu\text{-}O)_2(L)_2]$ compounds, Dalton Trans. 45 (2016) 17464–17473, https://doi.org/10.1039/C6DT02020H.
[221] C. Nagel, S. McLean, R.K. Poole, H. Braunschweig, T. Kramer, U. Schatzschneider, Introducing $[Mn(CO)_3(tpa\text{-}\kappa^3\text{-}N)]+$ as a novel photoactivatable CO-releasing molecule with well-defined iCORM intermediates – synthesis, spectroscopy, and antibacterial activity, Dalton Trans. 43 (2014) 9986–9997, https://doi.org/10.1039/C3DT51848E.
[222] B.S. Lim, R.H. Holm, Molecular Heme−Cyanide−Copper Bridged Assemblies: Linkage Isomerism, Trends in νCN Values, and Relation to the Heme-a3/CuB Site in Cyanide-Inhibited Heme−Copper Oxidases, Inorg. Chem. 37 (1998) 4898–4908, https://doi.org/10.1021/ic9801793.
[223] T. Fujii, A. Naito, S. Yamaguchi, A. Wada, Y. Funahashi, K. Jitsukawa, S. Nagatomo, T. Kitagawa, H. Masuda, Construction of a square-planar hydroperoxo-copper(II) complex inducing a higher catalytic reactivity, Chem. Commun. (2003) 2700–2701, https://doi.org/10.1039/B308073K.
[224] A.L. Ward, L. Elbaz, J.B. Kerr, J. Arnold, Nonprecious Metal Catalysts for Fuel Cell Applications: Electrochemical Dioxygen Activation by a Series of First Row Transition Metal Tris(2-pyridylmethyl)amine Complexes, Inorg. Chem. 51 (2012) 4694–4706, https://doi.org/10.1021/ic2026957.
[225] S. Yan, C. Li, P. Cheng, D. Liao, Z. Jiang, G. Wang, X. Yao, Honggen. Wang, Copper, a chemical Janus: two copper(II) complexes with different ligand in one single crystal, J. Chem. Crystallogr. 29 (1999) 1085–1088.
[226] A.G. Blackman, E.B. Schenk, R.E. Jelley, E.H. Krenske, L.R. Gahan, Five-coordinate transition metal complexes and the value of τ_5: observations and caveats, Dalton Trans. 49 (2020) 14798–14806, https://doi.org/10.1039/D0DT02985H.
[227] A.A. Massie, M.C. Denler, L.T. Cardoso, A.N. Walker, M.K. Hossain, V.W. Day, E. Nordlander, T.A. Jackson, Equatorial Ligand Perturbations Influence the Reactivity of Manganese(IV)-Oxo Complexes, Angew. Chem. Int. Ed. 56 (2017) 4178–4182, https://doi.org/10.1002/anie.201612309.
[228] W. Rasheed, A. Draksharapu, S. Banerjee, V.G. Young Jr., R. Fan, Y. Guo, M. Ozerov, J. Nehrkorn, J. Krzystek, J. Telser, L. Que Jr., Crystallographic Evidence for a Sterically Induced Ferryl Tilt in a Non-Heme Oxoiron(IV) Complex that Makes it a Better Oxidant, Angew. Chem. Int. Ed. 57 (2018) 9387–9391, https://doi.org/10.1002/anie.201804836.
[229] S. Rana, J.P. Biswas, A. Sen, M. Clémancey, G. Blondin, J.-M. Latour, G. Rajaraman, D. Maiti, Selective C-H halogenation over hydroxylation by non-heme iron(IV)-oxo, Chem. Sci. 9 (2018) 7843–7858, https://doi.org/10.1039/C8SC02053A.
[230] E. Ramírez, M.K. Hossain, M. Flores-Alamo, M. Haukka, E. Nordlander, I. Castillo, Oxygen Transfer from Trimethylamine N-Oxide to Cu^{I} Complexes Supported by Pentanitrogen Ligands, Eur. J. Inorg. Chem. 2020 (2020) 2798–2808, https://doi.org/10.1002/ejic.202000488.
[231] J.P. Biswas, M. Ansari, A. Paik, S. Sasmal, S. Paul, S. Rana, G. Rajaraman, D. Maiti, Effect of the Ligand Backbone on the Reactivity and Mechanistic Paradigm of Non-Heme Iron(IV)-Oxo during Olefin Epoxidation, Angew. Chem. Int. Ed. 60 (2021) 14030–14039, https://doi.org/10.1002/anie.202102484.
[232] S. Munshi, A. Sinha, S. Yiga, S. Banerjee, R. Singh, M.K. Hossain, M. Haukka, A. F. Valiati, R.D. Huelsmann, E. Martendal, R. Peralta, F. Xavier, O.F. Wendt, T. K. Paine, E. Nordlander, Hydrogen-atom and oxygen-atom transfer reactivities of iron(IV)-oxo complexes of quinoline-substituted pentadentate ligands, Dalton Trans. 51 (2022) 870–884, https://doi.org/10.1039/D1DT03381F.
[233] D.F. Leto, R. Ingram, V.W. Day, T.A. Jackson, Spectroscopic properties and reactivity of a mononuclear oxomanganese(IV) complex, Chem. Commun. 49 (2013) 5378–5380, https://doi.org/10.1039/C3CC00244F.
[234] J. Chen, Y.-M. Lee, K.M. Davis, X. Wu, M.S. Seo, K.-B. Cho, H. Yoon, Y.J. Park, S. Fukuzumi, Y.N. Pushkar, W. Nam, A Mononuclear Non-Heme Manganese(IV)–Oxo Complex Binding Redox-Inactive Metal Ions, J. Am. Chem. Soc. 135 (2013) 6388–6391, https://doi.org/10.1021/ja312113p.
[235] E.J. Klinker, J. Kaizer, W.W. Brennessel, N.L. Woodrum, C.J. Cramer, L. Que Jr., Structures of Nonheme Oxoiron(IV) Complexes from X-ray Crystallography, NMR Spectroscopy, and DFT Calculations, Angew. Chem. Int. Ed. 44 (2005) 3690–3694, https://doi.org/10.1002/anie.200500485.
[236] A. Geersing, N. Ségaud, M.G.P. van der Wijst, M.G. Rots, G. Roelfes, Importance of Metal-Ion Exchange for the Biological Activity of Coordination Complexes of the Biomimetic Ligand N4Py, Inorg. Chem. 57 (2018) 7748–7756, https://doi.org/10.1021/acs.inorgchem.8b00714.
[237] R. Turcas, B. Kripli, A.A.A. Attia, D. Lakk-Bogáth, G. Speier, M. Giorgi, R. Silaghi-Dumitrescu, J. Kaizer, Catalytic and stoichiometric flavanone oxidation mediated by nonheme oxoiron(IV) complexes as flavone synthase mimics: kinetic, mechanistic and computational studies, Dalton Trans. 47 (2018) 14416–14420, https://doi.org/10.1039/C8DT03519A.
[238] D. Lakk-Bogáth, P. Török, M. Giorgi, J. Kaizer, Catalase and catecholase-like activities of manganese and copper complexes supported by pentadentate polypyridyl ligands in aqueous solution, J. Mol. Struct. 1262 (2022), 133100, https://doi.org/10.1016/j.molstruc.2022.133100.
[239] A. Hazell, O. Mønsted, J.C. Rasmussen, H. Toftlund, Three overcrowded zinc(II) complexes with potentially hexadentate polypyridyl ligands, Acta Crystallogr. Sect. C. 64 (2008) m185–m189. https://doi.org/10.1107/S0108270108007014.
[240] Y. Mikata, S. Takeuchi, E. Higuchi, A. Ochi, H. Konno, K. Yanai, S. Sato, Zinc-specific intramolecular excimer formation in TQEN derivatives: fluorescence and zinc binding properties of TPEN-based hexadentate ligands, Dalton Trans. 43 (2014) 16377–16386, https://doi.org/10.1039/C4DT01847H.
[241] S. Vuong, L. Stefan, P. Lejault, Y. Rousselin, F. Denat, D. Monchaud, Identifying three-way DNA junction-specific small-molecules, Biochimie 94 (2012) 442–450, https://doi.org/10.1016/j.biochi.2011.08.012.
[242] A.C.M. Appel, R. Hage, D. Tetard, R.S. Twisker, Bleaching composition and bleaching laundered fabrics with atmospheric oxygen in the presence of a ligand/metal complex, 2001.
[243] A. Guillou, L.M.P. Lima, M. Roger, D. Esteban-Gómez, R. Delgado, C. Platas-Iglesias, V. Patinec, R. Tripier, 1,4,7-Triazacyclononane-Based Bifunctional Picolinate Ligands for Efficient Copper Complexation, Eur. J. Inorg. Chem. 2017 (2017) 2435–2443, https://doi.org/10.1002/ejic.201700176.
[244] W. Han, Z.-D. Wang, C.-Z. Xie, Z.-Q. Liu, S.-P. Yan, D.-Z. Liao, Z.-H. Jiang, P. Cheng, Crystal structures and spectroscopic properties of copper(II) and zinc(II) complexes with the macrocycle 1,4,7-tris(2-pyridylmethyl)-1,4,7-triazacyclononane, J. Chem. Crystallogr. 34 (2004) 495–500, https://doi.org/10.1023/B:JOCC.0000042016.86927.1b.
[245] L. Christiansen, D.N. Hendrickson, H. Toftlund, S.R. Wilson, C.L. Xie, Synthesis and structure of metal complexes of triaza macrocycles with three pendant pyridylmethyl arms, Inorg. Chem. 25 (1986) 2813–2818, https://doi.org/10.1021/ic00236a031.
[246] G.-S. Park, Zn(II) Complex of Tachquin, N, N', N''-Tris(2-quinolinylmethyl)-cis, cis-1,3,5-triaminocyclohexane); Synthesis and X-ray Structure of [Zn(tachquin)] $(ClO_4)_2$. H_2O, Bull. Korean Chem. Soc. 26 (2005) 1849–1852, https://doi.org/10.5012/bkcs.2005.26.11.1849.
[247] T. Bowen, R.P. Planalp, M.W. Brechbiel, An improved synthesis of cis, cis-1,3,5-triaminocyclohexane. Synthesis of novel hexadentate ligand derivatives for the preparation of gallium radiopharmaceuticals, Bioorg. Med. Chem. Lett. 6 (1996) 807–810, https://doi.org/10.1016/0960-894X(96)00110-2.
[248] G. Park, N. Ye, R.D. Rogers, M.W. Brechbiel, R.P. Planalp, Effect of metal size on coordination geometry of N, N′, N″-tris(2-pyridylmethyl)-cis, cis-1,3,5-triaminocyclohexane: synthesis and structure of $[M^{II}L](ClO_4)_2$ (M=Zn, Cd and Hg), Polyhedron 19 (2000) 1155–1161, https://doi.org/10.1016/S0277-5387(00)00380-6.
[249] F. Matyuska, A. Szorcsik, N.V. May, Á. Dancs, É. Kováts, A. Bényei, T. Gajda, Tailoring the local environment around metal ions: a solution chemical and structural study of some multidentate tripodal ligands, Dalton Trans. 46 (2017) 8626–8642, https://doi.org/10.1039/C7DT00104E.
[250] Y. Mikata, A. Kizu, H. Konno, TQPHEN (N, N, N′, N′-tetrakis(2-quinolylmethyl)-1,2-phenylenediamine) derivatives as highly selective fluorescent probes for Cd^{2+}, Dalton Trans. 44 (2015) 104–109, https://doi.org/10.1039/C4DT02177K.
[251] Y. Mikata, M. Wakamatsu, S. Yano, Tetrakis(2-quinolinylmethyl)ethylenediamine (TQEN) as a new fluorescent sensor for zinc, Dalton Trans. (2005) 545–550, https://doi.org/10.1039/B411924J.
[252] Y. Mikata, Y. Sato, S. Takeuchi, Y. Kuroda, H. Konno, S. Iwatsuki, Quinoline-based fluorescent zinc sensors with enhanced fluorescence intensity, Zn/Cd selectivity and metal binding affinity by conformational restriction, Dalton Trans. 42 (2013) 9688–9698, https://doi.org/10.1039/C3DT50719J.
[253] C.A. Blindauer, M.T. Razi, S. Parsons, P.J. Sadler, Metal complexes of N, N, N′, N′-tetrakis(2-pyridylmethyl)ethylenediamine (TPEN): Variable coordination numbers and geometries, Polyhedron 25 (2006) 513–520, https://doi.org/10.1016/j.poly.2005.08.019.

[254] M. Nieger, J. Ratilainen, K. Rissanen, Private Communication to the Cambridge Structural Database. CCDC192006.
[255] Y. Mikata, K. Nozaki, M. Tanaka, H. Konno, A. Matsumoto, M. Kawamura, S. Sato, Switching of Fluorescent Zn/Cd Selectivity in N, N, N′, N′-Tetrakis(6-methoxy-2-quinolylmethyl)-1,2-diphenylethylenediamine by One Asymmetric Carbon Atom Inversion, Inorg. Chem. 59 (2020) 5313–5324, https://doi.org/10.1021/acs.inorgchem.9b03304.
[256] D. Lakk-Bogáth, N.P. Juraj, B.I. Meena, B. Perić, S.I. Kirin, J. Kaizer, Comparison of Nonheme Manganese- and Iron-Containing Flavone Synthase Mimics, Molecules 26 (2021) 3220, https://doi.org/10.3390/molecules26113220.